UNIVERSITÀ DEGLI STUDI DI PADOVA

Dipartimento di Ingegneria Industriale DII

Corso di Laurea Magistrale in Ingegneria Energetica

TESI DI LAUREA MAGISTRALE

Dynamic investigations of a domestic scale thermally driven heat pump application

Relatore: Prof. Andrea Lazzaretto[a]
Correlatori: Prof. Sotirios Karellas[b]
Dr. Giannis Mandilaras[b]
Msc-Ing. Tryfonas Roumpedakis[b]
Dipl-Ing. Stratis Varvagiannis[b]

Laureando: Paris Pasqualin
Matricola: 1152777

[a] Università degli Studi di Padova, Italy
[b] National Technical University of Athens, Greece

Anno Accademico 2017-2018

Contents

i Nomenclature

A_b	Heat transfer area of the beds
A_c	Heat transfer area of the condenser
A_e	Heat transfer area of the evaporator
A_{frame}	Area of the frame of the window
A_{window}	Total area of the window
COP	Coefficient of performance
COP_c	Coefficient of performance for cooling
COP_h	Coefficient of performance for heating
D_{s0}	Pre-exponent constant in the kinetics equation
E_a	Activation energy of surface diffusion
L	Latent heat of evaporation
P_s	Saturation pressure
Q_{ads}	Heating power produced in the adsorber
Q_c	Heating power produced in the condenser
Q_{des}	Heating power provided to the desorber
Q_e	Cooling power produced in the evaporator
Q_h	Total heating power produced by the chiller
Q_{st}	Adsorption heat
R_p	Average radius of silica gel
R_w	Universal gas constant of water
T_a	Temperature at the adsorption bed
T_{a0}	Initial temperature at the adsorption bed
T_c	Temperature at the condenser
T_{c0}	Initial temperature at the condenser
T_{chw_in}	Inlet chilled water temperature
$T_{cw\_b\_out}$	Outlet chilled water temperature
$T_{cw\_c\_out}$	Outlet cool water from the bed
T_{cw_in}	Outlet cool water from the condenser
T_d	Temperature at the desorption bed
T_{d0}	Initial temperature at the desorption bed
T_e	Temperature at the evaporator
T_{e0}	Initial temperature at the evaporator
T_{hw_in}	Inlet hot water temperature
$time_A$	Time of working of phase A of the chiller
$time_B$	Time of working of phases B and A of the chiller
U	Heat transfer coefficient of the surfaces
U_b	Heat transfer coefficient of the beds
U_c	Heat transfer coefficient of the condenser
U_e	Heat transfer coefficient of the evaporator
U_{glass}	Heat transfer coefficient of the glazing
W_{b_cu}	Mass of the copper in the beds
W_{c_cu}	Mass of the copper in the condenser
W_{c_w}	Mass of the water in the condenser
W_{e_cu}	Mass of the copper in the evaporator
W_{e_w}	Mass of the water in the evaporator
W_s	Mass of silica gel
cp_{cu}	specific heat capacity of copper
cp_s	specific heat capacity of silica gel
cp_w	specific heat capacity of water
g_{glass}	Solar factor of the glazing
$\dot{m}_{chw}$	Mass flow rate of chilled water
$\dot{m}_{cw}$	Mass flow rate of cooling water
$\dot{m}_{cw\_b}$	Mass flow rate of cooling water in the beds
$\dot{m}_{cw\_c}$	Mass flow rate of cooling water in the condenser
$\dot{m}_{hw}$	Mass flow rate of hot water
q	Fraction of refrigerant adsorbed or desorbed by the adsorbent
q_a	Fraction of refrigerant adsorbed by the adsorber
q_{a0}	Initial fraction of refrigerant adsorbed by the adsorber
q_d	Fraction of refrigerant desorbed by the desorber
q_{d0}	Initial fraction of refrigerant desorbed by the desorber
q^*	Fraction of refrigerant which can be adsorbed by the adsorbent under saturation condition

1 Italian summary

L'argomento consiste nell'impiego dell'energia solare per il riscaldamento e il raffrescamento di un gruppo di edifici tramite l'utilizzo di un chiller ad adsorbimento. Il chiller ad adsorbimento fa parte delle tecnologie di raffrescamento solare che sfruttano energia solare per produrre potenza frigorifera. Questa macchina può essere utilizzata per il riscaldamento degli edifici dove il suo funzionamento rimane uguale durante i periodi di raffrescamento e riscaldamento. Il chiller ad adsorbimento assorbe potenza frigorifera da un ambiente e cede potenza termica ad un altro ambiente. Durante il periodo di riscaldamento la potenza utile è la potenza termica ceduta all'ambiente mentre nel periodo di raffrescamento la potenza utile è la potenza frigorifera assorbita dall'ambiente.
L'obbiettivo è di creare un modello dinamico composto da un modello 3D degli edifici, un modello dinamico del chiller ad adsorbimento e un sistema di controllo. Il sistema dinamico complessivo dovrà calcolare il fabbisogno energetico degli edifici, la frazione di energia primaria risparmiata, la frazione di energia solare e il tempo di ritorno dell'investimento iniziale. Questi quattro parametri verranno utilizzati per analizzare il sistema energeticamente ed economicamente per 20 configurazioni. Le configurazioni hanno quattro volumi di accumulo: 500, 1000, 2000 e 3000 l e cinque aree di collettori solari: 37.71, 58.66, 79.61, 96.37 e 113.13 m^2. L'obbiettivo finale è di trovare la configurazione col minor tempo di ritorno dell'investimento.
Gli edifici considerati nella simulazione sono dei tipici fabbricati in architettura Greca costruiti ad Atene nel periodo 1980-2011. Si assume che gli edifici utilizzino una caldaia a gasolio e una pompa di calore per il riscaldamento e raffrescamento degli edifici mediante l'impiego di fan coil. Per questo motivo il calcolo dell'investimento iniziale non comprende i prezzi della caldaia e dei fan coil. Ogni edificio è composto da un piano terra e un seminterrato, entrambi con area in pianta di 80 m^2, dove solo il piano terra è riscaldato e raffrescato e pertanto il fabbisogno energetico totale coincide con quello del piano terra.
Il chiller ad adsorbimento è composto da quattro componenti: l'evaporatore, il condensatore e i due letti ad adsorbimento che contengono il silica gel. Il chiller lavora con tre livelli di temperatura dell'acqua: calda (70 - 95 °C con portata uguale a 1.28 kg/s), media (25 - 45 °C con portata uguale a 2.89 kg/s) e fredda (10 - 18 °C con portata uguale a 0.7 kg/s). Il modello dinamico si basa su un chiller ad adsorbimento reale che è stato studiato sperimentalmente.
Il metodo impiegato consiste nella costruzione di un modello dinamico che possa simulare il comportamento dei componenti che costituiscono il sistema in modo da prevedere il funzionamento del sistema durante l'anno. Gli input nel sistema sono i dati climatici dell'anno tipo della località, la temperatura del terreno, i parametri di design del chiller, le caratteristiche dei muri e delle finestre dei edifici, i parametri di design dei componenti del sistema e i loro prezzi. Gli output sono il fabbisogno energetico degli edifici e il consumo energetico della caldaia

che consentono di valutare le quattro grandezze definite negli obiettivi. I componenti ausiliari non sono stati considerati perché si assume che il loro consumo energetico sia molto minore rispetto a quello della caldaia. Inoltre sono trascurati i consumi elettrici e le pressioni di lavoro di tutti i componenti perché alcuni componenti di TRNSYS non calcolano il consumo elettrico e le pressioni dei fluidi. Infine, si considera che i dati climatici dell'anno tipo vengono ripetuti ugualmente ogni anno.

Il problema del raffrescamento degli edifici presenta dei transitori che possono essere inclusi nei calcoli utilizzando un modello dinamico. Un modello dinamico esprime il suo funzionamento in funzione del tempo. In TRNSYS si può scegliere il passo temporale che è stato posto pari ad un'ora. Il modello degli edifici non considera variazioni nello spazio della temperatura all'interno degli edifici e delle temperature dell'acqua all'interno delle tubazioni e pertanto e considerato un modello zero dimensionale.

TRNSYS è stato confrontato con il software TEE K.Eν.A.K creato dall'istituto tecnico nazionale Greco per il calcolo del fabbisogno energetico degli edifici. Sono state studiate 28 configurazioni per un semplice edificio per verificare i risultati di TRNSYS. I due software forniscono risultati diversi perché hanno diversi input e diversi metodi di calcolo. Dalle 28 simulazioni si conclude che i risultati di TRNSYS sono più ragionevoli.

Il chiller ad adsorbimento è stato ottimizzato per produrre maggior potenza frigorifera. Il tempo del "switching" e il tempo del ciclo sono le variabili che sono state variate durante l'ottimizzazione. Valori di switching time uguale a 20 s e tempo di ciclo uguale a 800 s permettono di massimizzare la potenza frigorifera prodotta dal chiller. Il calcolo annuale, ora per ora, delle temperature in uscita dal chiller impiega 6 giorni. Per questo è stata usata un interpolazione tri-lineare che diminuisce il tempo di calcolo a 5 minuti con un errore massimo di 2 %.

I risultati del modello del chiller dimostrano come maggiori potenze frigorifere siano prodotte con elevata temperatura dell'acqua calda, bassa temperatura dell'acqua media ed elevata temperatura dell'acqua fredda. Inoltre, l'acqua media provoca elevate variazioni della COP e della potenza frigorifera il che suggerisce ad investire in una buona torre evaporativa per aumentare la COP e la potenza frigorifera prodotta.

I risultati del modello complessivo dimostra che energeticamente conviene avere grandi superfici di collettori solari e grandi volumi di accumulo mente economicamente conviene avere piccole superfici di collettori solari e grandi volumi di accumulo. Questo contrasta con il fatto che il raffrescamento solare necessita grandi superfici di collettori solari per ottenere maggiori frazioni di energia solare. Il passaggio da un piccolo ad uno medio volume di accumulo provoca elevate riduzioni del tempo di ritorno dell'investimento, elevati aumenti della frazione di energia risparmiata e della frazione solare. Il miglioramento decresce continuando ad aumentare l'accumulo con benefici economici marginali per le configurazioni con aree di collettori solari pari a 58.66, 96.37 e 113.13 m^2 e volume di accumulo maggiore di 2000 l. Il minor tempo di

ritorno dell'investimento compreso tra 26.3 e 32.1 anni, ottenuto con un accumulo di 3000 l e area di collettori solari pari a 37.71 m^2, è molto elevato e senza un incentivo economico questa scelta non è ragionevole.

2 Abstract

The subject is to employ an adsorption chiller to heat and cool two identical single family buildings. Its target is the creation of a dynamic model of a solar hot water system (SHWS) which includes a 3D model of the buildings, a dynamical model of the adsorption chiller and an automatic control system. The energetic and economic evaluation of the SHWS requires the calculation of the energy demands of the buildings, the fraction of primary energy savings, the solar fraction during cooling and the payback period (PBP) of the initial investment.
The method consists in the creation of a dynamic model which simulates the components of the SHWS to predict the behavior of the SHWS during the entire year.
The lowest PBP without incentives, between 26.3 and 32.1 years, can be achieved with a tank volume of 3000 l and a collector area of 37.71 m^2. This too high value of the PBP shows that the adsorption solar cooling technologies are not a competitive solution for heating and cooling and thus more research is needed.

3 Introduction

In this work solar energy is utilized to produce heating and cooling power through an adsorption chiller which is part of the solar cooling technologies. The adsorption chillers work with hot water temperatures between 70 and 95 °C and can be coupled with flat plate solar collectors. Solar cooling systems require high solar fractions (ratio between input solar energy and total input energy to the system) which are achievable with large solar collectors areas. These solar collectors can also operate during winter to generate heating power. During both cooling and heating periods adsorption chillers absorb heat from one environment and reject heat to another one: the absorbed heat is the useful outcome during the cooling period whereas the rejected heat is the useful outcome during the heating period.
There are two categories of chillers, absorption and adsorption chillers, which operate with liquid working fluids (LiBr or ammonia) and solid adsorbents (silica gel or zeolite) respectively. Several papers about dynamic simulations of absorption solar cooling technologies have been performed in the literature (e.g., [25], [37], [45], [48]) which include utilities with energy demands and the weather data of the location. Conversely, in the dynamic simulations of adsorption chillers (e.g., [16], [17], [44], [54]) the behavior is described independently of utilities and weather data. Hassan et al. [28] proposed a theoretical simulation model for a tubular solar

adsorption refrigerating system which includes a solar flat plate collector with a 1 square meter area. They also considered ambient temperature and solar radiation variations along the day without including utilities. Palomba et al. [42] developed a TRNSYS model and performed dynamic simulations of an adsorption chiller connected with a building and operating only in cooling mode. They simply utilized the TRNSYS block "type 909", which relies on user provided performance data files containing normalized capacity and COP ratios correlated to the hot, cooling and chilled water inlet temperature [8]. Also Vasta et al. [50] performed dynamic simulations with TRNSYS to evaluate the economic feasibility of three adsorption systems for three different cities in Italy. The model equations of the adsorption chiller operating in cooling mode were built on the basis of experimental tests of a commercial unit. The payback period, calculated without incentives, ranged from 33 to 35 years. Calise et al. [13] developed a TRNSYS dynamic model of an adsorption system which generates both heating and cooling power to maximize the primary energy savings. No information was given about the model of the adsorption chiller.

The novelty of this work consists in the development of a dynamic model for a real silica gel-water adsorption chiller based on a set of differential equations which accurately describes its behavior over time. The equations and their experimental validation were performed by Papoutsis [44]. Both heating and cooling modes are considered in order to increase the operating period and in turn the economic savings.

The case studies consider four storage tank volumes: 500, 1000, 2000 and 3000 l and five solar collectors areas: 37.71, 58.66, 79.61, 96.37 and 113.13 m^2. The goal is to find the pair of storage tank volume and solar collectors area with the lowest PBP. This is achieved by evaluating the energetic and economic performance of the SHWS starting from the estimate of the energy demands of the buildings. The fraction of primary energy savings, the solar fraction during the cooling period and the PBP are also calculated.

4 Solar cooling technologies

Solar cooling popularity has increased in the last years because cooling power can be produced from solar energy. The electric vapor compression cycle is the main technology utilized for cooling due to its low cost, approcimately of 500 €/kW, and its high cooling performance with COP values of 4.5 [39]. Electric vapor compression requires electrical energy which in most countries is produced from fossil fuels. Renewable energies have become necessary due to the negative environmental impact origineted from the utillization of fossil fuels, the increasing global population and the aim of COP21 to keep the global temperature rise below 2 °C. 40% of the total global energy demand is required from residential buildings and cooling energy demand is expected to increase by 6% per year [5].
Solar cooling has the advantage that the availability of solar energy corresponds with the cooling demand. High solar fractions can be obtained with large solar collectors areas. These collectors can be employed during the heating period to produce heating power. Adsorption solar cooling technologies can produce heating and cooling power by exploiting solar energy without affect negatively the environment.
Adsorption and absorption systems require a specific solar flat plate collector area higher than 2 m^2/kW and lower than 5 m^2/kW. Absorption ammonia-water systems require specific collector areas larger than the water-LiBr systems and therefore ammonia-water systems have higher installations costs. The water-LiBr systems show the best performance while the adsorption systems are generally less efficient [11].
The PBP of solar heating and cooling (SHC) installation is still considered too high and consequently the performance of solar cooling technologies aims to maximize the primary energy savings, reduce the auxiliary energy demands and extend the operational hours in order to increase the economic savings [39].

4.1 Adsorption solar cooling

The common working pairs for adsorption cooling systems are water-silica gel, water-zeolite and ammonia-$CaCl_2$. Adsorption chillers have limit applications because of their negative aspects which are low COP and high initial costs. The developments of silica gel-water adsorption chiller concentrates on improving efficiency, decreasing size and costs [26]. The SACE database [2] includes completed questionnaires for 54 projects where only 10% of these projects employ adsorption chillers.
Typical working conditions are chilled water temperature of 14 °C, cooling temperature of 31 °C and hot temperature of 70 – 85 °C [9], [30], [34], [43], [49]. Corrosion problems can be avoided with adsorption chillers because water is the refrigerant while silica gel is the adsorbent [10]. Adsorption technologies can be driven by low heat source temperatures without crystal-

lization problems with average COP values of 0.59. The average COP is lower compared to other solar cooling technologies. Adsorption technologies have the highest initial costs among the solar cooling technologies with values of 5,000 €/kW [11].

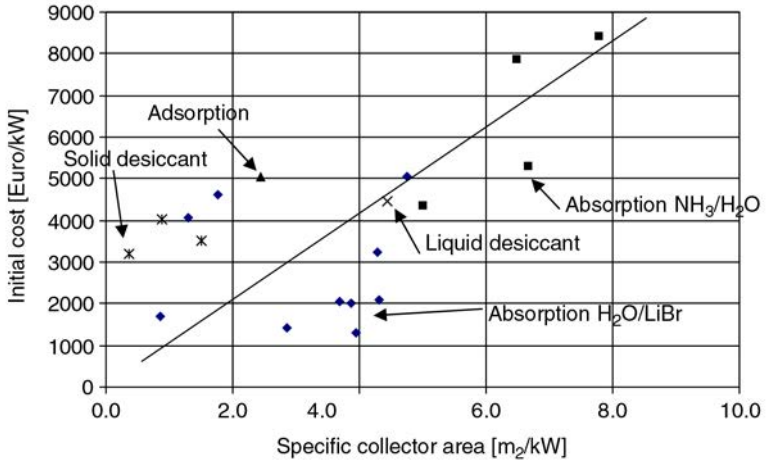

Fig. 1. Initial system cost as a function of the specific collector area. Cited from Balaras [11]

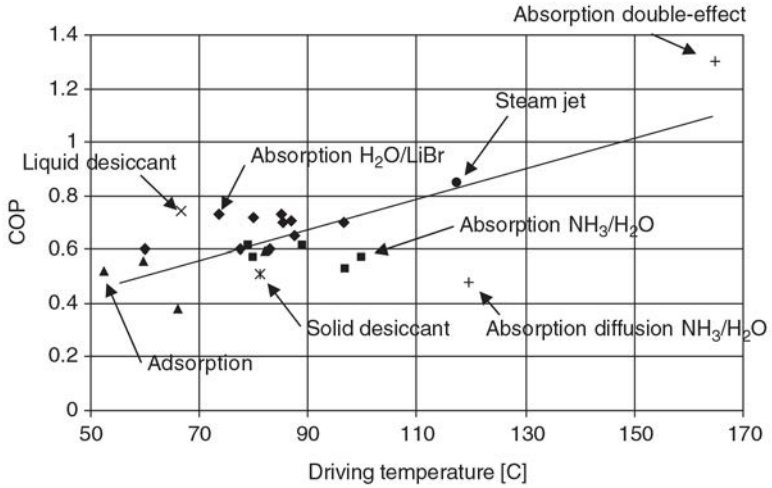

Fig. 2. COP as a function of heating medium temperature. Cited from Balaras [11]

Adsorption chillers have poor heat exchange between the solid adsorbent and the water and their systems are affected by intrinsic intermittence. These problems have been partly solved and adsorption chillers which require driving temperatures of 60 - 70 °C are commercially available with low COP values [53]. COP values between 0.3 and 0.5 can be reached with adsorption silica gel-water chillers powered by hot water temperatures of 60 - 85 °C [52].
Silica gel-water adsorption chillers have also been developed to exploit low waste heat temperatures to improve the energy conversion efficiency from waste heat to useful cooling [54]. Saha et al. [46] developed a multi stage silica gel-water adsorption chiller that operated with temperatures of 50 °C with very low COP values.

Models of silica gel-water adsorption chillers have been developed from theoretical and experimental studies, such as [16], [17], [54]. Other models of adsorption chillers with zeolite as the refrigerant have been proposed from various authors: [31],[33], [36], [38],[56].
Desideri et al. [20] evaluated the PBP for two cases: an absorption chiller for a food-processing factory and a hybrid tri-generation plant for a hotel. The PBP was equal to 10 and 12 years respectively for the two cases considering a tax allowance of 55 % and effective interest rate of 5 %.

4.2 Absorption solar cooling

Absorption refrigeration was introduced by Ferdinand Carrè in 1858 and has been developed in the last years. Common working pairs for absorption cooling system are water-LiBr and ammonia-water. In the SACE database [2] approximately 70% of the systems employ absorption chillers. Single-effect absorption is the most popular system with COP values of 0.5 - 0.8. A COP value of 0.7 can be achieved with driving, ambient and evaporation temperature of 90 °C, 30 °C and 5 °C respectively. Higher COP values can be reached with double-effect cycles that require driving temperatures of 140 °C. Novel concepts are proposed to improve the performance of solar thermal cooling systems [26].
Absorption systems employ a refrigerant that expands from the condenser to the evaporator through a throttle. Conventional vapor compression systems operate in a similar way. The absorbent absorbs refrigerant vapor from the evaporator at low pressure and desorbs it to the condenser at high pressure when heat (Qsol) is supplied to the generator. The absorption system acts as a heat driven heat pump. The heat can be provided from solar energy, heat waste or other sources. The system operates between the pressures of the evaporator and the condenser and interacts with three temperature levels: the cooling temperature in the evaporator, the intermediate temperature in the absorber and condenser and the high temperature in the generator [11].

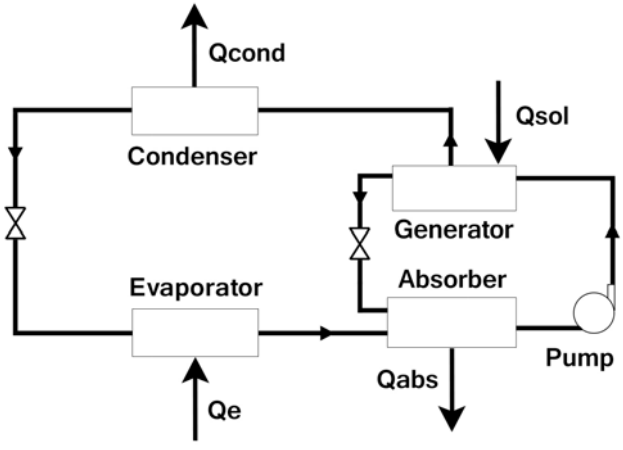

Fig. 3. Simplified absorption scheme

Single-effect absorption systems can reach COP values up to 0.7 with LiBr–water and up to 0.6 with ammonia–water. These two pairs require large solar collector areas which can be reduced by employing systems with improved COP driven by higher heat source temperatures. Developments in gas-fired absorption systems made possible to commercialize double-effect systems with COP of 1.0 – 1.2. Triple-effect systems are still under development with COP of 1.7 [11].

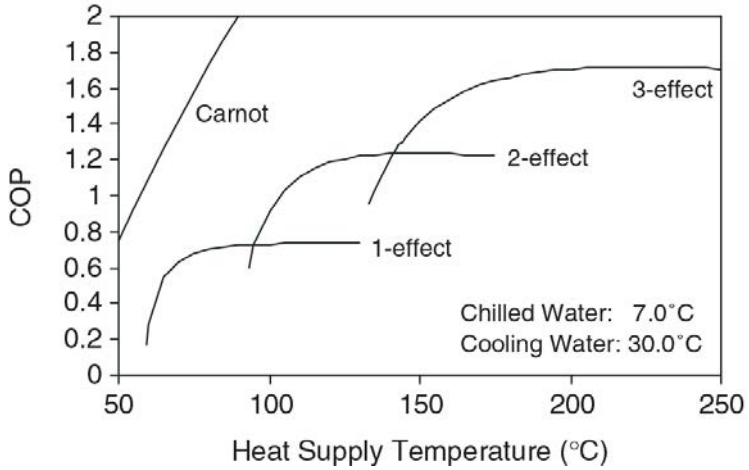

Fig. 4. COP of LiBr–water absorption chillers as a function of heat supply temperature for single, double and triple-effect. Cited from Balaras [11]

Xu and wang [57] simulated a solar cooling system based on variable effect LiBr-water. Increasing the solar collects area from 150 to 275 m^2 increases the COP from 0.82 to 1.00, increases the solar fraction from 0.24 to 0.37 and decreases the PBP. The COP decreases from 1.00 to 0.82 by increasing the storage tank volume from 1.0 to 4.5 m^3. The solar fraction increases from 0.31 to 0.36 by increasing the storage tank volume from 1.0 to 2.5 m^3 and decreases from 0.36 to 0.30 by increasing the storage tank volume from 2.5 to 4.5 m^3. The PBP ranges from 12 to 19 years based on the fuel prices.

4.3 Desiccant cooling

Desiccant cooling systems operate desiccant materials to cool air without employing refrigerant fluids. The desiccant material, solid or liquid, dehumidifies air by removing its moisture. Open loop desiccant systems are directly connected with air while close loop dehumidify air indirectly. Solid desiccant systems employ desiccants such as silica gel and zeolite in a rotating bed with flexible utilization [19]. Liquid desiccant systems work with a surface submerged in lithium chloride or calcium chloride [4] and are more compact and less subject to corrosion compared to the solid desiccant systems [19]. In the SACE database [2] 10% of the systems employ desiccant cooling systems.

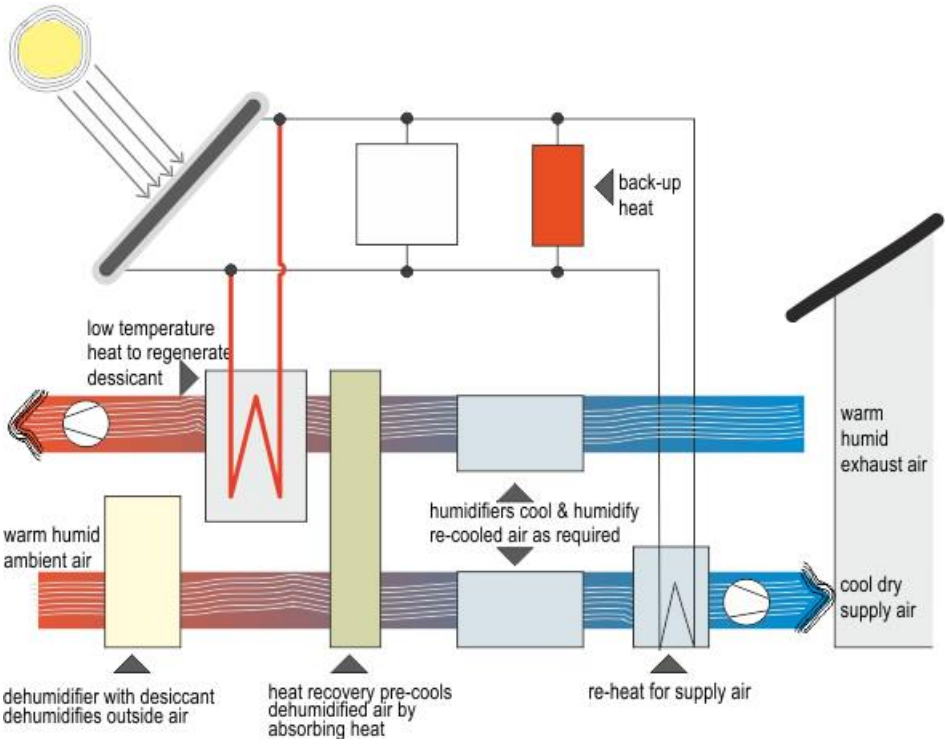

Fig. 5. Scheme of a solid desiccant system. Cited by nzeb [4]

Desiccant cooling systems are driven by low heat source temperatures and are compatible for residential and commercial applications by increasing energy savings and by reducing the operating costs. The initial costs of the desiccant system are comparatively high and hence the focus of research for the past decade has been to develop desiccant systems with high COP. Recent studies have emphasized computer modeling and hybrid systems that combine desiccant dehumidifiers with conventional systems [55].

Liquid desiccant systems have been investigated to improve the performance of electrical vapor compression cycles [18]. Desiccant cooling can attenuate the negative effects of the vapor compression cycles to achieve more accessible, economical and cleaner air conditioning. Combinations of desiccant cooling with electrical vapor compression cycles can reach fractions of primary energy savings equal to 0.5 [29].

Water vapor must be driven out continuously to guarantee proper internal conditions which is achieved by heating the desiccant material to its regeneration temperature. Desiccant cooling systems can be divided in the regeneration heat source, the dehumidifier and the cooling unit. The regeneration heat source provides the required thermal energy to the desiccant material in order to absorb the water vapor of the air. The thermal energy source can be solar energy, heat waste or natural gas [19].

Henning et al. [29] investigated the potential of solar energy in desiccant cooling with TRNSYS by evaluating 12 cases with three storage tank volumes and four collectors areas. The calculated solar fraction ranged from 0.4 to 1. The calculated COP during a typical summer

week is equal to 0.6. Their study suggests installing desiccant cooling systems in warm and humid climates for good energetic and economic performance. Halliday et al. [27] proved the feasibility of the desiccant systems for the UK.
Bourdoukan et al. [12] investigated experimentally the desiccant system. The overall performance of the installation was evaluated over a day for a moderate humid climate with regeneration solely by solar energy. The overall efficiency of the solar installation was equal to 0.55 with COP equal to 0.45.

4.4 Future developments

The forecast proposed by Otanicar et al. [41] expect a major improvement of the COP for desiccant and adsorption cycles. Absorption COP is expected to increase slower compared to desiccant and adsorption cycles. In 2030 desiccant cooling are expected to reach a maximum COP of 1.2 while adsorption cycles a COP of 0.6.

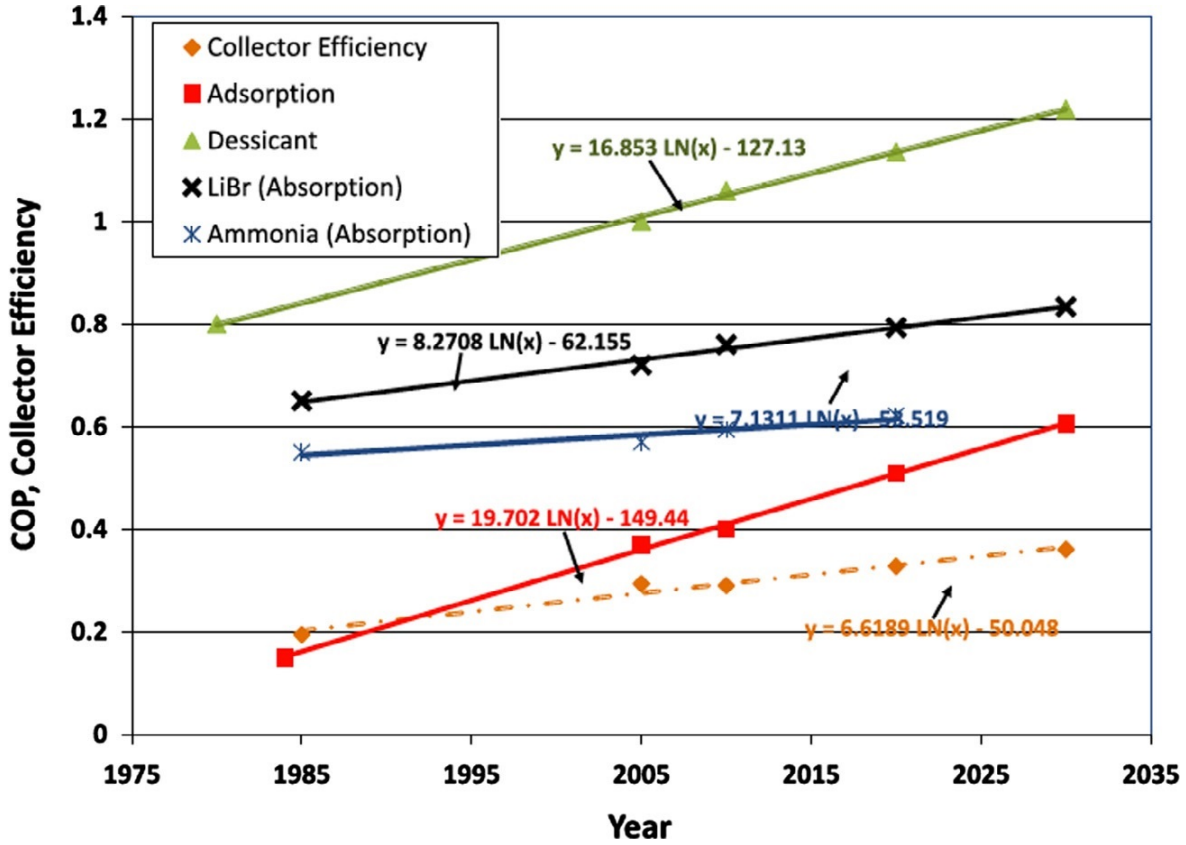

Fig. 6. Current and projected efficiencies for thermal AC and medium temperature ST collectors. Cited from Otanicar et al. [41]

5 Solar hot water systems (SHWS)

5.1 Description

The SHWS heats and cools the buildings through air ventilation. The buildings before the integration of the adsorption chiller were heated and cooled from fan coils powered by a heat pump and an oil boiler. The components added to the SHWS are the solar collectors, the storage tank, the adsorption chiller, the water-to-water heat exchanger, the cooling tower and the water-to-air heat exchanger. TRNSYS doesn't include a water-to-air heat exchanger and thus a cool coil was added instead (indicated as cool coil-2 in the following figures).
The SHWS heats the buildings with a heat coil and cools the buildings with a cool coil. Two components are required because TRNSYS doesn't include a component which can heat and cool during different periods. The adsorption chiller isn't directly connected to the heat coil due to the high flow rate of the cooling water equal to 2.89 kg/s. A water-to-water heat exchanger was introduced between the adsorption chiller and the heat coil to solve the problem of the high cooling water flow rate. The boiler heats the hot water when the solar collectors can't maintain the hot water temperature above 75 °C. The adsorption chiller works with three temperature levels: hot (70 - 95 °C, flow rate equal to 1.28 kg/s), cooling (25 - 45 °C, flow rate equal to 2.89 kg/s) and chilled water (10 - 18 °C, flow rate equal to 0.7 kg/s). A model in TRNSYS can include only one building and thus the flow rates of the cooling water during heating and the chilled water during cooling are divided by two to simulate a system with two buildings. The flow rates of the cooling and chilled water return to their real values through the components called "flowrate cw" and "flowrate chw" respectively. The production of cooling or heating power decreases the hot, increases the cooling and decreases the chilled water temperature.
The SHWS equilibrium requires components which can increase the hot, decrease the cooling and increase the chilled water temperature during both cooling and heating. The operating components during cooling and heating are different. During the cooling period the hot water temperature increases with the solar collectors, the boiler and the storage tank. The cooling water temperature decreases with the cooling tower and the chilled water temperature increases with the cool coil which cools the buildings. During the heating period the hot water temperature increases with the solar collectors, the boiler and the storage tank. The cooling water temperature decreases with the heat coil which heats the buildings and the chilled water temperature increases with the water-to-air heat exchanger. The operating components without cooling or heating demand are the solar collectors, the storage tank and the boiler.
The operating components depend on the control system which is necessary to keep in operation the SHWS during the entire year. The control system, which includes six differential controllers, commands the four divergent valves and send the water flow rates to the proper components.

A real adsorption chiller was investigated by Papoutis [44] who provided the differential equations which define the operation of the adsorption chiller over time. This chiller has a nominal cooling power of 16 kW produced with chilled, cooling and hot water temperature of 12, 30 and 90 °C respectively. This work investigated which utilities could be coupled with this adsorption chiller to exploit it the most efficient way. It was assumed that the proposed adsorption chiller could cool contemporaneously two identical typical Greek units, each with flat area equal to 80 m^2, built in Athens between 1980 and 2011. It was considered that in Greece thermal insulation regulations are applied to buildings built after 1980. Each of these buildings has already installed a fan coil with nominal cooling power equal to 7 kW. Both of the buildings are supplied by an oil boiler with rated capacity of 20 kW. These nominal powers are typical powers installed in Greece during the period 1980-2011. The total nominal cooling power for two building of 14 kW is close to the nominal power of the adsorption chiller. The water-to-water heat exchanger added to the system has a nominal power of 8 kW to match it with the nominal power of the fan coil.
The inputs of the SHWS are the typical meteorological data of Athens, the ground temperature, the design parameters of the adsorption chiller, the initial parameters of the SHWS, the walls and windows characteristics of the buildings, the design parameters of the components and their prices. The outputs of the components are calculated based on the operational curves, which are included in every component of TRNSYS, and the inputs of the components. The outputs of the SHWS are the energy demands of the buildings and the energy required from the boiler which are necessary to calculate the fraction of primary energy savings, the solar fraction during cooling and the PBP.
The inputs and outputs of the SHWS during a typical meteorological year (TMY) are assumed to remain constant every year. The auxiliary energy consumption is assumed to be neglected compared to the energy required from the boiler. The electric consumption and the working pressures of the components are not calculated because TRNSYS doesn't provide a calculation for the electric consumption and the working pressures for all the components. The electric consumption of the fan coils will be calculated from the final thermal energy required for their functioning

Finally, it's assumed that the two buildings are identical with the same energy demands.

5.2 Flowsheets

The SHWS operates in three cases: cooling, heating or without cooling and heating. The SHWS flowsheets for the three cases are represented in the following figures. The collectors water is indicated in orange, the hot water in red, the cooling water in blue, the chilled water in green, the water between the heat exchanger and the heat coil in purple, the heated air in pink

and the cooled air in cyan.

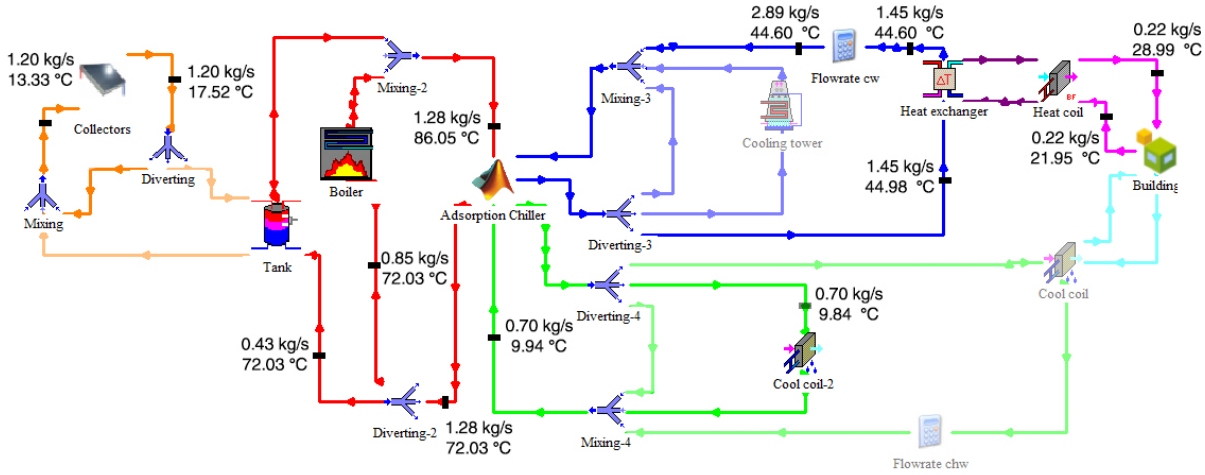

Fig. 7. SHWS during heating, time equal to 1500 h

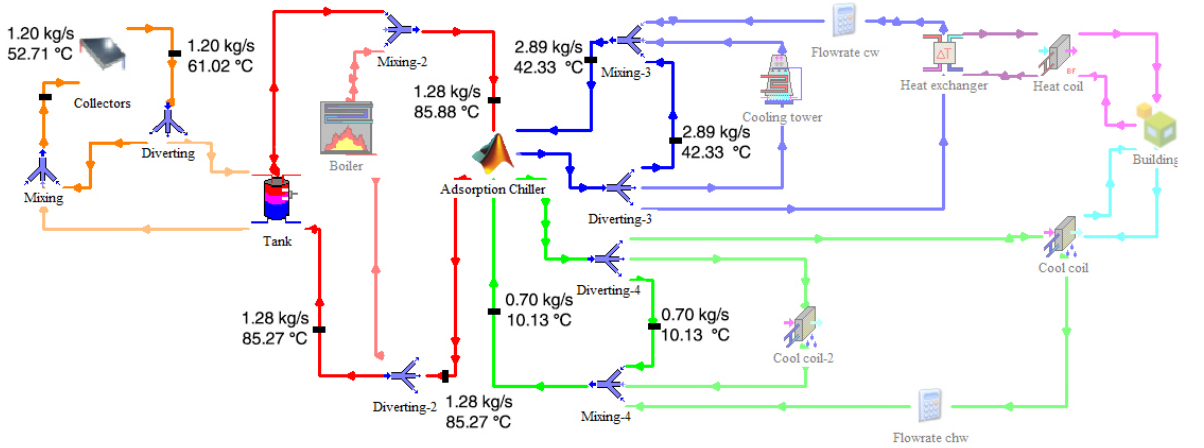

Fig. 8. SHWS without cooling and heating, time equal to 2750 h

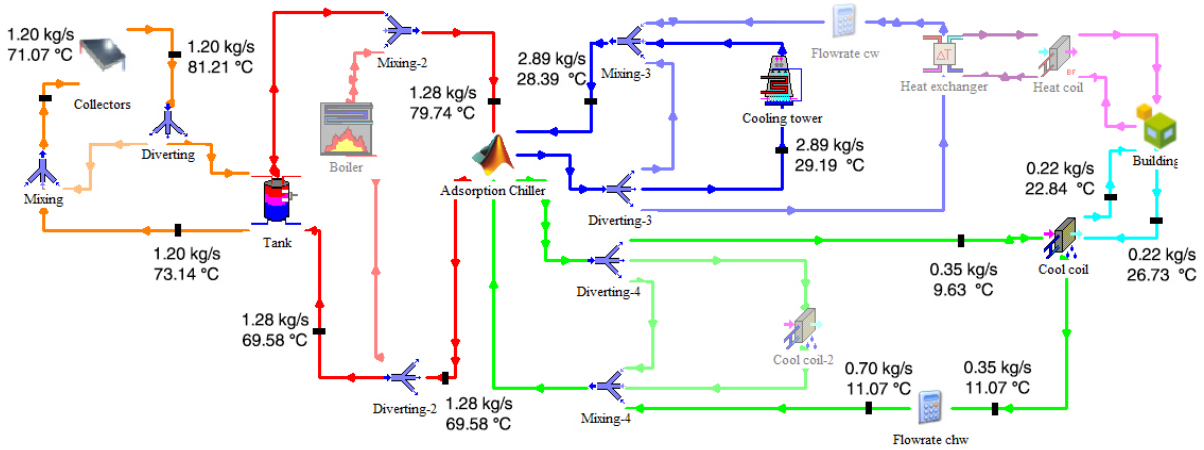

Fig. 9. SHWS during cooling, time equal to 4550 h

6 Method

The method consists in the creation of a dynamic model which simulates the components constituting the SHWS to predict the functioning of the model throughout the year with a time step equal to one hour. The overall system is composed by a dynamical model for the adsorption chiller created in Matlab Simulink and by dynamical model for the SHWS created in TRNSYS. Both of these programs include blocks for the creation of the systems. In Matlab simulnk there are blocks which represent mathematical operations while in TRNSYS the blocks represent different components. The creation of their models consist in the proper connection of the utilized blocks. The simulation of the SHWS, through the dynamic model, under typical meteorological conditions for Athens allows to achieve the objectives defined in the introduction.
Transient conditions occur during cooling due to the thermal inertia of the building structures and dynamic models can calculate their effect. Dynamic models can accurately calculate the energy consumption of a building during cooling which would be different from the results provided by a steady state model. Steady state and dynamic models produce similar results only for the calculation of the energy consumption during heating. A dynamic model represents a system which state evolves over time. The time step of the simulation was set equal to one hour because the weather data has hourly values. The future state of the system depends on the inputs and the present state of the system. These systems are typically represented via differential equations. The dynamic model is zero dimensional and doesn't consider temperature variations over space for the internal air of the buildings and the three water flow rates inside the pipes of the SHWS.

7 Comparison between simulation results of TRNSYS and TEE K.Eν.A.K

The software SketchUp was utilized to create the 3D model of the buildings. The 3D model was loaded in TRNSYS through the type 56 (Multi-Zone Building). TRNSYS was also employed to load the weather data, to create the SHWS and to couple TRNSYS with Matlab Simulink through the type 155 (TRNSYS - Matlab link). The weather data for Athens was taken from the Tess libraries which are integrated in TRNSYS. These libraries also include components like heat and cool coils which are part of the SHWS.
A comparison was done with the software TEE K.Eν.A.K made by TEE (Technical Chamber of Greece) which calculates the final and primary energy demands of a building. The two software gave different results because they have different input values and calculation methods. A simple building was investigated in twenty eight cases and it was found that TRNSYS provided more reasonable results. A dynamic model with only the buildings was executed to calculate the annual energy demands and the power peaks of the buildings without the adsorption chiller. TEE [22] divides the buildings in four zones. The division is based on the degree-day (DD) of the location which goes from lower DD (zone A) to higher DD (zone D). Athens is in the zone B. The buildings can also be divided in three periods based on the year of construction: from 1955 until 1980, from 1980 until 2011 and from 2011 until today. In the years 1955, 1980 and 2011 changes of the construction laws for the layers of the walls were made. It is assumed that the buildings were built in the period from 1980 until 2011. TEE also defines the cooling and heating periods, the design internal temperatures and the internal gains which are defined as boundary conditions for the dynamic model of the buildings.

7.1 Weather data

TEE KENAK's weather data is taken from TEE [23] which lists, for different Greek locations, the average monthly values for the: maximum, minimum and medium air temperature, air humidity, wind velocity and solar total horizontal irradiation. The weather data in TRNSYS uses hourly values. The following figure shows the difference between TEE K.Eν.A.K and TRNSYS for the external air temperature.

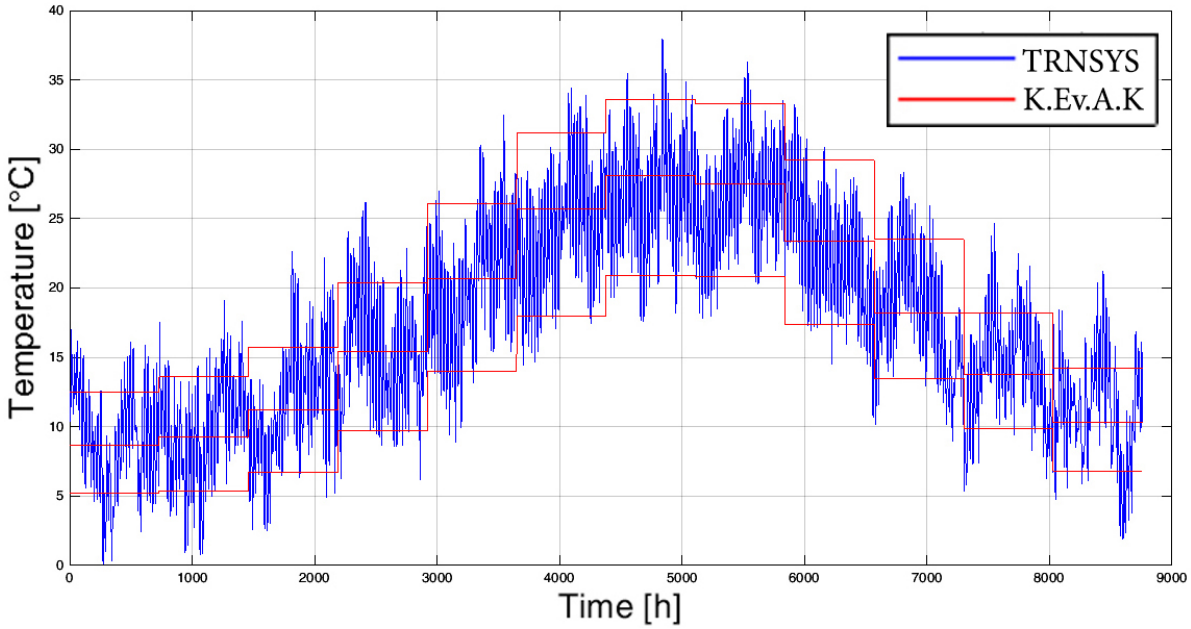

Fig. 10. External air temperature of TRNSYS and TEE K.Eν.A.K indicated in blue and red respectively

7.2 Ground temperature data

TEE K.Eν.A.K calculates the ground temperature based on the following equation:

$$T_{grd}(z,t) = T_m - A_s * \exp\left(-z * \frac{\pi}{365 * \alpha}\right)^{1/2} * cos\left[\left(\frac{2\pi}{365}\right) * \left(t - t_0 - \frac{z}{2} * \left(\frac{365}{\pi * \alpha}\right)^{1/2}\right)\right] \quad (1)$$

where:

- z in [m] is the depth of the calculation
- t is day of the year
- $T_{grd}(z,t)$ in [°C] is the ground temperature
- T_m in [°C] is the average yearly surface temperature. Assumed equal to the yearly average external air temperature
- A_s in [°C] is the width of the yearly ground temperature fluctuation, equal to (Tm_{max}-Tm_{mead})$*$ 2 where Tm_{max} is the maximum average temperature and Tm_{mead} is the average medium temperature of the location
- α in [m^2/day] is the coefficient of the thermal diffusion of the ground, equal to 0.06 m^2/day for Athens
- t_0 is the day of the year with the lowest ground temperature, equal to 30 for Athens

The ground temperature calculation for the SHWS is provided by RSE (Ricerca Sistema Energetico) [14]. The requested inputs are the hourly values of the external air temperature, the

total horizontal irradiation and the thermal ground properties of Athens. The thermal ground properties are:

- Conductivity equal to 1.8 $W/(mK)$
- Capacity equal to 0.836 $kJ/(kgK)$
- Density equal to 1800 kg/m^3

The following figure shows the yearly ground temperature calculated at four depths.

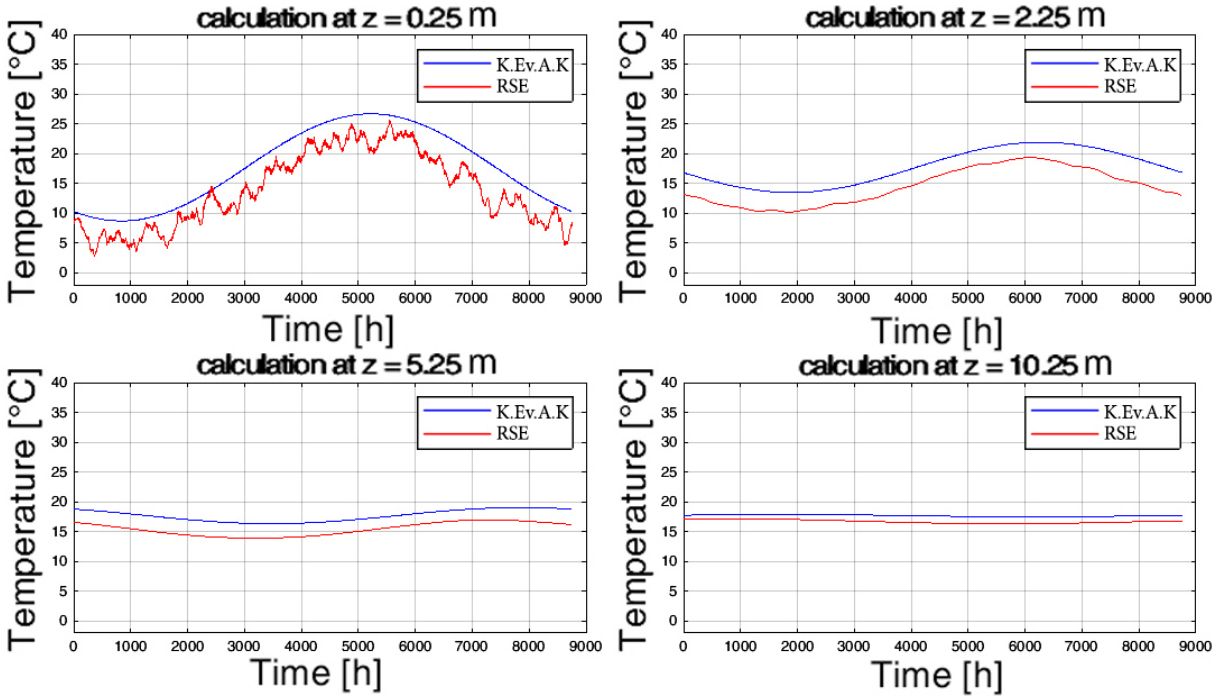

Fig. 11. Variation of the ground temperature calculated at four depths. The calculations with RSE and TEE K.Ev.A.K are indicated in red and blue respectively

The two methods gave similar results for depth greater than 6 m. The depth at which the ground temperature is calculated can affect the energy demands of the buildings. The floor will be adjacent to a heating surface in the winter and to a cooling surface in the summer if the ground temperature is calculated at a high depth. The floor will be adjacent to a surface with high temperatures in the summer if the ground temperature is calculated at a low depth and hence a good compromise is to calculate the ground temperature at a depth of 2 m.

7.3 Simulation of a simple building

The characteristics of the simple building are:

- Walls with U value of 0.7 $W/(m^2K)$, dimensions of 30 m^2 with orientations towards S,W,E,N
- Solar absorptance equal to 0.4 for the walls and the floor and 0.6 for the roof

- Longwave emission coefficient equal to 0.9 for all the surfaces
- Roof with U value of 0.5 $W/(m^2K)$, dimension of 100 m^2
- Floor with U value of 1 $W/(m^2K)$, dimension of 100 m^2 in contact of the ground
- Heating working from 6:00 until 24:00 and when the internal temperature goes bellow 20 °C
- Period of heating: 1/11 - 15/4
- Cooling working from 6:00 until 24:00 and when the internal temperature goes above 26 °C
- Period of cooling: 15/5 - 15/9
- Internal gains equal to 4.5 $W/(m^2)$
- Infiltration of air equal to 0.333 V/h
- Thermal capacitance equal to 150 $kJ/(m^2K)$
- Volume of the building equal to 300 m^3
- Window with U_{glass} of 5.68 $W/(m^2K)$, g_{glass} of 0.855, dimensions of 5 m^2 with orientation towards S

The energy demands of the two software were calculated for twenty eight cases. An ”open” surface has the U value mention above while a ”closed” one has an U value equal to 0.001 $W/(m^2K)$. The case studies were:
- Surface with orientation towards S open and all other surfaces closed
- Surface with orientation towards N open and all other surfaces closed
- Surface with orientation towards E open and all other surfaces closed
- Surface with orientation towards W open and all other surfaces closed
- Roof open and all other surfaces closed
- Floor open and all other surfaces closed
- All surfaces open

The cases were investigated under different conditions with:
1) Solar absorptance of walls equal to 0.001 and longwave emission coefficient equal to 0.001
2) Solar absorptance of walls and longwave emission coefficient as mentioned in the characteristics
3) Solar absorptance of walls and longwave emission coefficient as mentioned in the characteristics and air infiltration
4) Solar absorptance of walls and longwave emission coefficient as mentioned in the characteristics, infiltration and a window towards S

The results for the heating and cooling demands calculated with TEE K.Eν.A.K and TRNSYS are shown in the following tables:

TEE K.Eν.A.K	1		2		3		4	
Cases	Heating	Cooling	Heating	Cooling	Heating	Cooling	Heating	Cooling
S	3.9	14.4	3.1	15.5	12.5	15.5	2.3	32.3
N	3.9	14.4	3.8	15.1	13.5	15.2	8.3	30
E	3.9	14.4	3.6	15.8	13.1	15.8	8.1	30.7
W	3.9	14.4	3.6	15.8	13.1	15.8	8.1	30.7
R	11.9	14.6	9.4	22.7	19.4	22.8	6.6	39.6
F	0.2	14.5	0.2	14.5	7.1	14.4	3.9	29.4
ALL	39.8	16.1	33.5	27.7	43.9	28.2	34.7	42.8

Table 1. Annual heating and cooling demands calculated with TEE K.Eν.A.K in $kWh/(m^2y)$

TRNSYS	1		2		3		4	
Cases	Heating	Cooling	Heating	Cooling	Heating	Cooling	Heating	Cooling
SW	0.00	12.74	0.00	11.75	3.58	10.94	3.99	18.30
NW	0.00	12.74	0.00	11.34	4.17	10.55	5.27	17.67
EW	0.00	12.74	0.00	11.92	3.98	11.12	5.12	18.22
WW	0.00	12.74	0.00	11.94	3.96	11.12	5.10	18.22
R	2.41	11.97	2.63	16.62	11.92	15.78	12.06	22.76
F	0.82	1.37	0.86	1.35	9.41	12.69	9.23	14.86
ALL	41.88	19.55	44.97	24.77	55.60	27.46	41.63	39.50

Table 2. Annual heating and cooling demands calculated with TRNSYS in $kWh/(m^2y)$

TEE K.Eν.A.K and TRNSYS provided different results. The internal gains added in TRNSYS and TEE K.Eν.A.K are similar because they have similar cooling demands. The cooling demand calculated with TEE K.Eν.A.K remains constant when the floor is the only open surface while for the same case the cooling demand calculated with TRNSYS drops drastically. The maximum ground temperature during the heating period is equal to 20 °C end thus the floor represents a cooling surface which reduces the cooling demand. The energy demands of the two software increase and decrease similarly. The fact that TRNSYS has hourly and TEE K.Eν.A.K monthly values for the weather data and that TRNSYS consider the mutual irradiation between the internal surfaces are the reasons of the difference between the results of two software. It can be concluded that TRNSYS gives more reasonable results.

8 Modeling of the SHWS

8.1 Buildings

8.1.1 Boundary conditions

The boundary conditions of the buildings are:
- Solar absorptance equal to 0.4 for the walls and the floor and 0.6 for the roof
- Longwave emission coefficient equal to 0.9 for all the surfaces
- Heating working from 6:00 until 24:00 and when the internal temperature goes bellow 20 °C
- Period for heating: 1/11 - 15/4
- Cooling working from 6:00 until 24:00 and when the internal temperature goes above 26 °C
- Period for cooling: 15/5 - 15/9
- Internal gains equal to 4.5 $W/(m^2)$

8.1.2 Geometry

Every building can be divided in two zones: the ground floor and the basement. Both of these zones have a surface of 80 m^2 and height equal to 3.13 m. The basement is in contact with the ground from the floor and its internal walls. From these two zones only the ground floor is heated and cooled and hence the total energy demands correspond to the energy demands of this zone. Shadings have also been added for the south and east orientations.

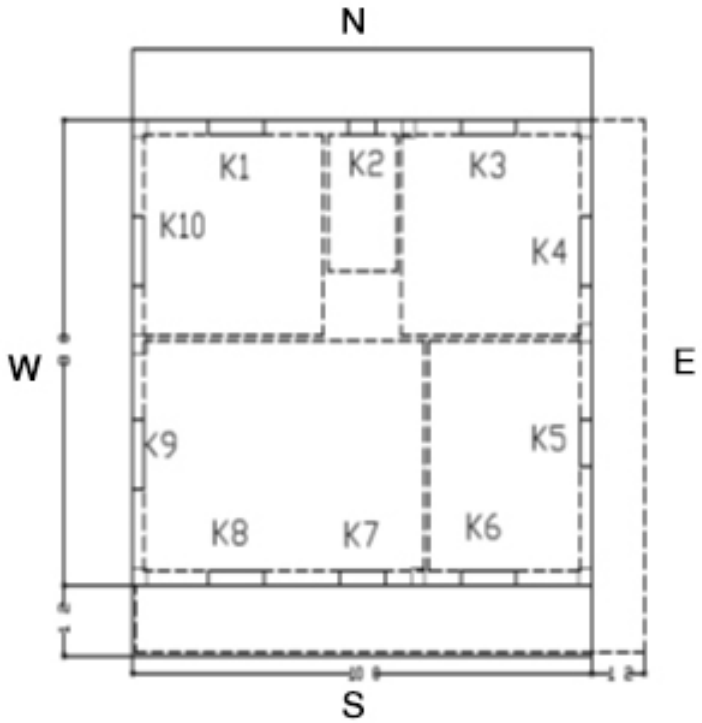

Fig. 12. Sketch of the typical building

The values from K1 to K10 represent the windows. In the following table are listed the characteristics of each window.

	Window			Glass			Frame	U	g	Infiltration
	Width	height	Area	Width	height	Area	Area	window	window	V_{inf}
	m	m	m^2	m	m	m^2	m^2	$W/(m^2K)$	(–)	m^3/h
K1	1.4	1.2	1.68	0.5	1	1	0.68	4.571	0.4	11.42
K2	0.6	0.6	0.36	0.4	0.4	0.16	0.2	5.222	0.3	2.45
K3	1.4	2.2	3.08	0.5	2	2	1.08	4.338	0.44	16.32
K4	1.4	1.2	1.68	0.5	1	1	0.68	4.571	0.4	11.42
K5	0.9	2.2	1.98	0.7	2	1.4	0.58	4.085	0.48	10.49
K6	1.4	1.2	1.68	0.5	1	1	0.68	4.571	0.4	11.42
K8	1.4	2.2	3.08	0.5	2	2	1.08	4.338	0.44	16.32
K9	1.4	1.2	1.68	0.5	1	1	0.68	4.571	0.4	11.42
K10	1.4	2.2	3.08	0.5	2	2	1.08	4.338	0.44	16.32

Table 3. Characteristics of the windows of the buildings

The typical building was modeled in SketchUp 2018. In the following figure it seems that the building is composed of two floors. The upper floor represents the ground floor and the lower floor the basement which walls were switched from external to boundary in contact with the ground.

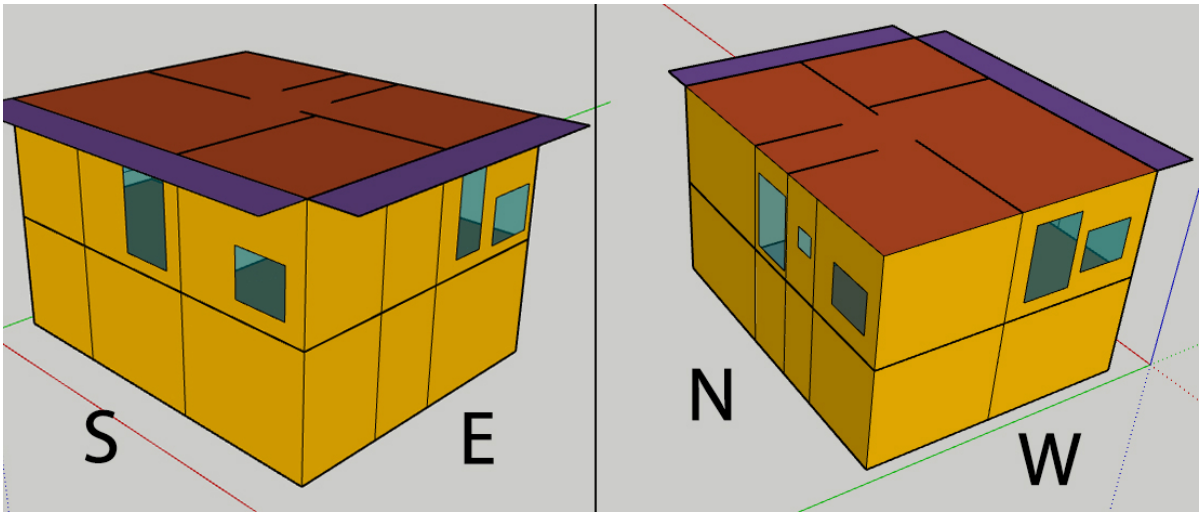

Fig. 13. 3D SketchUp model of the typical building

8.1.3 Energy demands and power peaks

In the following figure is shown the model in TRNSYS which was automatically generated by loading the SketchUp file.

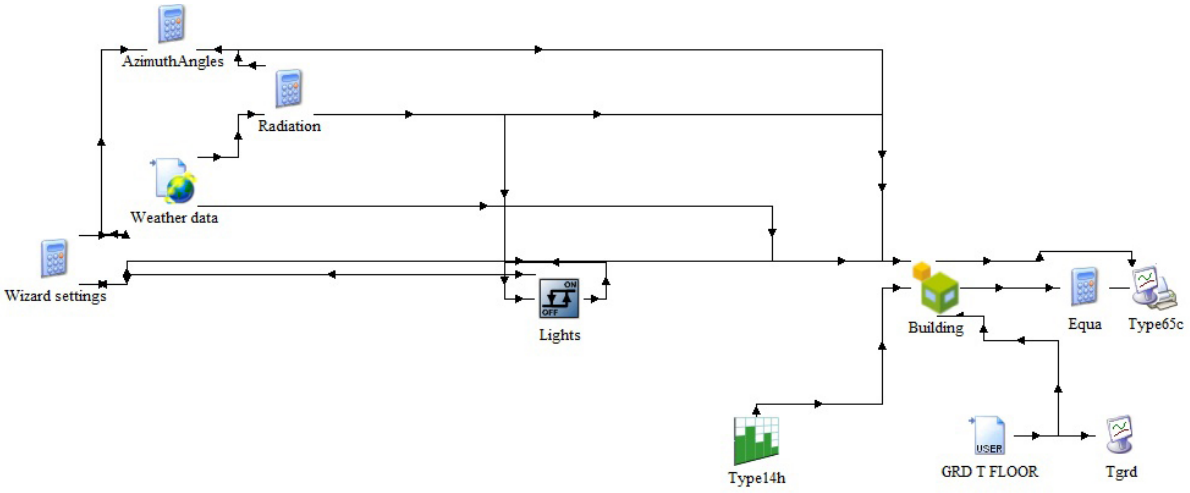

Fig. 14. TRNSYS model of the buildings without the adsorption chiller

The results for the cooling and heating demands and the internal air temperature are:

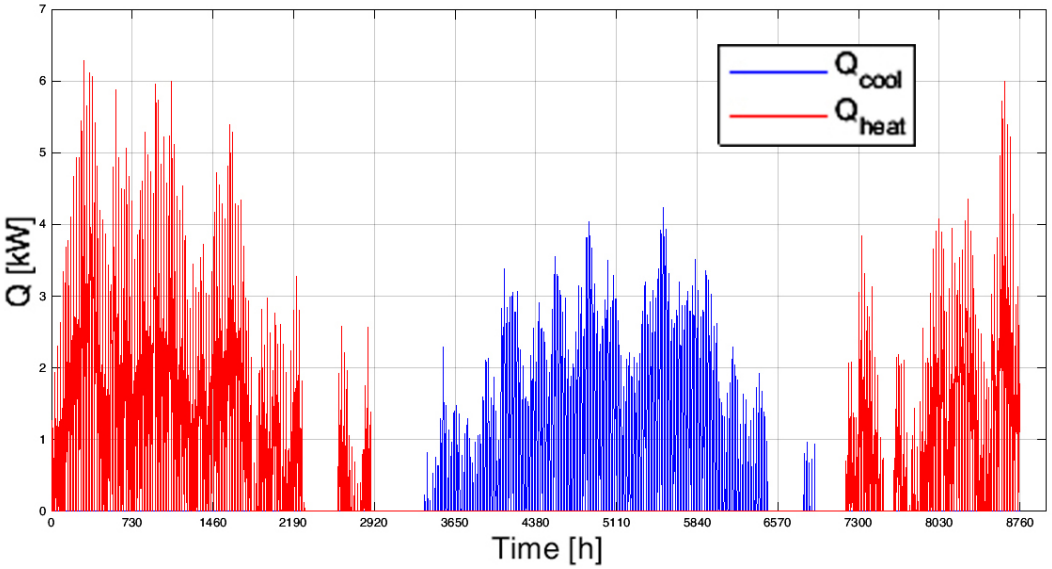

Fig. 15. Heating and cooling demands of the buildings in [kW]

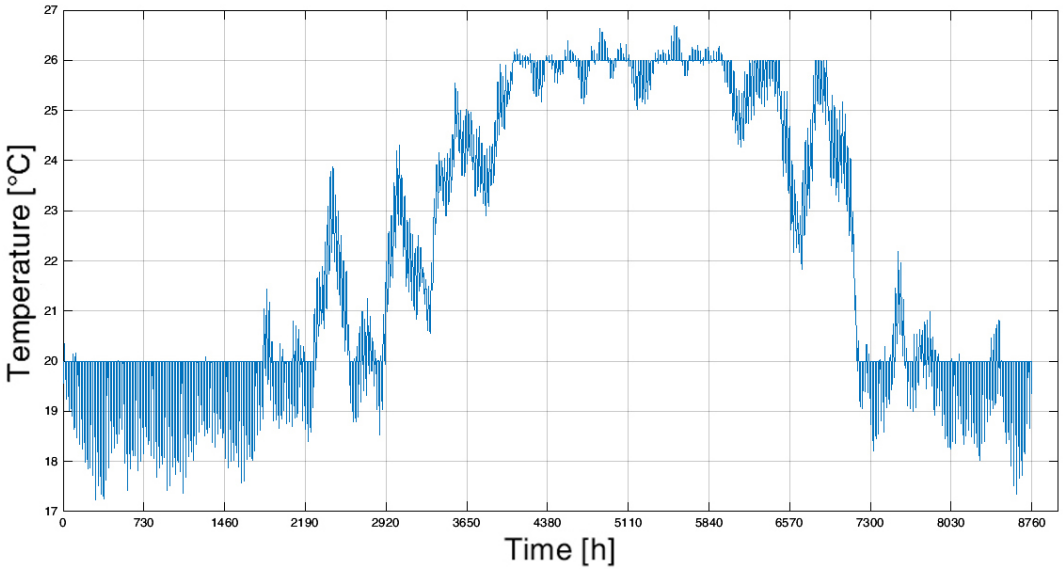

Fig. 16. Internal temperature of the buildings in [°C]

The annual energy demands and the power peaks of the buildings are:

- Cooling demand equal to 34.77 $kWh/(m^2y)$
- Heating demand equal to 60.02 $kWh/(m^2y)$
- Cooling peak power equal to 4.23 kW
- Heating peak power equal to 6.29 kW

8.2 Adsorption chiller

Matlab Simulink was utilized to create the dynamic model of the adsorption chiller, to find the initial values needed as inputs for the model which guarantee a proper function of the adsorption chiller, to calculate the optimal time variables of the adsorption chiller and to reduce the calculation time through a tri-linear interpolation.

An iterative method was implemented to guarantee a proper functioning of the adsorption chiller because some of its design parameters are affected from the temperature. The adsoprtion chiller produce the maximum cooling or heating power with a switching time of 20 s and cycle time of 800 s. The tri-linear interpolation reduced the calculation time from 6 days to 5 minutes with a maximum error of 1 % compared with the detailed calculation. It was found that not all the temperature pairs of the water are possible working points.

8.2.1 Functioning

The adsorption chiller is composed of four components: the condenser the evaporator and the two adsorption beds which contain the silica gel. Water is the refrigerant and silica gel the adsorbent. There is a connection between the condenser and the evaporator from where worm

condensate is allowed to flow back to the evaporator through a pressure reduction valve.
This cycle works with three levels of temperature: hot (hw), cooling (cw) and chilled (chw) water. When a bed is cooled by the cooling water the adsorption process starts and steam from the evaporator is adsorbed by the cool bed. The adsorption process is exothermic and heat has to be extracted by the cooling water. The other bed is heated by the hot water, the desorption process starts and steam from the bed is rejected to the condenser. The desorption process is endothermic and heat is provided by the hot water. While the adsorption process proceeds the silica gel gets saturated, when it's completely saturated the cooling and hot water supply are switched. The switching isn't instantaneous because the connection of the regenerated hot bed with the evaporator would desorb the adsorbed refrigerant and this would reduce the cooling power. A certain time (called switching time) is needed in order for the cool bed to heat up and for the hot bed to cool down. The premature connection of the saturated cool bed with the condenser doesn't reduce the pressure of the condenser because the condensate in the condenser evaporates and the pressure is maintained.

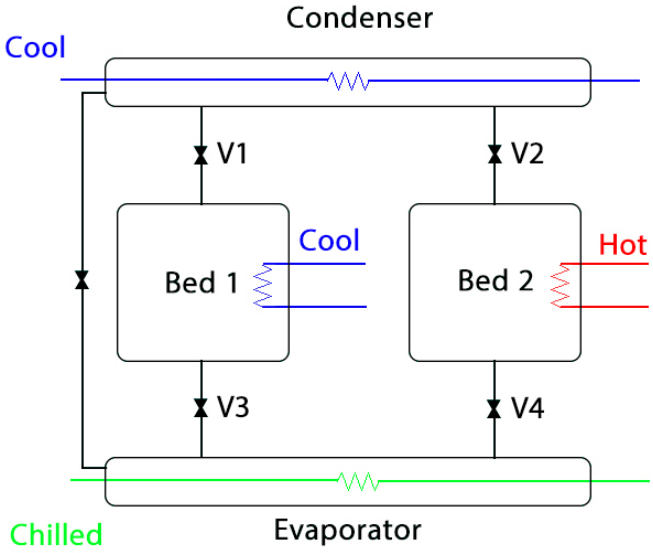

Fig. 17. Simplified representation of the adsorption chiller

The cycle is divided in four phases: A, B, C and D.
- Phase A: the valves V1, V2, V3 and V4 are closed for a time period called $time_A$ (switching time), this is the phase needed for the beds to reach the desired temperatures.
- Phase B: the valves V1 and V4 are closed for a time period called $time_B$ (half cycle time), in this phase cooling or heating power is produced in the evaporator or in the condenser respectively. When the cool bed is completely saturated the valves close and the cooling and hot water supply are switched.
- Phase C: the valves V1, V2, V3 and V4 are closed for the same period as for phase A, this is

the phase needed for the cool bed to heat up and for the hot bed to cool down.
- Phase D: the valves V2 and V3 are closed for the same period as for phase B, in this phase cooling or heating power is produced in the evaporator or in the condenser respectively.

8.2.2 Model equations

The adsorption chiller was modeled in Matlab Simulink. The differential equations of the system were provided by the PhD thesis of Papoutsis [44]. These equations included a parameter ϕ which is equal to 1 for the phases B and D and is equal to 0 for the phases A and C. The design parameters of the adsorption model are:

Parameter	Value	Unit	Parameter	Value	Unit
U_bA_b	4241.38	W/K	D_{s0}	$2.54 * 10^{-4}$	m^2/s
U_cA_c	15349.8	W/K	R_w	8.314	J/mol K
U_eA_e	4884.9	W/K	R_p	$1.74 * 10^{-4}$	m
W_{c_cu}	24.28	kg	Q_{st}	$2.8 * 10^6$	J/kg
W_{e_cu}	12.28	kg	L	$2.5 * 10^6$	J/kg
W_s	35	kg	E_a	$4.2 * 10^4$	J/kg
W_{b_cu}	51.2	kg	$\dot{m}_{chw}$	0.7	kg/s
W_{c_w}	20	kg	$\dot{m}_{cw\_b}$	1.52	kg/s
cp_w	4186	J/kgK	$\dot{m}_{cw\_c}$	1.37	kg/s
cp_s	924	J/kgK	$\dot{m}_{hw}$	1.28	kg/s
cp_{cu}	386	J/kgK			

Table 4. Design parameters of the Adsorption model

The equations implemented in Matlab Simulink are the following:
- Equations for the kinetics of the adsorption beds:

$$\frac{dq}{dt} = \frac{15 * D_s}{R_p^2} * (q^* - q) \tag{2}$$

where:

$$D_s = D_{s0} * \exp\left(-\frac{E_a}{R * T}\right) \tag{3}$$

$$q^* = A(T_b) * \left(\frac{P_s(T_w)}{P_s(T_b)}\right)^{B(T_b)} \tag{4}$$

$$A(Tb) = A0 + A1 * T_b + A2 * T_b^2 + A3 * T_b^3 \tag{5}$$

$$B(Tb) = B0 + B1 * T_b + B2 * T_b^2 + B3 * T_b^3 \tag{6}$$

Parameter	Value	Unit	Parameter	Value	Unit
A0	-6.5314	kg/kg	B0	-15.857	-
A1	0.072452	kg/(kg K)	B1	0.15915	K^{-1}
A2	$-0.23951 * 10^{-3}$	$kg/(kgK^2)$	B2	$-0.50612 * 10^{-3}$	K^{-2}
A3	$0.25493 * 10^{-6}$	$kg/(kgK^3)$	B3	$0.5329 * 10^{-6}$	K^{-3}

Table 5. Coefficients of the equations 4 and 5. Cited from H.T. Chua [17]

For the adsorption process $T_b = T_a$ and $T_w = T_e$ while for the desorption process $T_b = T_d$ and $T_w = T_c$.

- Equations for the adsorption beds:

$$\Big(W_s * C_{ps} + W_s * q_a * c_{pw} + W_{b\_cu} * c_{pw}\Big) * \frac{dT_a}{dt} = \phi * Q_{st} * W_s * \frac{dq_a}{dt} + \phi * W_s * c_{pv} * \frac{dq_a}{dt} * \Big(T_e - T_a\Big) + \\ + \dot{m}_{cw\_b} * c_{pw} * (T_{cw\_in} - T_{cw\_b\_out}) \tag{7}$$

$$T_{cw\_b\_out} = T_a + (T_{cw\_in} - T_a) * \exp\Big(-\frac{U_b A_b}{\dot{m}_{cw\_b} * c_{pw}}\Big) \tag{8}$$

$$\Big(W_s * C_{ps} + W_s * q_d * c_{pw} + W_{b\_cu} * c_{pw}\Big) * \frac{dT_d}{dt} = \phi * Q_{st} * W_s * \frac{dq_d}{dt} + \\ + \dot{m}_{hw\_b} * c_{pw} * (T_{hw\_in} - T_{hw\_b\_out}) \tag{9}$$

$$T_{hw\_out} = T_d + (T_{hw\_in} - T_d) * \exp\Big(-\frac{U_b A_b}{\dot{m}_{hw} * c_{pw}}\Big) \tag{10}$$

- Equations for the condenser:

$$\Big(W_{c\_cu} * cp_{cu} + W_{c\_cu} * c_{pw}\Big) * \frac{dT_c}{dt} = -\phi * L * W_s * \frac{dq_d}{dt} - \phi * W_s * c_{pv} * \frac{dq_d}{dt} * \Big(T_d - T_c\Big) + \\ + \dot{m}_{cw\_c} * c_{pw} * (T_{cw\_in} - T_{cw\_c\_out}) \tag{11}$$

$$T_{cw\_c\_out} = T_c + (T_{cw\_in} - T_c) * \exp\Big(-\frac{U_c A_c}{\dot{m}_{cw\_c} * c_{pw}}\Big) \tag{12}$$

- Equations for the evaporator:

$$\Big(W_{e\_cu} * cp_{cu} + W_{e\_cu} * c_{pw}\Big) * \frac{dT_e}{dt} = -\phi * L * W_s * \frac{dq_a}{dt} - \phi * W_s * c_{pv} * \frac{dq_d}{dt} * \Big(T_c - T_e\Big) + \\ + \dot{m}_{chw\_c} * c_{pw} * (T_{chw\_in} - T_{chw\_out}) \tag{13}$$

$$T_{chw\_out} = T_e + (T_{chw\_in} - T_e) * \exp\left(-\frac{U_e A_e}{\dot{m}_{chw\_c} * c_{pw}}\right) \tag{14}$$

- Mass balance equations:

$$\frac{dW_{e\_w}}{dt} = -W_s * \left(\frac{dq_a}{dt} + \frac{dq_d}{dt}\right) \tag{15}$$

- Calculation of the power of the components and the cooling and heating COP:

$$Q_e = \frac{\int_0^{2*time_B} \dot{m}_{chw} * c_{pw} * (T_{chw\_in} - T_{chw\_out})dt}{2 * time_B} \tag{16}$$

$$Q_{des} = \frac{\int_0^{2*time_B} \dot{m}_{hw} * c_{pw} * (T_{hw\_in} - T_{hw\_out})dt}{2 * time_B} \tag{17}$$

$$Q_c = \frac{\int_0^{2*time_B} \dot{m}_{cw} * c_{pw} * (T_{cw\_c\_out} - T_{cw\_in})dt}{2 * time_B} \tag{18}$$

$$Q_{ads} = \frac{\int_0^{2*time_B} \dot{m}_{cw\_b} * c_{pw} * (T_{cw\_b\_out} - T_{cw\_in})dt}{2 * time_B} \tag{19}$$

$$COP_c = \frac{Q_e}{Q_{des}} \tag{20}$$

$$COP_h = \frac{Q_c + Q_{ads}}{Q_{des}} \tag{21}$$

The following figure shows the adsorption cycle on a Clapeyron diagram:

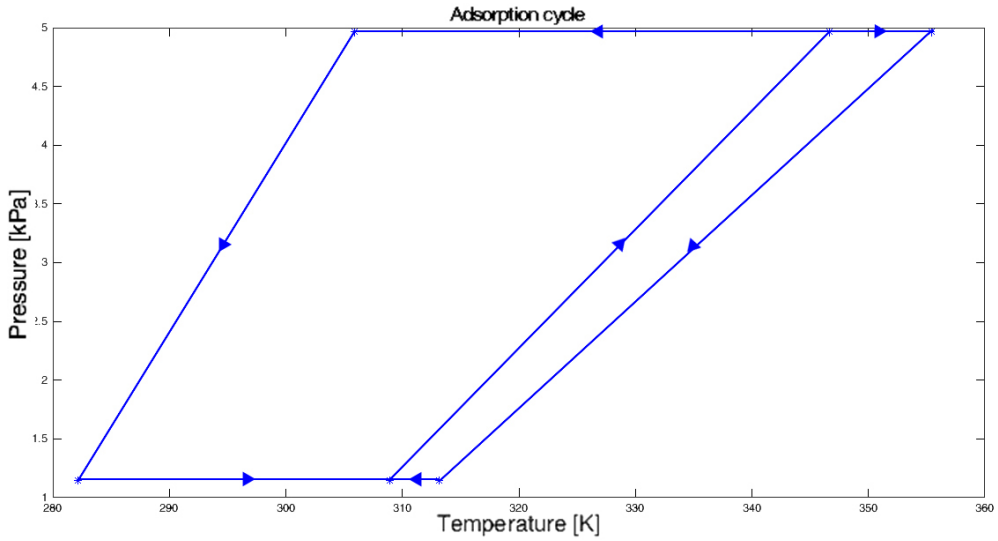

Fig. 18. Adsorption cycle on Clapeyron diagram with $time_A$ = 45 s, $time_B$ = 450 s, Thw_in = 85.7 °C, Tcw_in = 31.1°C and Tchw_in = 14.8°C

8.2.3 Initial values in the simulation of the operation

The dynamic model of the adsorption chiller requires to fix the values: T_{a0}, T_{e0}, T_{c0}, T_{d0}, W_{e_w}, q_{a0} and q_{d0}. The dynamic model is executed two times but the cooling and heating power are calculated only in the second run to eliminate the noise due to the influence of the initial values. The initial values of the temperatures and water mass in the condenser are fixed as:

- $T_{e0} = T_{chw\_in}$ K
- $T_{c0} = T_{cw\_in} + 5$ K
- $T_{d0} = T_{cw\_in} + 5$ K
- $T_{a0} = T_{hw\_in} - 5$ K
- $W_{e\_w} = 50$ kg

The design values of Table 4 are set for a steady state system with constant temperatures of the hot, cooling and chilled water. In order to evaluate the performance of the adsorption chiller in a dynamical simulation, it has to be considered that the activation energy of surface diffusion (E_a), the pre-exponent constant (D_{s0}) and the initial fractions of the silica gel in the beds (q_d0 and q_a0) vary with the temperature. The concentration of the silica gel which is adsorbed or desorbed remains constant for the phase A and C. For the phases B and D, the value of the final concentration of the silica gel which was adsorbed or desorbed has to be equal to the initial value of the concentration of the silica gel which was desorbed or adsorbed.
An iterative equation was implemented which changes the concentration of the silica gel in the two beds. Initially the contents of the two beds are equal to 0.1 kg_w/kg_s. At the end of the simulation the final values of the contents which were adsorbed or desorbed are set equal to the initial values of the contents that will be desorbed or adsorbed during the next simulation. This equation is repeated until the difference between the initial and final values is lower than 1 %.

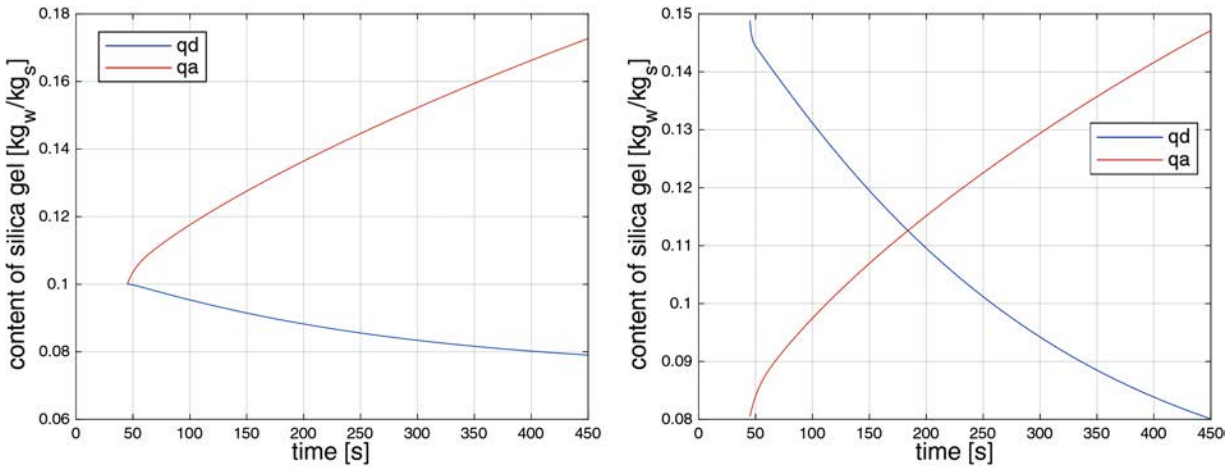

Fig. 19. First and last calculation of q_d and q_a with Tchw_in = 14.8 °C, Tcw_in = 31.1 °C and Thw_in = 85.7 °C

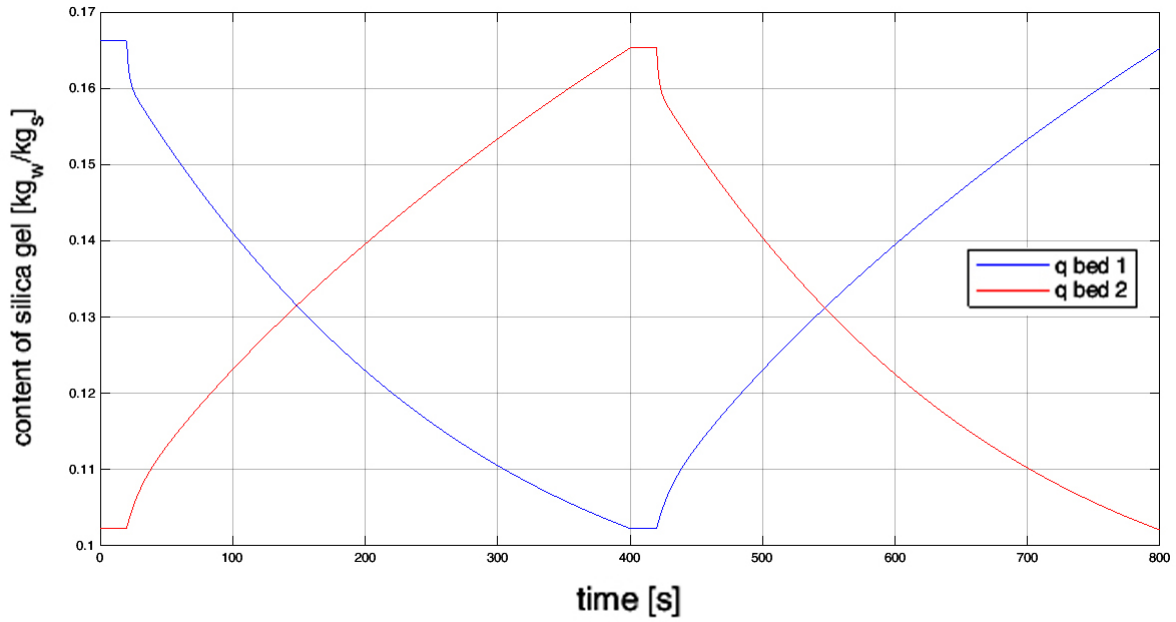

Fig. 20. Complete cycle for q_d and q_a with Tchw_in = 10 °C, Tcw_in = 25 °C and Thw_in = 70 °C

This method gives reasonable results by taking into consideration that E_a, D_{s0}, q_d and q_a change with the temperature but it doesn't represent what really happens in the beds. This iterative equation is executed before starting the Simulink model.

8.2.4 Optimization of the operation

The switching time has to be evaluated correctly, if it's too short then the beds are not cooled or heated enough while if too long the cooling power is reduced and hence an optimal value of the switching time may exist.

Also, the cycle time has to be considered. Long cycle time increase the COP but reduce the cooling power, while low cycle time reduces both the cooling power and the COP. By executing the model for $time_A$ = 20:10:70 and $time_B$ = 300:50:700 it was found that the pair with $time_A$ = 20 s and $time_B$ = 400 s allows to maximize the cooling or heating power.

The model of the adsorption chiller works in the same way during the cooling and heating periods which absorbs heat from one environment and rejects heat to another one. The total heating power (Q_h) is given by the sum of the heating power produced by the adsorber and the condenser while the cooling power is equal to the power produced in the evaporator (Q_e).

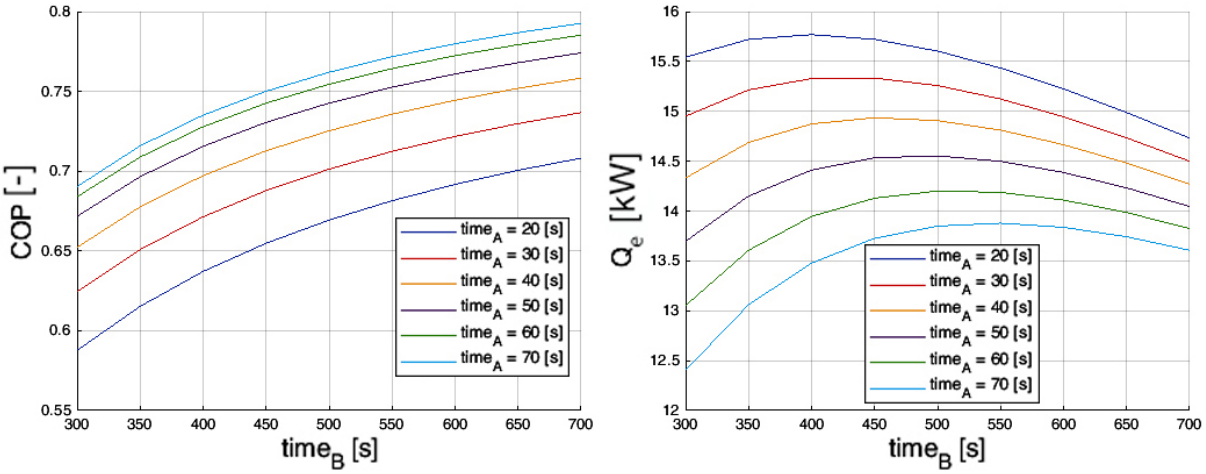

Fig. 21. Variation of COP and Q_e for different values of $time_A$ and $time_B$

From the three levels of temperatures, the cooling one has the greatest effect on the COP and the cooling power. In the following figure it's shown the variation of the COP for different hot and cooling water temperatures and chilled water temperature equal to 14 °C.

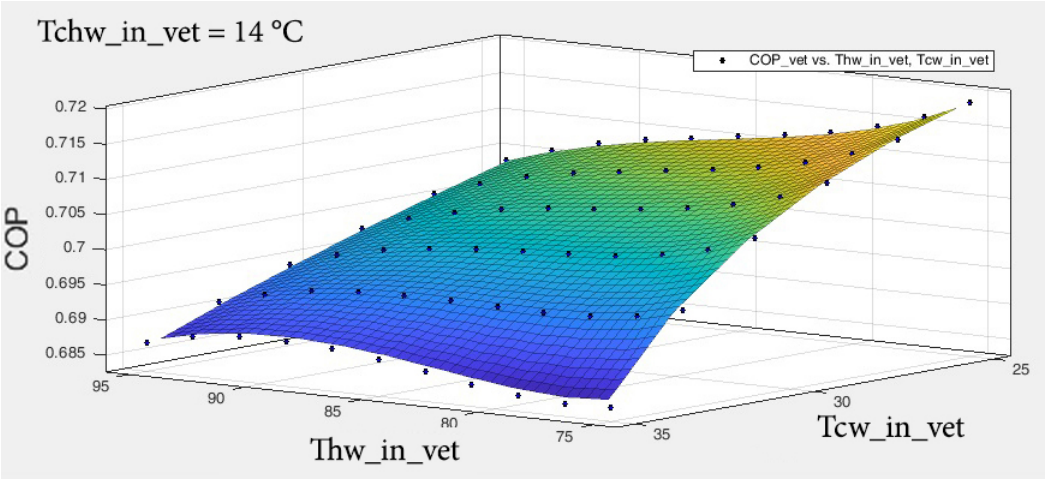

Fig. 22. COP as function of the hot and cool water

By decreasing the cool water from 35 to 25 °C the COP increases from 0.685 to 0.72 while the COP remains almost constant for different hot water temperatures which suggests investing in a good cooling tower to achieve higher COP values. The outlet temperature from the cooling tower is limited by the wet bulb temperature which was set equal to 27.8 °C.

8.2.5 Reduction of the computational time in the optimization of the operation

The method proposed by R. Wagner [51] was implemented to evaluate the value $V(x, y, z)$ for a generic point P = (x_p,y_p,z_p)

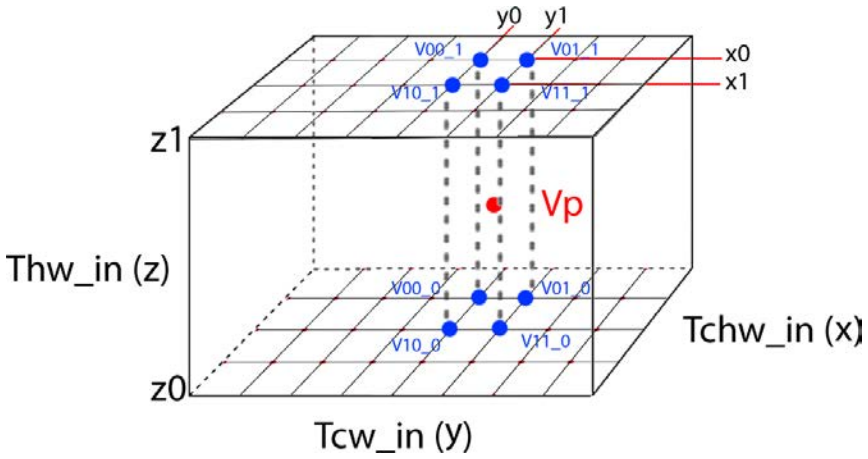

Fig. 23. Scheme of the tri-linear interpolation method

The values x_0 and x_1 are temperatures that belong to $Tchw\_in$, the values y_0 and y_1 are temperatures that belong to Tcw_in and the values z_0 and z_1 are temperatures that belong to Thw_in where:

- $x_0 < x_p < x_1$
- $y_0 < y_p < y_1$
- $z_0 < z_p < z_1$

The evaluation of $V_p(x_p, y_p, z_p)$ requires to calculate the coefficients a, b, c, d, e, f, g, h and to load the values: $V00_0$, $V01_0$, $V10_0$ and $V11_0$, $V00_1$, $V01_1$, $V10_1$ and $V11_1$ from the tables 18 through 29 listed in the appendix.

$$a = \frac{(x_1 - x_p) * (y_1 - y_p) * (z_p - z_0)}{(x_1 - x_0) * (y_1 - y_0) * (z_1 - z_0)} \tag{22}$$

$$b = \frac{(x_1 - x_p) * (y_p - y_0) * (z_p - z_0)}{(x_1 - x_0) * (y_1 - y_0) * (z_1 - z_0)} \tag{23}$$

$$c = \frac{(x_p - x_0) * (y_1 - y_p) * (z_p - z_0)}{(x_1 - x_0) * (y_1 - y_0) * (z_1 - z_0)} \tag{24}$$

$$d = \frac{(x_p - x_0) * (y_p - y_0) * (z_p - z_0)}{(x_1 - x_0) * (y_1 - y_0) * (z_1 - z_0)} \tag{25}$$

$$e = \frac{(x_1 - x_p) * (y_1 - y_p) * (z_1 - z_p)}{(x_1 - x_0) * (y_1 - y_0) * (z_1 - z_0)} \tag{26}$$

$$f = \frac{(x_1 - x_p) * (y_p - y_0) * (z_1 - z_p)}{(x_1 - x_0) * (y_1 - y_0) * (z_1 - z_0)} \tag{27}$$

$$g = \frac{(x_p - x_0) * (y_1 - y_p) * (z_1 - z_p)}{(x_1 - x_0) * (y_1 - y_0) * (z_1 - z_0)} \tag{28}$$

$$h = \frac{(x_p - x_0) * (y_p - y_0) * (z_1 - z_p)}{(x_1 - x_0) * (y_1 - y_0) * (z_1 - z_0)} \tag{29}$$

$$V_p(x_p, y_p, z_p) = V00_1 * a + V01_1 * b + V10_1 * c + V11_1 * d + V00_0 * e + V01_0 * f + V10_0 * g + V11_0 * h \quad (30)$$

The tri-linear interpolation is necessary due to time issues. To evaluate with the detailed method the heating and cooling power for every hour of the year the adsorption model requires six days to terminate the calculations. The tri-linear interpolation requires 5 minutes for the calculations with a percentage error between the two methods lower than 1 %. The error was evaluated for random values of the Tcw_in, Thw_in and Tchw_in. In the following tables are listed the values of the Q_e, Q_h in [kW] from the tested values.

Q_h [kW]	Detailed	calculation		Tri-linear	calculation	
Thw_in = 74.9	Tcw_in = 41.2	Tcw_in = 43.4	Tcw_in = 44.7	Tcw_in = 41.2	Tcw_in = 43.4	Tcw_in = 44.7
Tchw_in = 10.1	0	0	0	0	0	0
Tchw_in = 13.2	2.826	0	0	2.834	0	0
Tchw_in = 17.6	9.417	4.113	0.9486	9.398	4.109	0.958
Thw_in = 84.1	Tcw_in = 25.4	Tcw_in = 35.5	Tcw_in = 44.7	Tcw_in = 25.4	Tcw_in = 35.5	Tcw_in = 44.7
Tchw_in = 10.1	7.181	2.411	0	7.104	2.399	0
Tchw_in = 13.2	11.649	6.794	3.89	11.585	6.764	3.863
Tchw_in = 17.6	18.346	13.37	10.396	18.285	13.329	10.347
Thw_in = 93.2	Tcw_in = 25.4	Tcw_in = 35.5	Tcw_in = 44.7	Tcw_in = 25.4	Tcw_in = 35.5	Tcw_in = 44.7
Tchw_in = 10.1	14.854	10.477	7.852	14.671	10.377	7.678
Tchw_in = 13.2	19.349	14.875	12.194	19.234	14.802	12.078
Tchw_in = 17.6	26.11	21.51	18.743	26.03	21.43	18.652

Table 6. Results for the Q_h in [kW] with the detailed and the linear calculation, all temperatures are in [°C]

Q_e [kW]	Detailed	calculation		Tri-linear	calculation	
Thw_in = 74.9	Tcw_in = 25.4	Tcw_in = 35.5	Tcw_in = 44.7	Tcw_in = 25.4	Tcw_in = 35.5	Tcw_in = 44.7
Tchw_in = 10.1	14.57	5.045	0	14.56	5.04	0
Tchw_in = 11.2	15.37	5.775	0	15.37	5.772	0
Tchw_in = 11.7	15.74	6.109	0	15.73	6.106	0
Thw_in = 84.1	Tcw_in = 25.4	Tcw_in = 35.5	Tcw_in = 44.7	Tcw_in = 25.4	Tcw_in = 35.5	Tcw_in = 44.7
Tchw_in = 10.1	17.16	8.489	0	17.14	8.474	0
Tchw_in = 11.2	17.98	9.231	0.4593	17.97	9.218	0.4504
Tchw_in = 11.7	18.36	9.571	0.769	18.34	9.556	0.7584
Thw_in = 93.2	Tcw_in = 25.4	Tcw_in = 35.5	Tcw_in = 44.7	Tcw_in = 25.4	Tcw_in = 35.5	Tcw_in = 44.7
Tchw_in = 10.1	19.19	11.38	3.447	19.37	11.36	3.429
Tchw_in = 11.2	20.03	12.13	4.122	20.09	12.11	4.107
Tchw_in = 11.7	20.41	12.47	4.431	20.42	12.46	4.415

Table 7. Results for the Q_e in [kW] with the detailed and the linear calculation, all temperatures are in [°C]

8.2.6 Conclusions

The iterative method which was implemented was necessary to guarantee a proper functioning of the adsorption chiller. It was found that $time_A = 20$ s and $time_B = 400$ s allow to produce the maximum Q_e. To increase the Q_e and the COP it's better to invest in a good cooling tower which achieves low outlet temperatures of the cooling water. The results with the implementation of

the tri-linear interpolation are in good correspondence with the results of the detailed method with a maximum error below 1 %. The approximate calculation is capable of calculating the cooling and heating power in all the possible working points with high accuracy.

8.3 Integration of buildings and adsorption chiller: the SHWS

TRNSYS was utilized to create the dynamic model of the SHWS, to create the control system and to find the case with the lowest PBP. It's assumed that the buildings before the integration of the adsorption chiller were heated and cooled through fan coils powered by an oil boiler and a heat pump. The prices of the boiler and the fan coils won't be included in the calculation of the PBP. The equations of the control system and the setpoint temperatures of the components are grouped in the "control panel". Twenty cases where investigated with four storage tank volumes: 500, 1000, 2000 and 3000 l and five solar collectors areas: 37.71, 58.66, 79.61, 96.37 and 113.13 m^2. It was found that the lowest PBP, between 26.3 and 32.1 years, is achieved with a storage tank volume of 3000 l and a solar collectors area of 37.71 m^2. The model in TRNSYS of the SHWS is shown in the following figure:

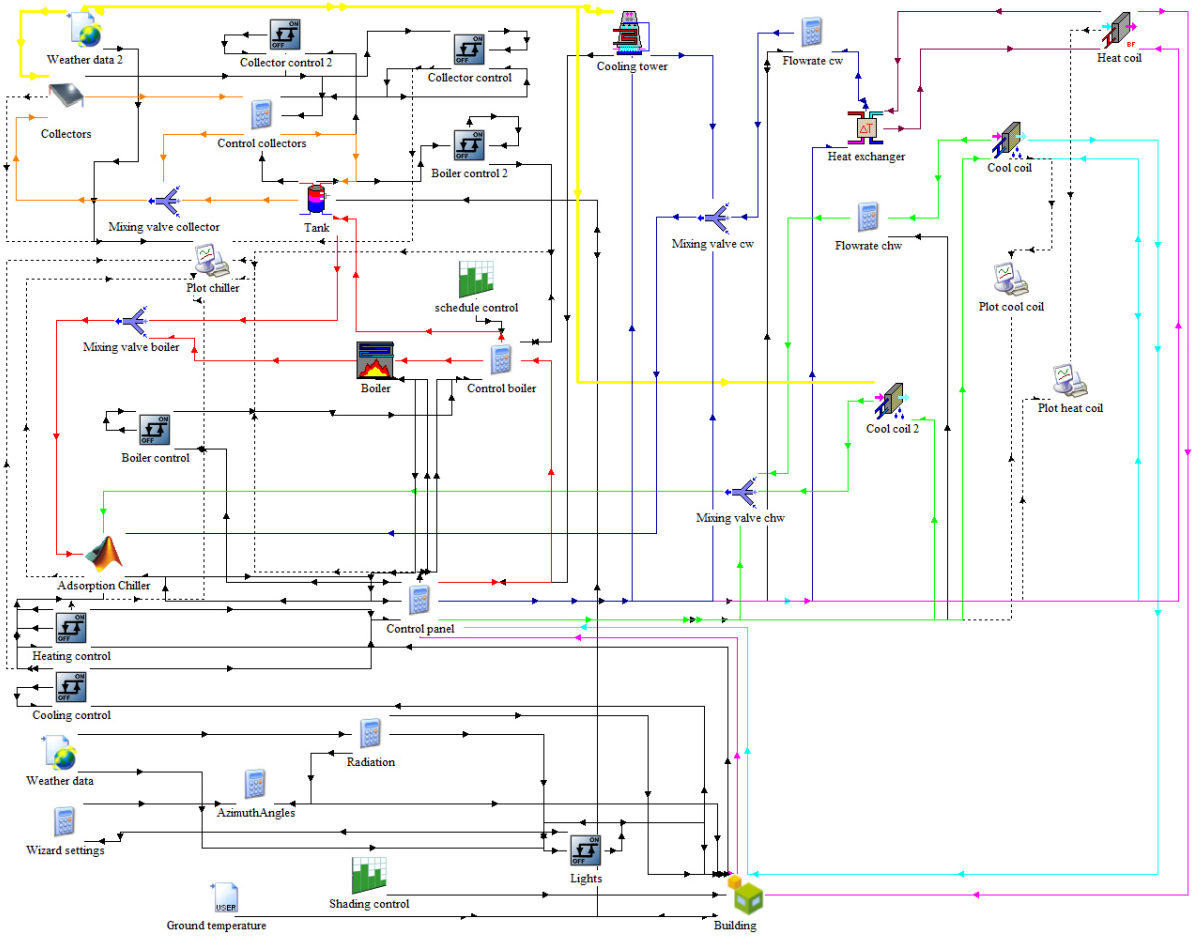

Fig. 24. TRNSYS model for the SHWS

8.3.1 Control panel

The control panel commands the water flow rates to guarantee a proper functioning of the SHWS during the entire year and includes the set point temperatures of the components. The control panel sends the water flow rates to different components based on the energy demand. Three cases can occur depending on the internal temperature of the buildings:
- Case 1, no heating nor cooling
- Case 2, cooling
- Case 3, heating

These cases are controlled by the parameters: SigC, SigH and V. The following rules are applied:
- If cooling is needed then the parameter 'SigC' is equal to 1 otherwise it's equal to 0
- If heating is needed then the parameter 'SigH' is equal to 1 otherwise it's equal to 0
- The parameter 'V' is the sum of 'SigC' and 'SigH'

The values defined in the control panel are:
- n_buildings [-], number of buildings
- $\dot{m}$_boiler = 3072 kg/h, flow rate of the hot water passing though the boiler
- $\dot{m}$_coldside = 1200 kg/h, flow rate of the cold side water of the heat exchanger
- SetpointCoolChw = 10.5 °C, set point of the outlet fluid temperature from the cool coil during the cooling period
- SetpointHeatChw = 10 °C, set point of the outlet fluid temperature from the cool coil-2 during the heating period
- SetpointBoiler = 90 °C, the desired temperature of the fluid exiting the boiler
- SetpointHeatingCoil = 29 °C, set point of the outlet air temperature from the heat coil
- SetpointCoolT = 29 °C, set point of the outlet fluid temperature from the cooling tower
- flowAir = 800 kg/h, air change rate of the cool and heat coil
- FlowAirHeatChw = 1840*n_buildings kg/h, air change rate in the cool coil-2 during the heating period

The cooling and chilled water flow rates can be represented as:

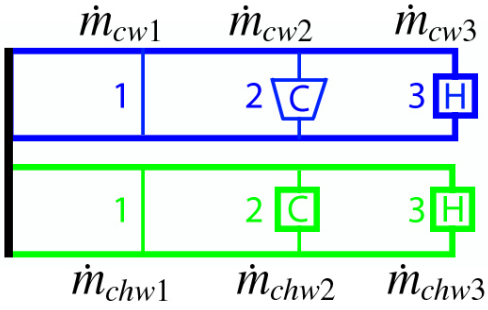

Fig. 25. Simplified representation of the two water flowarates,
in blue the cooling and in green the chilled

Where:
- $\dot{m}_{cw1} = \dot{m}_{cw} * (1 - V)$
- $\dot{m}_{cw2} = \dot{m}_{cw} * sigC$
- $\dot{m}_{cw3} = \dot{m}_{cw} * sigH/n\_buildings$
- $\dot{m}_{chw1} = \dot{m}_{chw} * (1 - V)$
- $\dot{m}_{chw2} = \dot{m}_{chw} * sigC/n\_buildings$
- $\dot{m}_{chw3} = \dot{m}_{chw} * sigH$

With these equations:
the cool water
- Pass thought $\dot{m}_{cw1}$ (no component) in case 1
- Pass thought $\dot{m}_{cw2}$ (cooling tower) in case 2
- Pass thought $\dot{m}_{cw3}$ (heat exchanger) in both 3

the chilled water
- Pass thought $\dot{m}_{chw1}$ (no component) in case 1
- Pass thought $\dot{m}_{chw2}$ (cool coil) in case 2
- Pass thought $\dot{m}_{chw3}$ (cool coil-2) in case 3

8.3.2 Energetic analysis

Twenty configurations were investigated by varying the solar collectors area and the storage tank volume. The energy required from the boiler, referred for both buildings, was calculated for every case divided it in energy required during cooling and heating. The results of the energy demands of the boiler are:

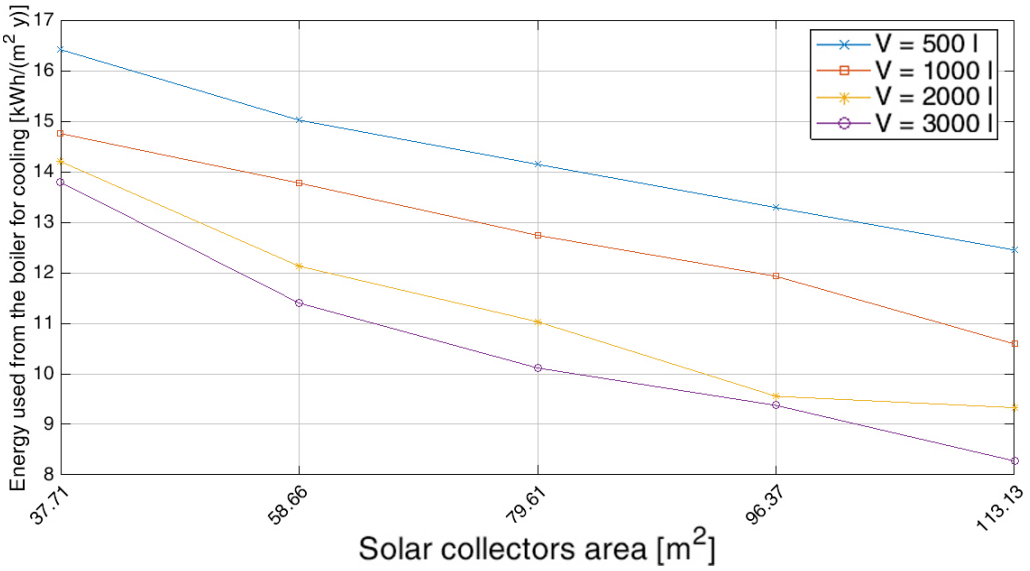

Fig. 26. Energy required from the boiler in [kWh/(m^2 y)] during cooling for the four tank volumes in [l] as function of the solar collectors area in [m^2]

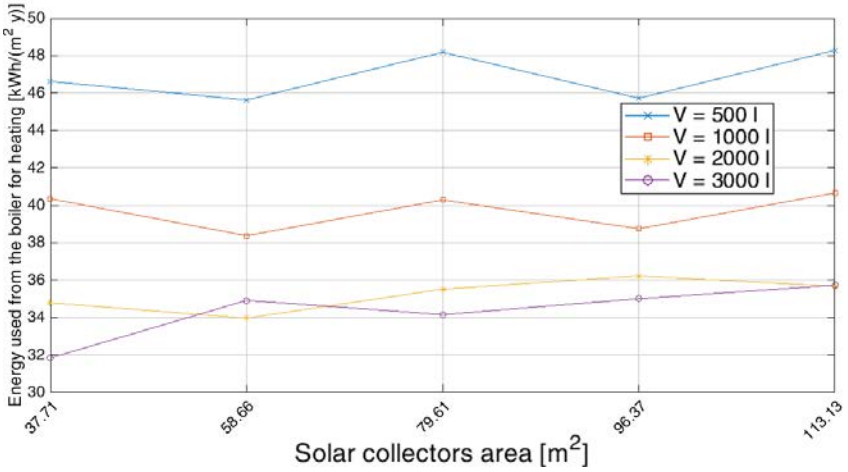

Fig. 27. Energy required from the boiler in [kWh/(m^2 y)] during heating for the four tank volumes in [l] as function of the solar collectors area in [m^2]

In fig. 26 it's shown that the energy required from the boiler during cooling decreases as the solar collectors area increases because larger collectors areas provide higher solar energy to the system. The energy required from the boiler during heating remains almost constant for different solar collectors areas because the fraction of solar energy is low during this period. The energy required from the boiler during heating decreases as the storage tank volume increases because with larger storage tank volumes the boiler turns on less times to maintain the hot water between 75 and 90 °C.

The energy required from the boiler along with the coefficients provided by TEE [22] allow to calculate the fraction of primary energy savings. These coefficients convert the final energy into primary energy.

Electric fan coils are operated for the generation of the cooling energy. TRNSYS calculates the energy demands in thermal energy. The calculated cooling energy is equal to 34.77 $kWh/(m^2y)$. The primary thermal energy is equal to final thermal energy multiplied by 2.9. The primary electric energy is calculated by dividing the primary thermal energy with the seasonal COP of the heat pump which has an average value of 3.1 based on the data sheet of DAIKIN [3]. The primary electric cooling energy is equal to 32.53 $kWh/(m^2y)$.

An oil boiler is operated for the generation of the heating energy. The final heating energy is equal to 60.02 $kWh/(m^2y)$. The primary thermal energy is equal to final thermal energy multiplied by 1.1. The primary thermal heating energy is equal to 66.03 $kWh/(m^2y)$ and thus the total primary energy required from the system is equal to 98.56 $kWh/(m^2y)$. The same coefficients are utilized to calculate the primary energy required from the boiler.

The annual fraction of primary energy savings is calculated as:

$$F\_prim\_s = 1 - \frac{Prim\_b}{Prim\_tot} \tag{31}$$

Where *F_prim_s* is the fraction of primary energy savings, *Prim_b* is the primary energy required from the boiler in [kWh/(m^2 y)] and *Prim_tot* is the total primary energy required from the system in [kWh/(m^2 y)]. The results for the annual fraction of primary energy savings are:

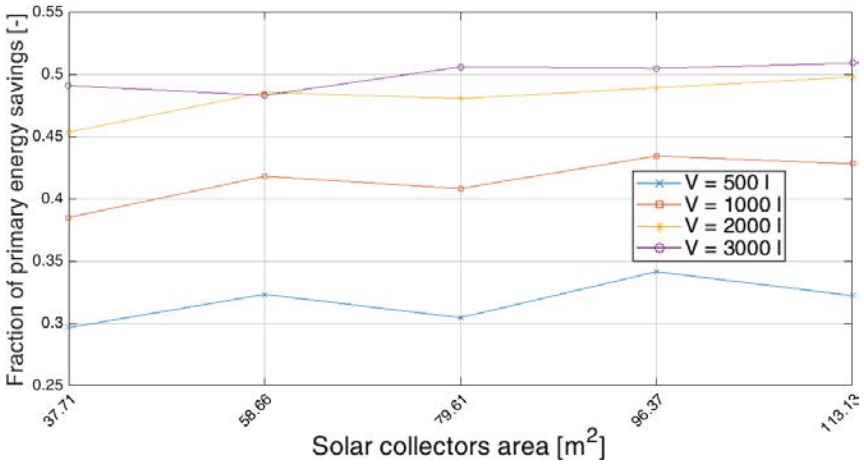

Fig. 28. Fraction of primary energy savings [-] for the four tank volumes in [l] as function of the solar collectors area in [m^2]

The fraction of primary energy savings remains almost constant for different solar collectors areas because the energy required from the boiler during heating is three times greater than the one required during cooling.

The energy required from the boiler during cooling allows to calculate the solar fraction:

$$f = \frac{Q_{col}}{Q_{col} + Q_{boiler\_c}} \quad [-] \tag{32}$$

where Q_{boiler_c} is the energy required from the boiler during cooling in [kWh/(m^2 y)] and Q_{col} is the energy provided from the solar collectors in [kWh/(m^2 y)]. The results for the solar fraction are:

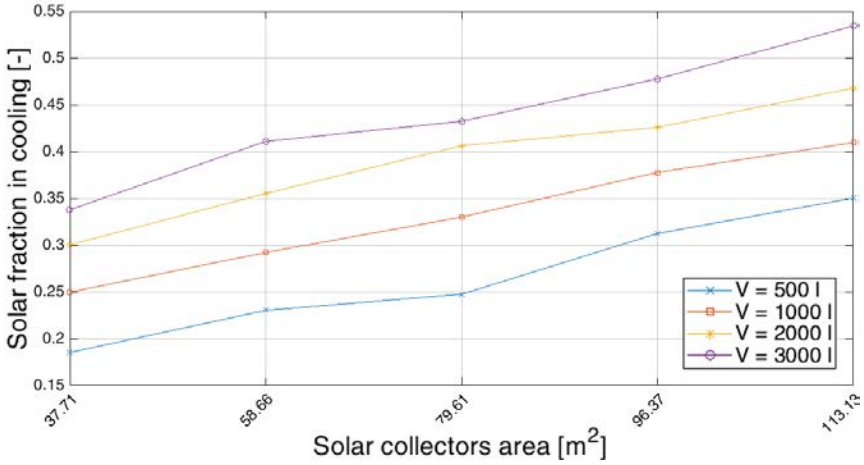

Fig. 29. solar fraction during cooling [-] for the four tank volumes in [l] as function of the solar collectors area in [m^2]

8.3.3 Techno-economic analysis

The prices of the components have to be defined in order to calculate the PBP. The boiler and the fan coils are already installed in the buildings and their prices won't be considered in the initial investment. The initial investment, calculated with the average prices, was multiplied by 0.9 and 1.1 to consider the variability of the prices in the market.

- The average price for a flat plate solar collector of 2 m^2 is 220 €. The cost of the transportation (40 €) and the cost of the base (90 €) have to be added to this price and therefore the total average price of every solar collector is equal to 350 €. The five cases with solar collectors areas: 37.71, 58.66, 79.61, 96.37 and 113.13 m^2 have a total price which range from 6,300 € to 18,900 €.

- The average price for a storage tank volume of: 500, 1000, 2000 and 3000 l is respectively 300, 525, 800 and 1100 €. The price for installing the tank in the basement is respectively: 100, 200, 300 and 400 € for the four cases. The transportation cost is equal to the cost of the installation and hence the total average price for the tank can range from 500 € to 1,900.

- The average price for an adsorption chiller is equal to 600 €/$kW_{cooling}$ based on Lazzarin [35] and thus the total average price of the adsorption chiller is equal to 12,600 € because its peak cooling power is equal to 21 kW

- The average price for a water-to-air heat exchanger with nominal power equal to 7 kW(fan coil-2) is equal to 350 €, the average price for a cooling tower with a cooling capacity of 20 kW is equal to 1,500 € and the average price for a water-to-water heat exchanger with nominal power of 8 kW is equal to 500 € based on the pricelist of AIRTECHNIC [1].

- The average prices for the pipes, the mixing and diverging valves and the control system were assumed equal to 3,000 €.

The initial investment is equal to the sum of the components prices. The following figure shows the lower and upper initial investment for the four storage tank volumes considering a variability of the prices in the market:

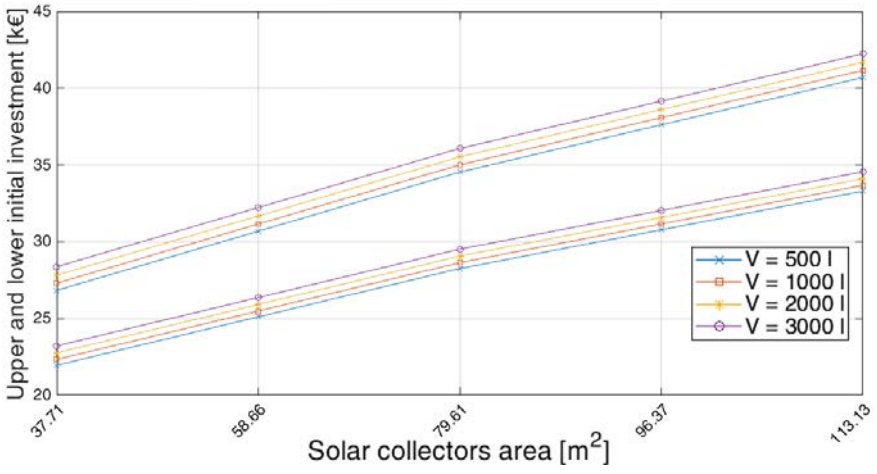

Fig. 30. Initial investments in [k€] as function of the solar collectors area in [m^2]

The coefficient for Greece provided by Eurostat [24] for the price of the electric energy allows to calculate the annual savings from the energy savings. The price of the electric energy is equal to 0.1620 for every kWh consumed. Typical values in Greece for the price of the oil is equal to 0.834 €/l. The price of the oil is equal to 0.0843 for every kWh consumed assuming an oil density equal to 834.5 kg/m^3 and an oil caloric value equal to 11.86 kWh/kg. These prices are referred to the year 2017. The annual savings for every building are:

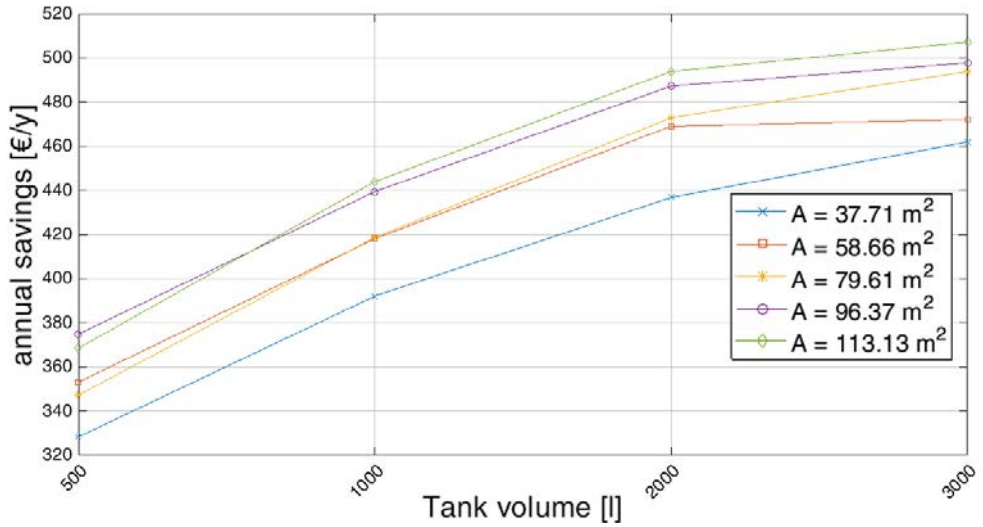

Fig. 31. Annual savings in [€/y] for every buildings as function of the tank volume in [l]

The PBP is calculated as:

$$PBP = \frac{I_0}{annual savings} \quad [y] \tag{33}$$

Where I_0 is the initial investment in [€] and the annual savings in [€/y]. The results for the average PBP are:

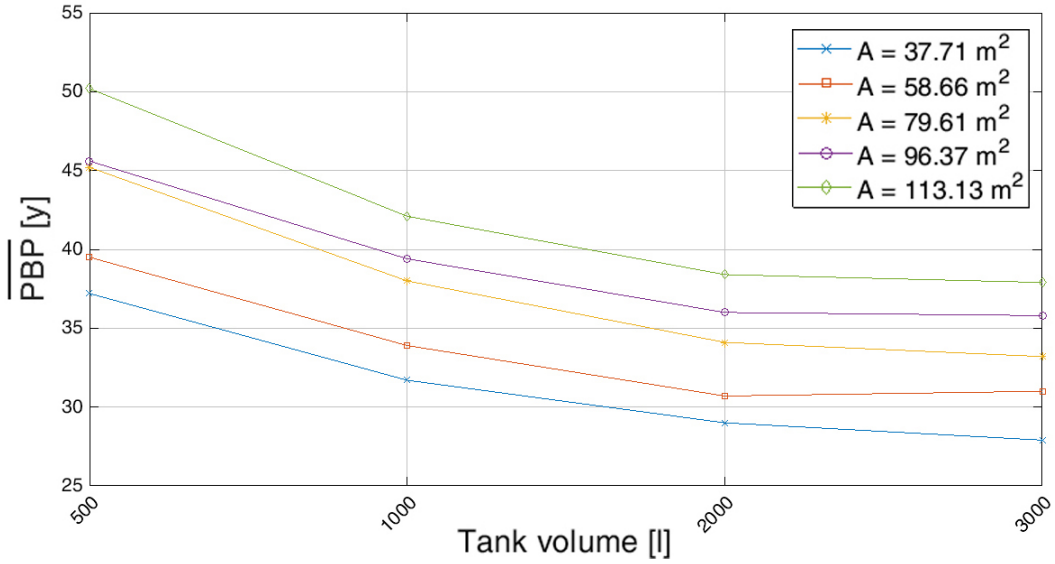

Fig. 32. Average PBP in [y] for the five solar collectors areas in [m^2] as function of the tank volume in [l]

The average PBP can be correlated to the fraction of primary energy savings and the solar fraction:

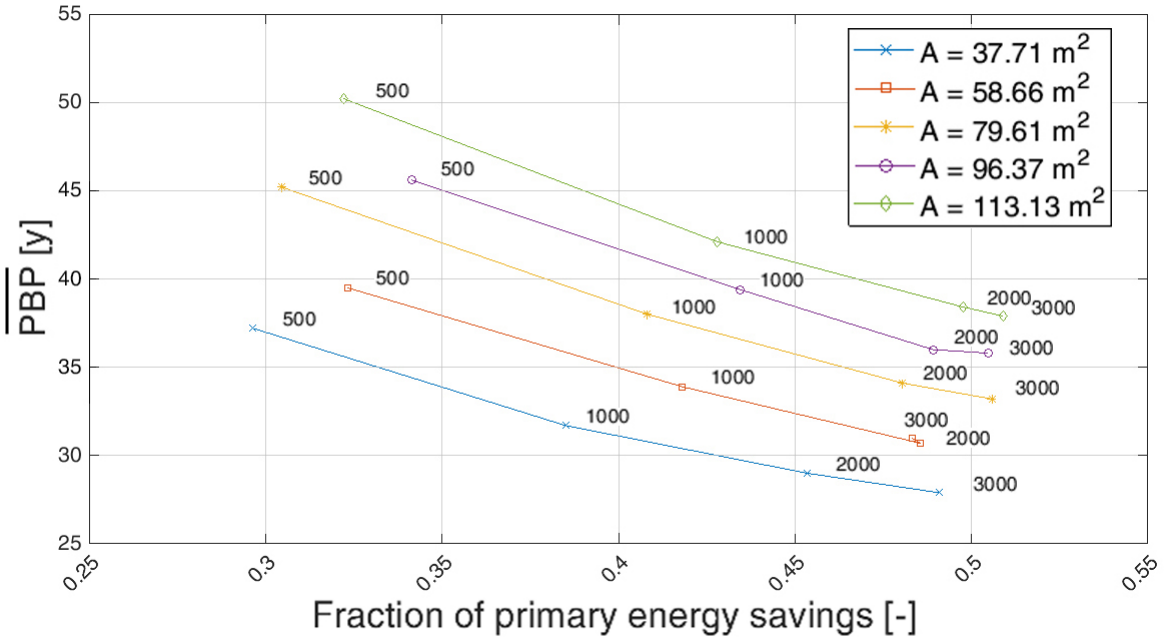

Fig. 33. Average PBP for the five solar collectors areas in [m^2]
as function of the fraction of primary energy savings [-]

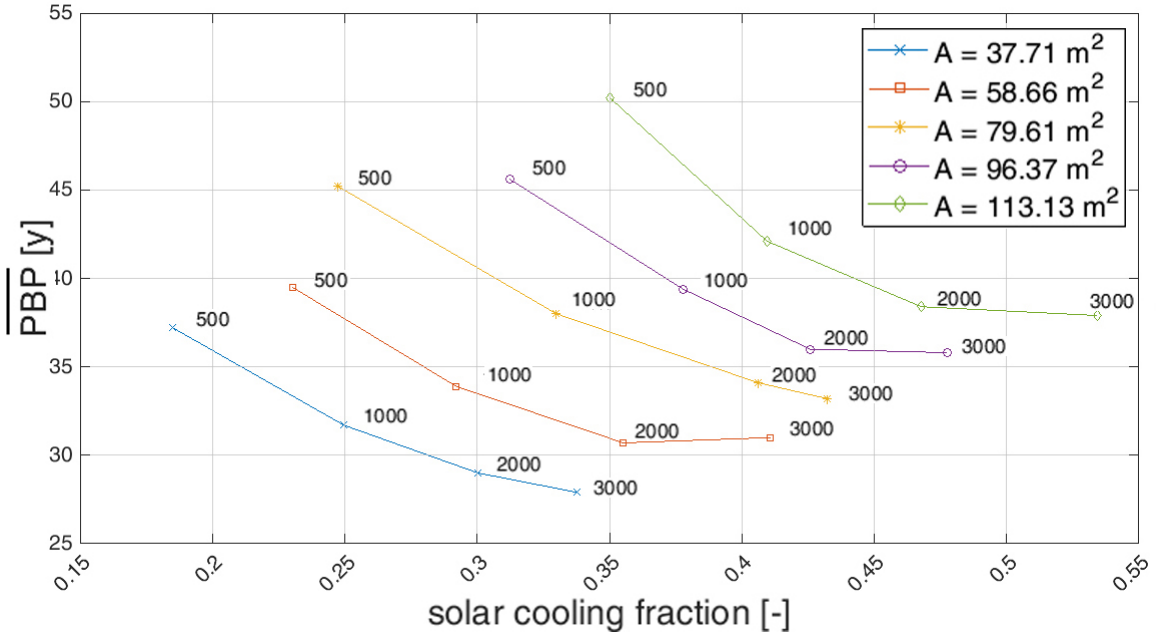

Fig. 34. Average PBP for the five solar collectors areas in [m^2]
as function of the solar fraction [-]

In the last two figures is shown that high solar collectors areas have higher PBP and that the PBP decreases as the storage tank volume increases. Increasing the tank from small to middle

size volume causes big differences to the PBP, the fraction of primary energy savings and the solar fraction.
In the fig. 33 the difference between the points for the fraction of primary energy savings gets smaller for larger storage tank volumes. Storage tank volumes larger than 2000 l have no economic advantage for the cases with solar collectors area of 58.66, 96.37 and 113.13 m^2.
In the fig. 34 the difference between the points for the solar fraction is constant for different storage tank volumes. Storage tank volumes larger than 2000 l have PBP that tend to increase for the cases with solar collectors area of 58.66, 96.37 and 113.13 m^2
The most economical solution is with high storage tank volumes and low solar collectors areas which provide low solar fractions. The optimal solution is not necessarily an environmental solution because the system keeps using oil to heat and cool the buildings.

8.3.4 Conclusions

Larger storage tank volumes and larger solar collectors areas improve the energetic performance of the system by increasing the fraction of energy savings during cooling. The fraction of energy savings during cooling increases as the storage tank volume and the solar collectors areas increase while the fraction of primary energy savings during heating increases only if the storage tank volume increases. The fraction of primary energy savings during heating remains almost constant for different solar collectors areas for a fixed storage tank volume because during the heating period the solar collectors can't reach temperatures higher than 70 °C and consequently the boiler provides energy to heat the buildings. The solar collectors are tilted at 20 ° to maximize the solar energy captured during the cooling period. The fraction of primary energy savings during heating is three times greater than the one during cooling and thus the total fraction of primary energy savings depends mainly to the fraction of primary energy savings during heating. The maximum solar fraction, equal to 0.534, can be achieved with a storage tank volume of 3000 l and a solar collectors area of 113.13 m^2.
Larger storage tank volumes and smaller solar collectors areas improve the economic performance of the system by decreasing the PBP. The minimum average PBP, equal to 29.2 years, can be achieved with a storage tank volume of 3000 l and a solar collectors area of 37.71 m^2.

9 Conclusions

The thesis describes the construction and simulation in TRNSYS environment of a solar hot water system which utilizes an adsorption chiller for the generation of the cooling and heating power required for two typical Greek buildings. The buildings were specifically tailored to optimally exploit the adsorption chiller. It is noted that in the literature, based on the knowledge of the author, none of the papers present a dynamic model which describe the performance of the adsorption chiller via differential equations.

The dynamic model accurately evaluates the cooling demands of the buildings based on the transient conditions which occur due to the thermal inertia of the building structures. The payback period is estimated by operating the system under realistic heating and cooling load curves.

The highest cooling and heating powers outputs of the adsorption chiller model are reached with high chilled, low cooling and high hot water temperature. The maximum cooling power calculated with hot water temperature of 70 °C and 90 °C is equal to 14.7 kW and 21.28 kW respectively. Conversely, the maximum heating power calculated with hot water temperature of 70 °C and 90 °C is equal to 7.62 kW and 30.43 kW respectively

The energetic and economic performance of the system is more efficient with larger storage tank volumes. From an energetic point of view, the case studies with larger solar collectors areas are more efficient with a solar fraction which range from 0.185 (storage tank volume of 500 l and solar collectors area of 37.71 m^2) to 0.534 (storage tank volume of 3000 l and solar collectors area of 113.13 m^2). From an economical point of view, the best cases are those with lower solar collectors areas. The average payback period can range from 51.8 years (storage tank volume of 500 l and solar collectors area of 113.13 m^2)to 29.2 years (storage tank volume of 3000 l and solar collectors area of 37.71 m^2). These results proves that efficient solar cooling systems do not require large solar collectors areas. A proper investigation for the limits of the solar fraction, which may change for different countries, has to be carried out before choosing the most economic solution.

The energetic and economic analysis of the system performance evaluated for the four storage tank volumes and the five solar collectors areas shows that the lowest payback period, between 26.3 and 32.1, is achieved with a storage tank volume of 3000 l and a solar collectors area of 37.71 m^2. The initial investment varies from 24,300 to 29,700 € with annual savings equal to 461.97 €/y for each building. Without incentives this solution has a really high payback period which suggests that more research is needed in order for the adsorption solar cooling technologies to became a competitive solution for heating and cooling. The following figures shows the annual variations of the internal air temperature of the buildings and the hot, cooling and chilled water outlet temperatures from the adsorption chiller.

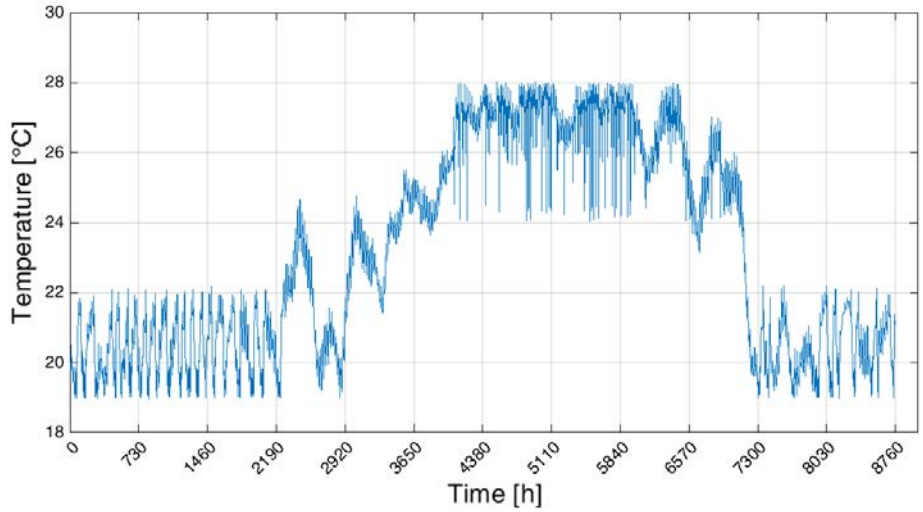

Fig. 35. Internal air temperature of the buildings in [°C]

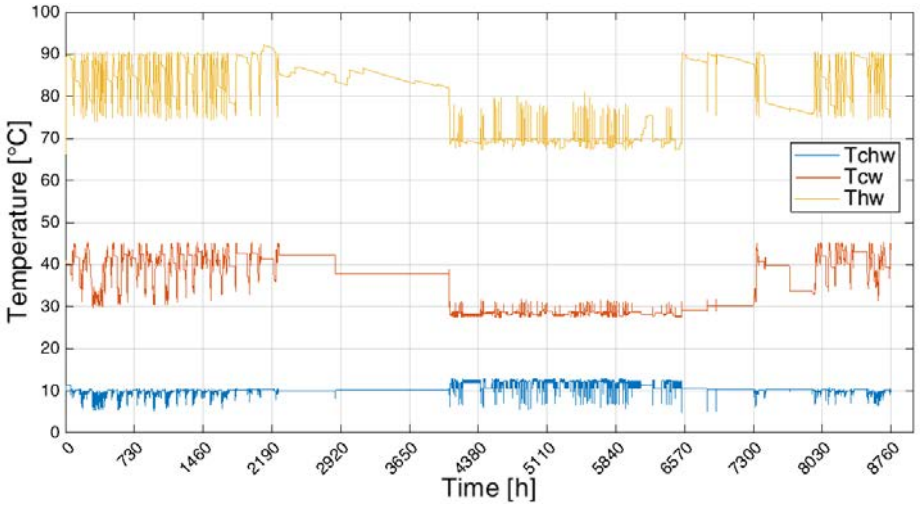

Fig. 36. Outlet temperatures from the chiller for the three water flow rates in [°C]

Fig. 35. shows that the system can guarantee the desired comfort with internal air temperatures that range from 18 to 22 °C during the heating period and from 24 to 28 °C during the cooling period.

The energy demands and the power peaks of the buildings without the adsorption chiller were estimated with a simple dynamic model with only the 3D model of the buildings. The cooling and heating peaks are equal to 4.23 and 6.29 kW respectively. At first sight it seems that there is a mismatch between the nominal cooling power of the adsorption chiller (16 kW) and the maximum cooling power required from the buildings (8.46 kW). Fig. 36 shows that during the cooling period the average chilled, cooling and hot water temperatures are equal to 10, 30 and 75 °C respectively. From the table 25 in the appendix it's shown that these temperatures produce a cooling power equal to 10.33 kW which proves that the utilization of two typical Greek units is the best match for the specific adsorption chiller.

Different buildings can easily be loaded to the TRNSYS model to evaluate the system performance for a variety of utilities and to investigate the optimal match between the number of the proposed adsorption chiller and the number of the buildings. Further developments considering a variety of utilities could consist in investigating for each case which commercial adsorption chiller would be the most suitable. Also, the model could get even more accurate by including the auxiliary energy consumption. Finally, concentrating solar collectors and a high temperature heat pump could be investigated to evaluate if these expensive components could produce an economic benefit.

10 Appendix I: buildings

10.1 Layers of the walls

External wall	Density ρ kg/m^3	Thickness d m	Conductivity λ $W/(mK)$	Capacity c $J/(kgK)$	Thermal Resistance d/λ $(m^2K)/W$
Lime and cement mortar	1800	0.020	0.870	1000	0.023
Bricks	1700	0.090	0.580	1000	0.155
Thermal insulation material	20	0.040	0.035	1000	1.143
Bricks	1700	0.090	0.580	1000	0.155
Lime and cement mortar	1800	0.020	0.870	1000	0.023

Table 8. Layers of the external wall

Concrete wall	Density ρ kg/m^3	Thickness d m	Conductivity λ $W/(mK)$	Capacity c $J/(kgK)$	Thermal Resistance d/λ $(m^2K)/W$
Lime and cement mortar	1800	0.020	0.870	1000	0.023
Reinforced concrete	2400	0.250	2.500	1000	0.100
Thermal insulation material	20	0.040	0.035	1000	1.143
Lime and cement mortar	1800	0.020	0.870	1000	0.023

Table 9. Layers of the concrete wall

Brick wall adjacent to an unheated zone	Density ρ kg/m^3	Thickness d m	Conductivity λ $W/(mK)$	Capacity c $J/(kgK)$	Thermal Resistance d/λ $(m^2K)/W$
Lime and cement mortar	1800	0.020	0.870	1000	0.023
Bricks	1700	0.090	0.580	1000	0.155
Thermal insulation material	20	0.030	0.035	1000	0.857
Bricks	1700	0.090	0.580	1000	0.155
Lime and cement mortar	1800	0.020	0.870	1000	0.023

Table 10. Layers of the brick wall adjacent to an unheated zone

Concrete wall adjacent to an unheated zone	Density ρ kg/m^3	Thickness d m	Conductivity λ $W/(mK)$	Capacity c $J/(kgK)$	Thermal Resistance d/λ $(m^2K)/W$
Lime and cement mortar	1800	0.020	0.870	1000	0.023
Reinforced concrete	2400	0.250	2.500	1000	0.100
Thermal insulation material	20	0.040	0.035	1000	1.143
Lime and cement mortar	1800	0.020	0.870	1000	0.023

Table 11. Layers of the concrete wall adjacent to an unheated zone

Concrete wall adjacent to the ground	Density ρ kg/m^3	Thickness d m	Conductivity λ $W/(mK)$	Capacity c $J/(kgK)$	Thermal Resistance d/λ $(m^2K)/W$
Lime and cement mortar	1800	0.020	0.870	1000	0.023
Reinforced concrete	2400	0.250	2.500	1000	0.100
Cement grout for smoothing	1800	0.020	1.400	1000	0.014
Single surface dressing	2300	0.002	0.170	1000	0.012
Thermal insulation material	20	0.020	0.035	1000	0.571

Table 12. Layers of the concrete wall adjacent to the ground

Wood floor adjacent to an unheated zone	Density ρ kg/m^3	Thickness d m	Conductivity λ $W/(mK)$	Capacity c $J/(kgK)$	Thermal Resistance d/λ $(m^2K)/W$
Wooden parquet	800	0.020	0.210	1000	0.095
Blind floor	700	0.020	0.180	1000	0.111
Air gap (5 cm)		0.050		1000	0.210
Reinforced concrete slab	2400	0.150	2.500	1000	0.060
Lime and cement mortar	1800	0.015	0.870	1000	0.017

Table 13. Layers of the wood floor adjacent to an unheated zone

Wood floor adjacent to the ground	Density ρ kg/m^3	Thickness d m	Conductivity λ $W/(mK)$	Capacity c $J/(kgK)$	Thermal Resistance d/λ $(m^2K)/W$
Wooden parquet	800	0.020	0.210	1000	0.095
Blind floor	700	0.020	0.180	1000	0.111
Air gap (5 cm)		0.060		1000	0.210
Smoothing layer of cement mortar	2000	0.010	1.400	1000	0.007
Reinforced concrete slab	2400	0.150	2.500	1000	0.060
Geotextile	80	0.001	0.040	1000	0.025
Single layer of bituminous board	1100	0.004	0.230	1000	0.017
Smoothing layer of cement mortar	2000	0.010	1.400	1000	0.007
Lean concrete	2300	0.100	1.500	1000	0.067
Nylon	1390	0.001	0.200	1000	0.003
Riprap	2700	0.200	1.000	1000	0.200

Table 14. Layers of the wood floor adjacent to the ground

Tile floor adjacent to the ground	Density ρ kg/m^3	Thickness d m	Conductivity λ $W/(mK)$	Capacity c $J/(kgK)$	Thermal Resistance d/λ $(m^2K)/W$
Tile parquet	2000	0.010	1.840	1000	0.005
Sagger grog	1800	0.020	1.400	1000	0.014
Grubbing as a balancing layer	1900	0.080	1.100	1000	0.073
Reinforced concrete slab	2400	0.150	2.500	1000	0.060
Nylon	1390	0.001	0.170	1000	0.003
Thermal insulation material	20	0.020	0.035	1000	0.571
Portland cement mortar lining	1100	0.004	0.230	1000	0.017
Smoothing layer of cement mortar	2000	0.010	1.400	1000	0.007
Lean concrete	2300	0.100	1.500	1000	0.067
Nylon	1390	0.001	0.200	1000	0.003
Riprap	2700	0.200	1.000	1000	0.200

Table 15. Layers of the tile floor adjacent to the ground

Tile roof	Density ρ kg/m^3	Thickness d m	Conductivity λ $W/(mK)$	Capacity c $J/(kgK)$	Thermal Resistance d/λ $(m^2K)/W$
Tile parquet	1000	0.030	0.440	1000	0.068
Air gap	700	0.030		1000	
Longitudinal roof-stiffener	800	0.050		1000	
PVC waterproofing membrane	1050	0.001		1000	
Roof boarding	700	0.010		1000	
Equivalent thermal resistance	759	0.091	0.303	1000	0.300
Thermal insulation material	20	0.060	0.035	1000	1.714
Smoothing layer of cement mortar	2000	0.010	1.400	1000	0.007
Reinforced concrete slab	2400	0.150	2.500	1000	0.060
Lime and cement mortar	1800	0.015	0.870	1000	0.017

Table 16. Layers of the tile roof

Paving slabs roof	Density ρ kg/m^3	Thickness d m	Conductivity λ $W/(mK)$	Capacity c $J/(kgK)$	Thermal Resistance d/λ $(m^2K)/W$
Paving slabs	2100	0.030	1.500	1000	0.020
Adhesive cement mortar	2000	0.020	1.400	1000	0.014
Geotextile	80	0.001	0.040	1000	0.025
Single layer of asphalt	1100	0.004	0.230	1000	0.017
Grubbing as a balancing layer	1700	0.080	0.810	1000	0.099
Thermal insulation material	20	0.060	0.035	1000	1.714
Asphalt coat as a vapor barrier	1050	0.001	0.170	1000	0.003
Softening layer of cement	2000	0.010	1.400	1000	0.007
Reinforced concrete slab	2400	0.150	2.500	1000	0.060
internal plaster	1800	0.015	0.870	1000	0.017

Table 17. Layers of the paving slabs roof

10.2 Characteristics of the windows

The windows were created with the software WINDOWS6. The characteristics of the windows of the buildings are:

- type1: $U_{glass} = 4.338\ W/(m^2K)$, $g_{glass} = 0.44$ and $A_{frame}/A_{window} = 0.3506$
- type2: $U_{glass} = 4.571\ W/(m^2K)$, $g_{glass} = 0.40$ and $A_{frame}/A_{window} = 0.4048$
- type3: $U_{glass} = 5.222\ W/(m^2K)$, $g_{glass} = 0.30$ and $A_{frame}/A_{window} = 0.5556$
- type4: $U_{glass} = 4.085\ W/(m^2K)$, $g_{glass} = 0.48$ and $A_{frame}/A_{window} = 0.2929$

Once these windows were created in WINDOWS6 a report was generated which had to be added in the window library of TRNSYS. All of the windows are double windows composed of two layers of 3 mm of clear glass and 12 mm of air cavity between the layers.

11 Appendix II: adsorption chiller

11.1 Simulink model

The model of the adsorption chiller in Matlab Simulink is based on the equations defined in chapter 7.2.2

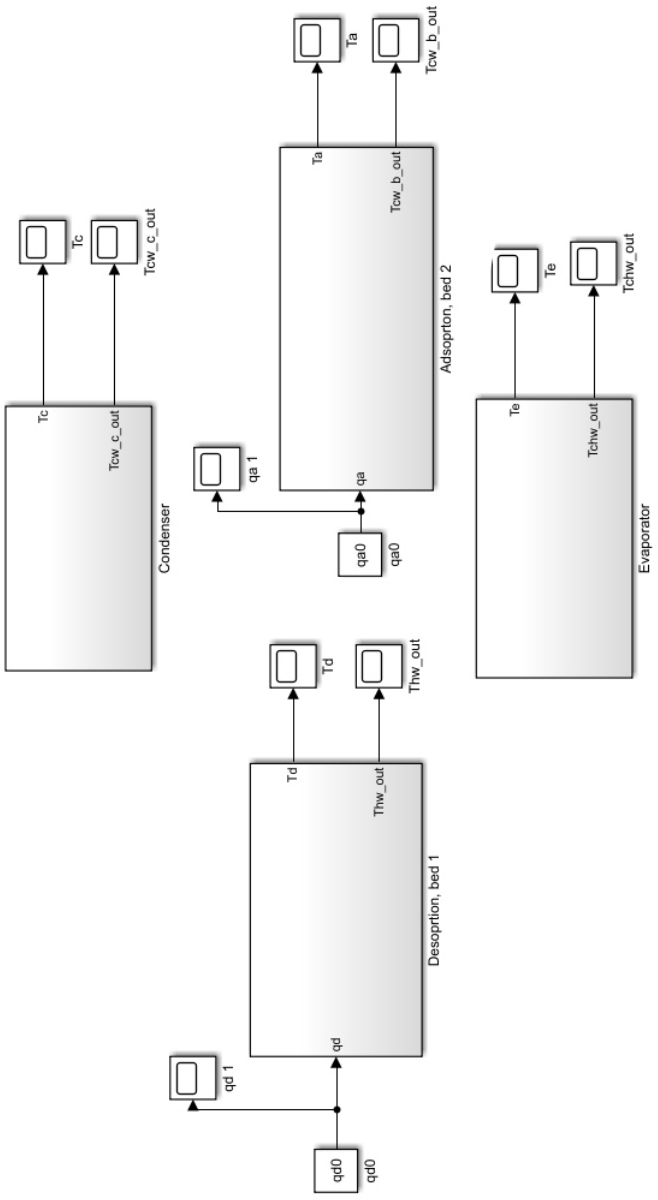

Fig. 38. Simulink model of the phase A

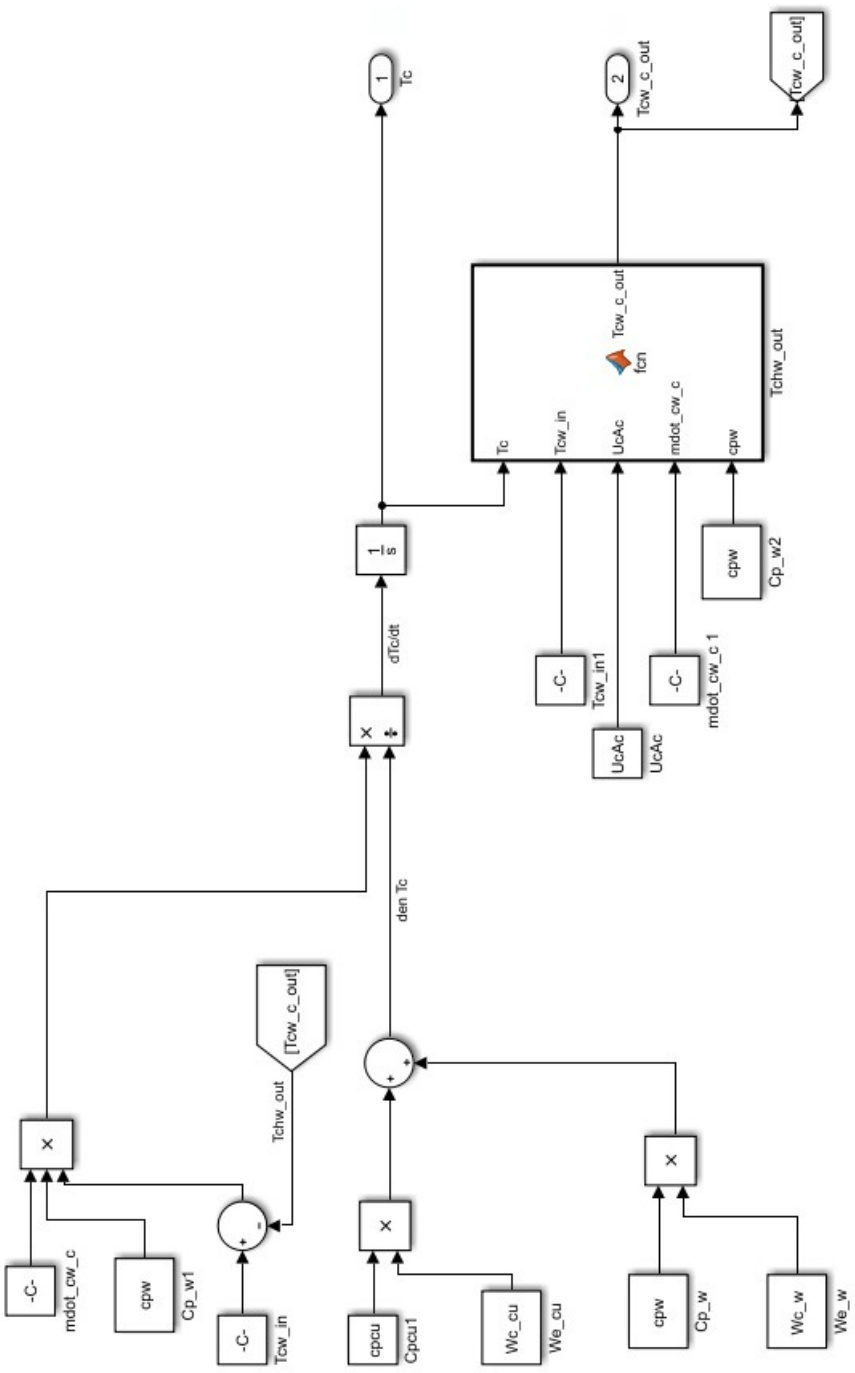

Fig. 39. Simulink model of the condenser in phase A

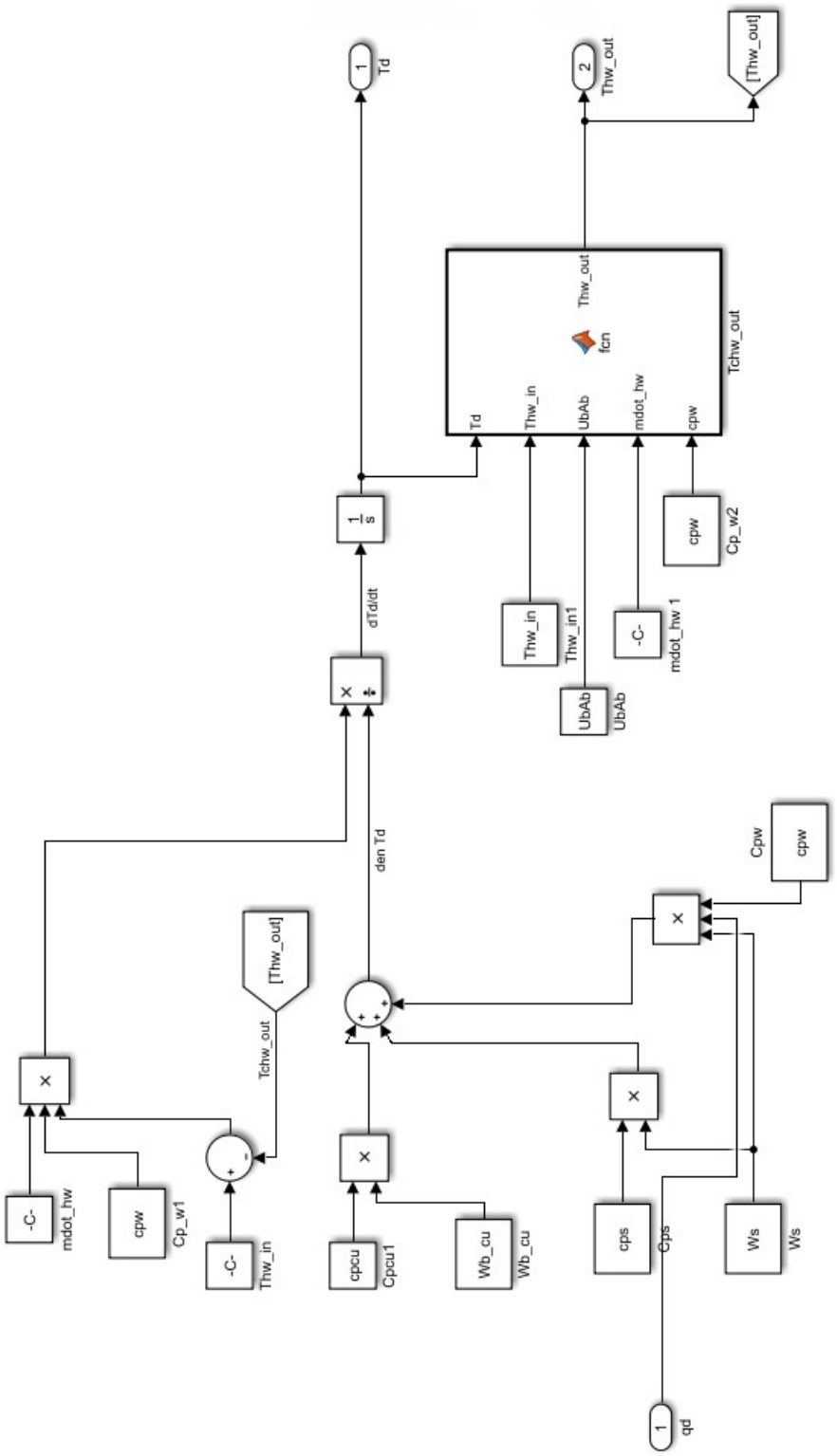

Fig. 40. Simulink model of the desorber in phase A

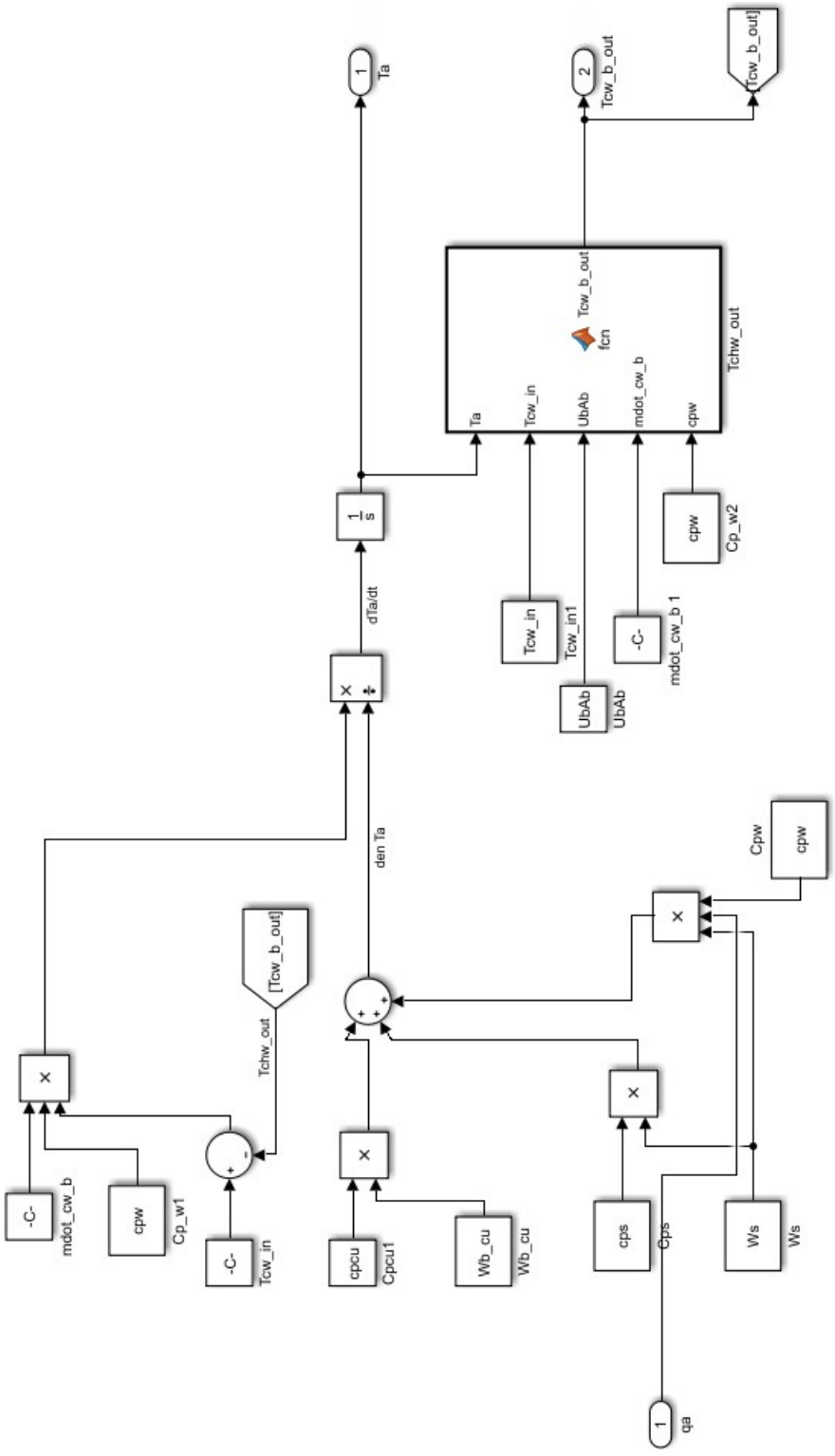

Fig. 41. Simulink model of the adsorber in phase A

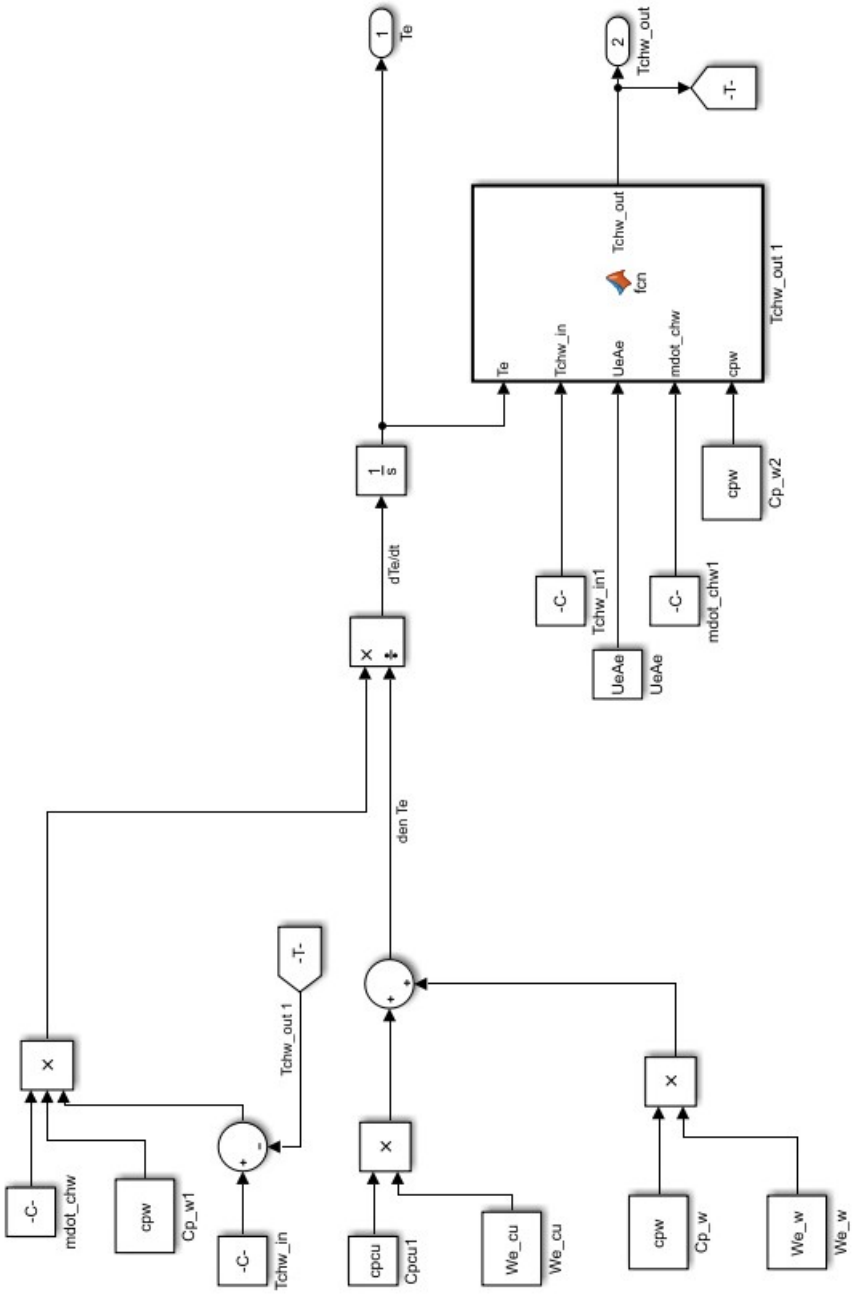

Fig. 42. Simulink model of the evaporator in phase A

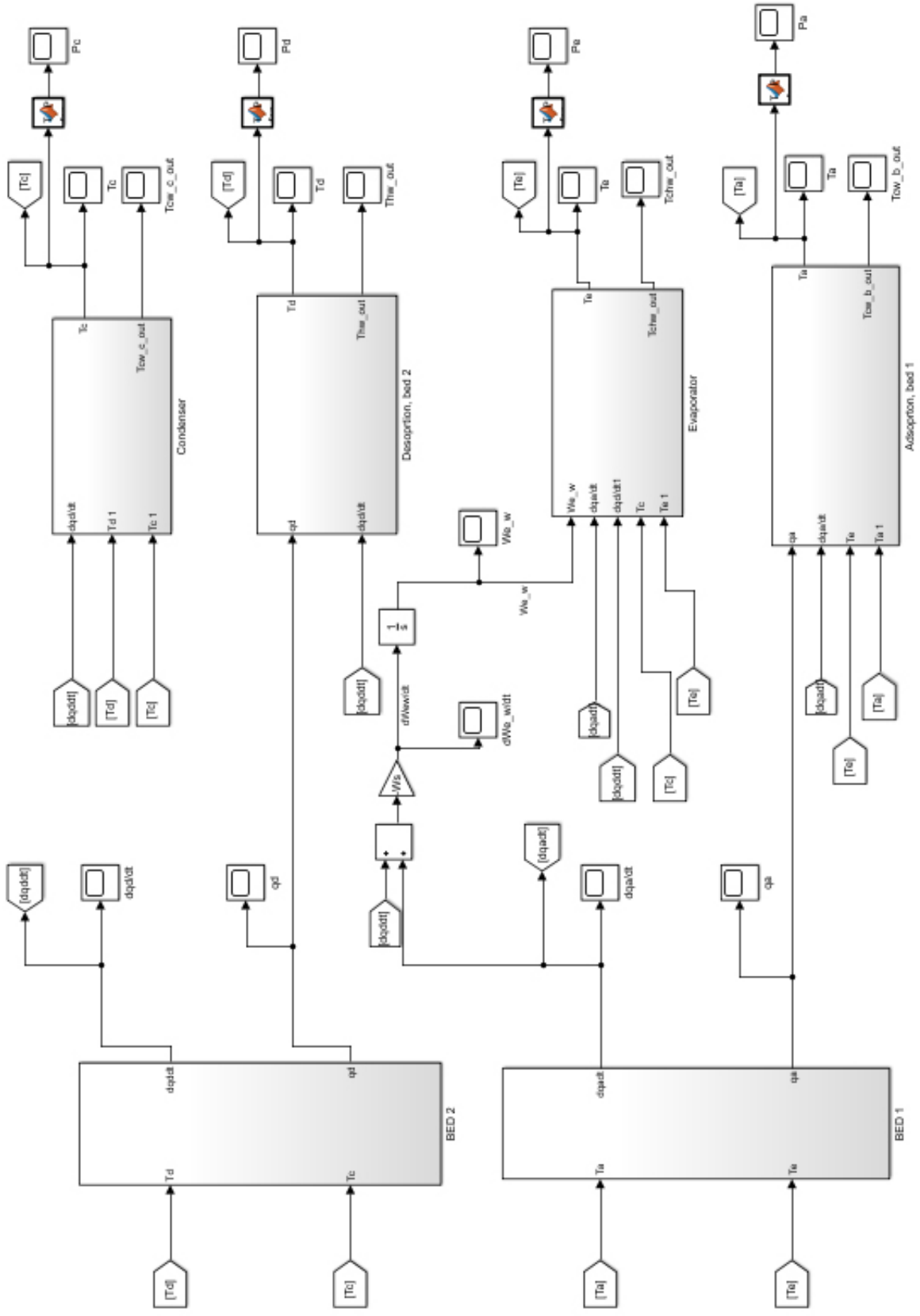

Fig. 43. Simulink model of the phase B

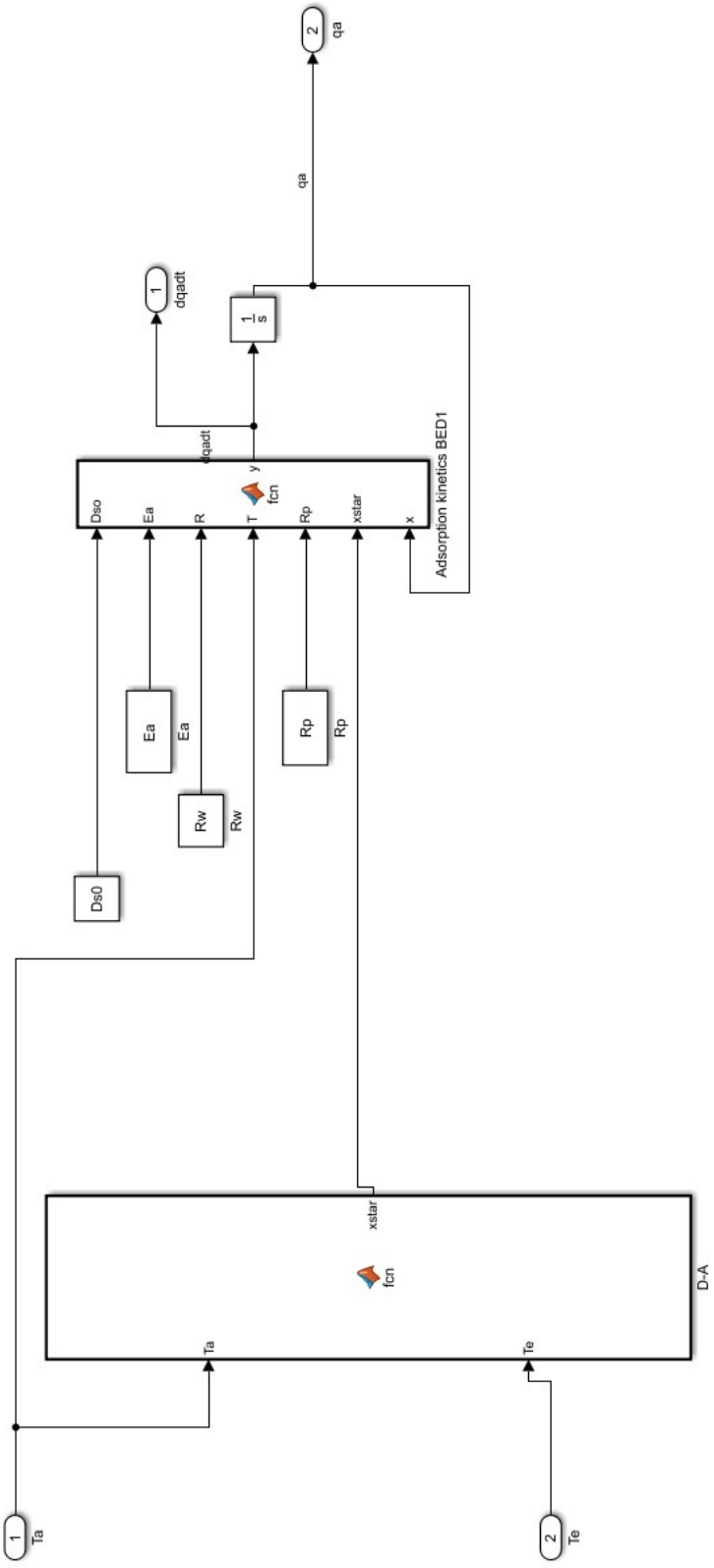

Fig. 44. Simulink model of the kinetics of the adsorption bed in phase B

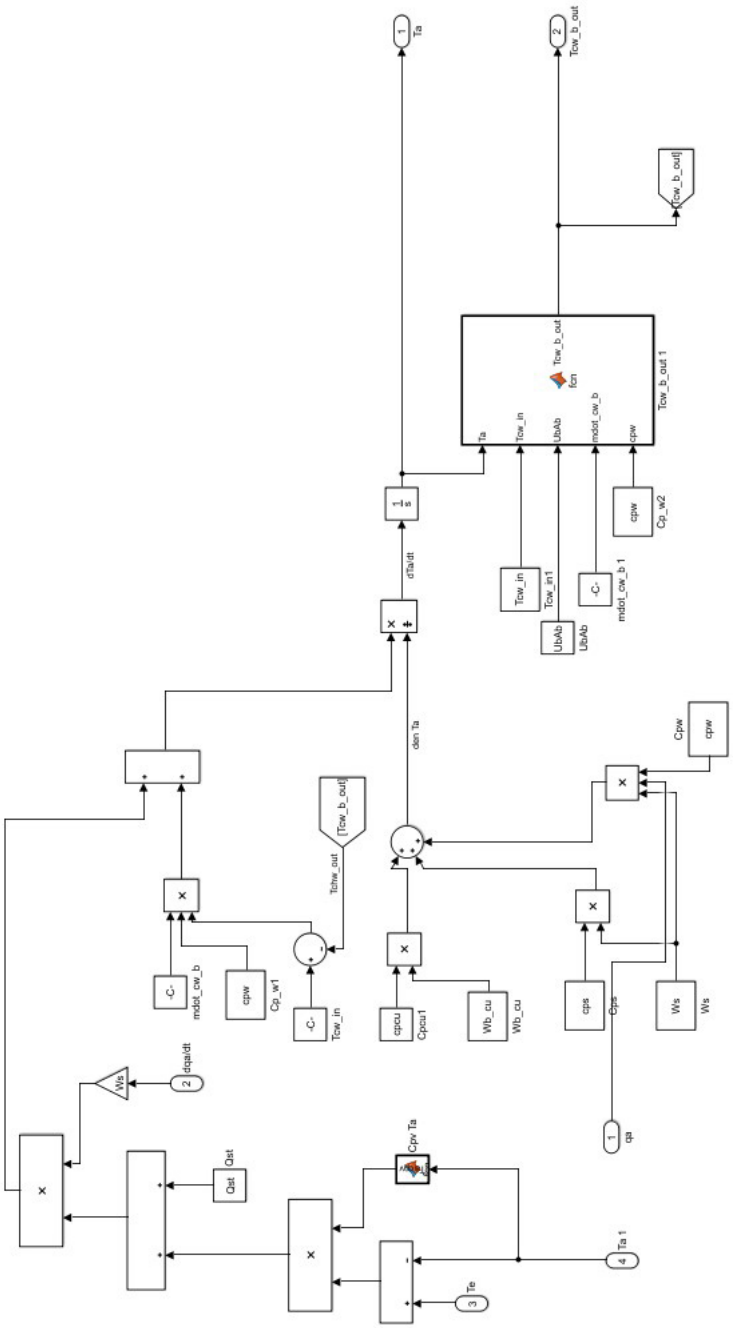

Fig. 45. Simulink model of the adsorber in phase B

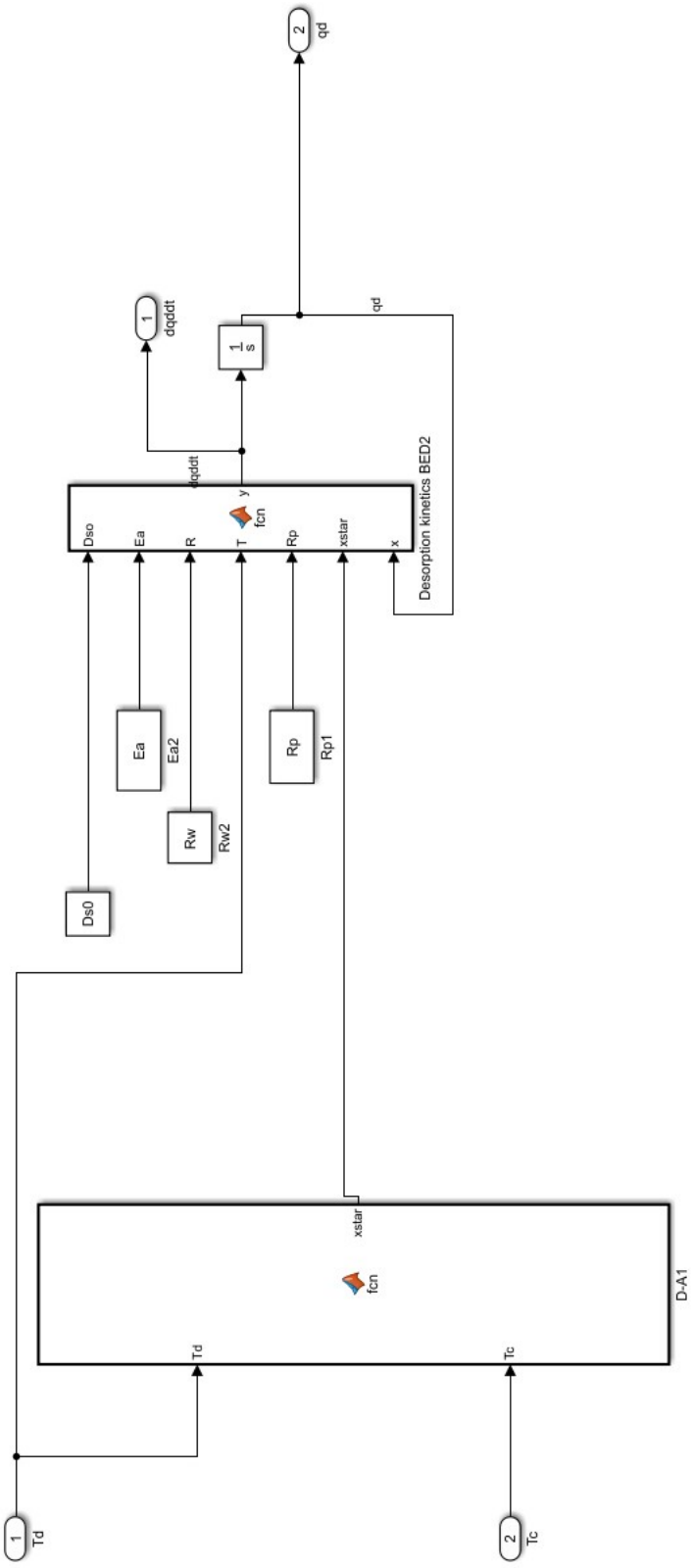

Fig. 46. Simulink model of the kinetics of the desorption bed in phase B

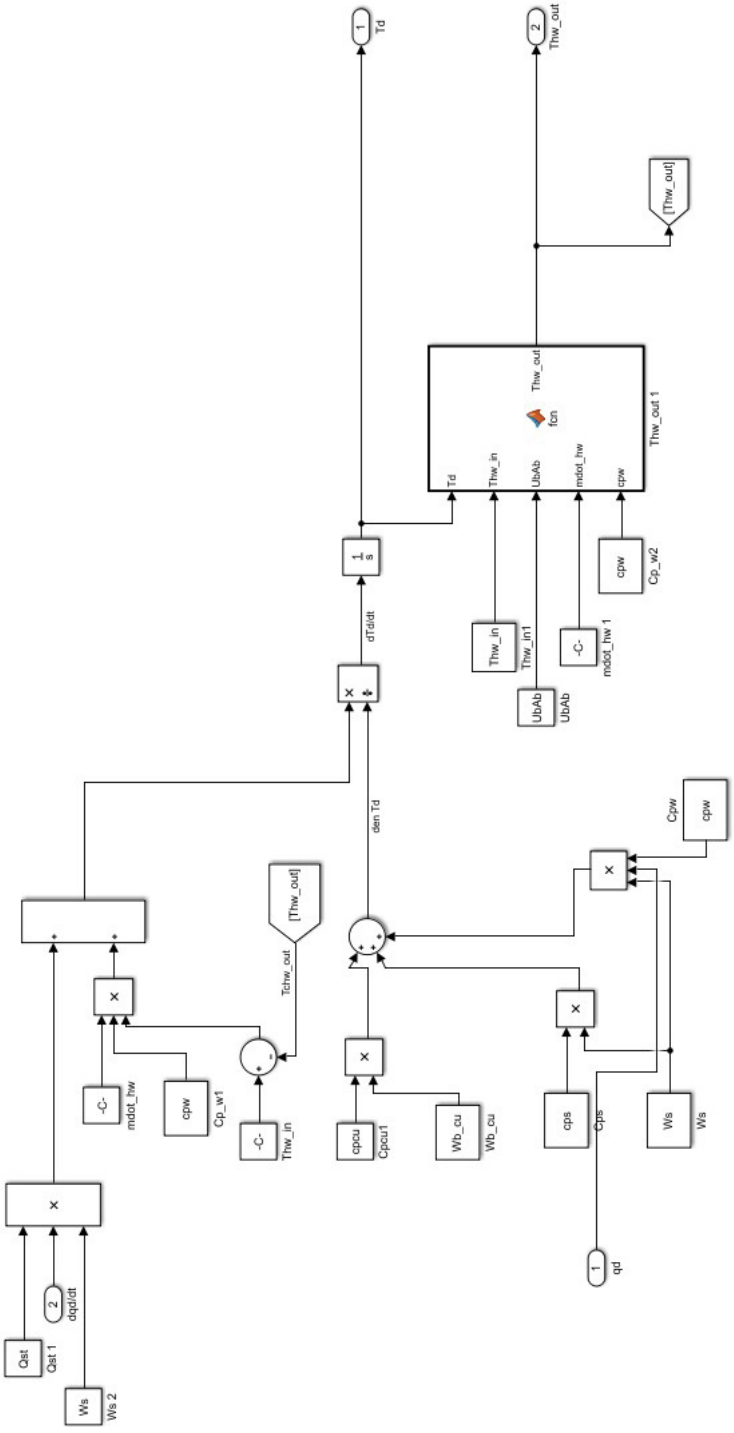

Fig. 47. Simulink model of the desorber in phase B

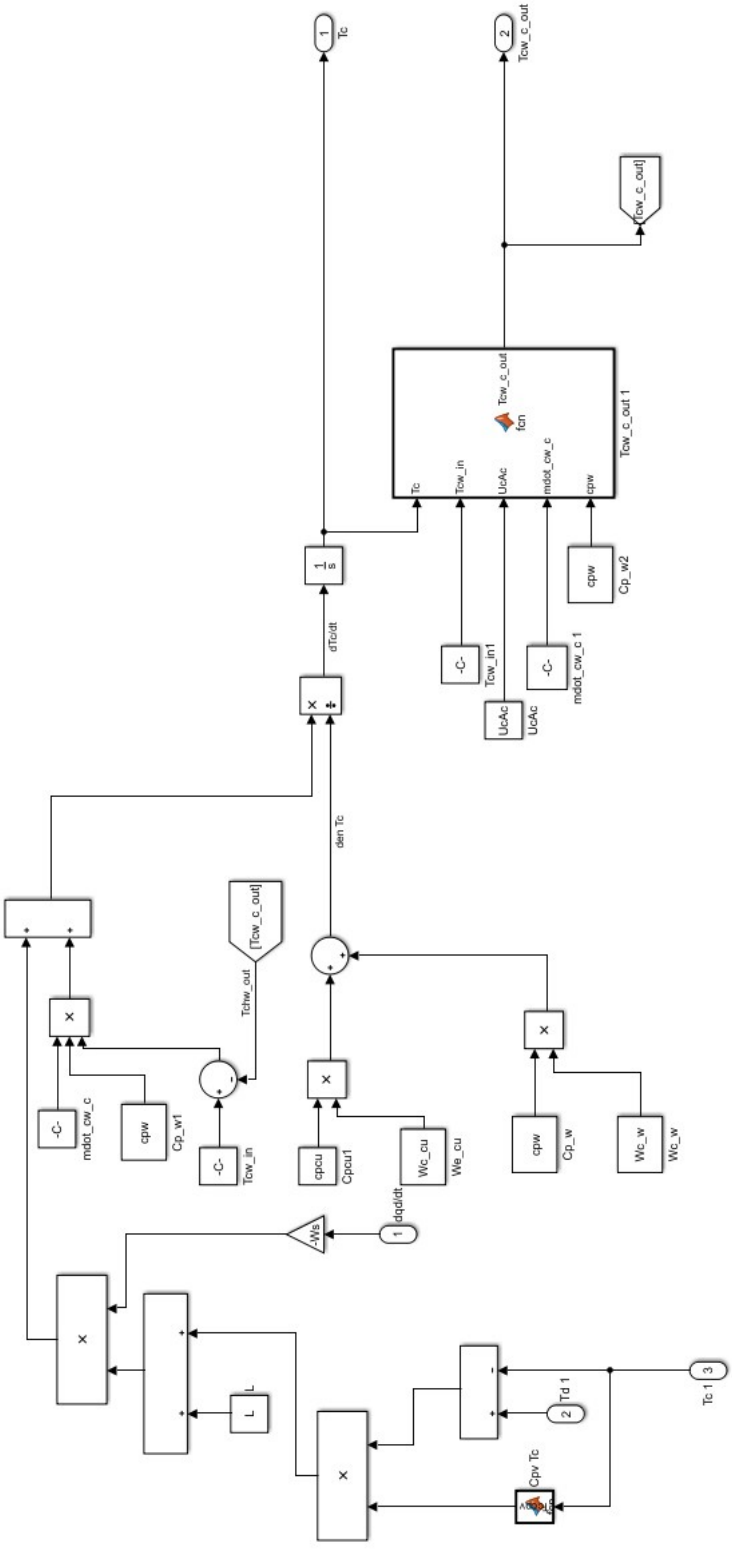

Fig. 48. Simulink model of the condenser in phase B

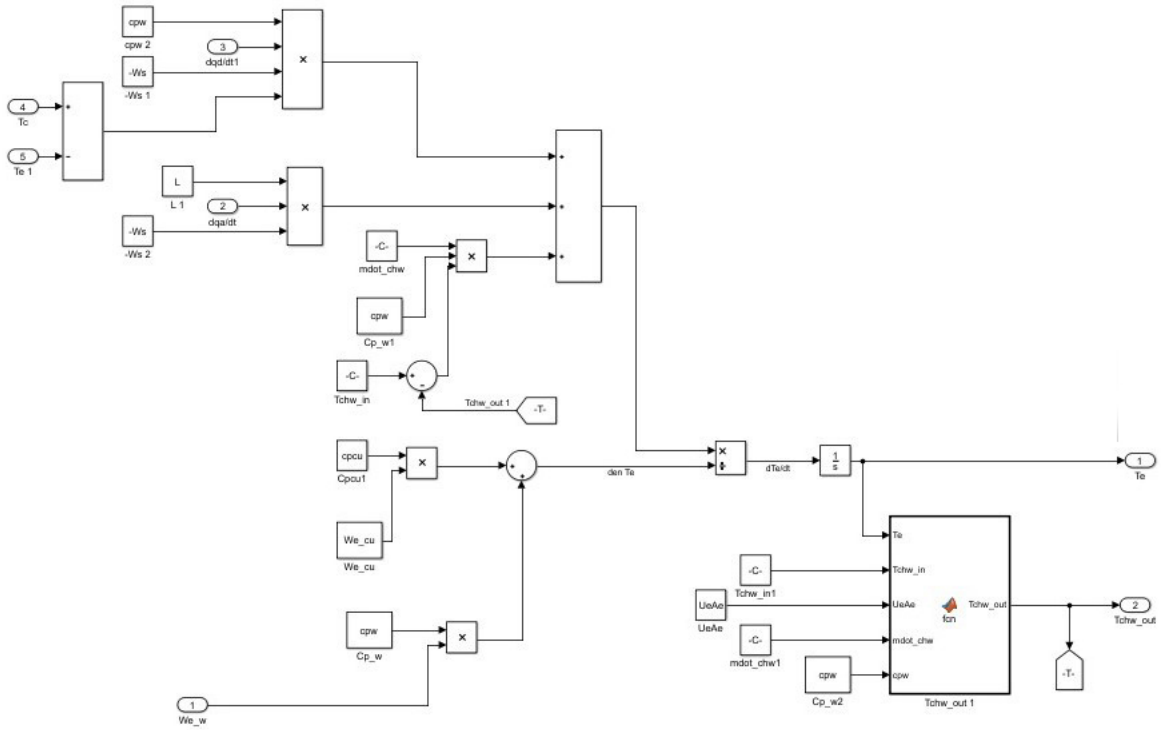

Fig. 49. Simulink model of the evaporator in phase B

11.2 Cooling and heating power outputs for different water temperatures

During the cooling period the Thw_in varies from 10 °C to 12 °C to cool efficiently the buildings. During the heating period the Tcw_in varies from 40 °C to 45 °C to heat efficiently the buildings. The values of the Q_e and Q_h that are negative represent impossible conditions for the chiller, mainly for low Thw_in and high Tcw_in. The dynamic model zeros the negative values of Q_e and Q_h and their corresponding COP. In this case, the outlet temperatures of the water are equal to their inlet temperatures. If the values of Q_e or Q_h are positive the outlet temperatures will be calculated by applying the energy balances:

$$Q_e = \dot{m}_{chw} * c_{pw} * (T_{chw\_in} - T_{chw\_out}) \quad [kW] \tag{34}$$

$$Q_{des} = \dot{m}_{hw} * c_{pw} * (T_{hw\_in} - T_{hw\_out}) \quad [kW] \tag{35}$$

$$Q_{ads} = \dot{m}_{cw\_b} * c_{pw} * (T_{cw\_b\_out} - T_{cw\_in}) \quad [kW] \tag{36}$$

$$Q_c = \dot{m}_{cw\_c} * c_{pw} * (T_{cw\_c\_out} - T_{cw\_in}) \quad [kW] \tag{37}$$

Thw_in = 70.00	Tcw_in = 40.00	Tcw_in = 40.63	Tcw_in = 41.25	Tcw_in = 41.88	Tcw_in = 42.50	Tcw_in = 43.13	Tcw_in = 43.75	Tcw_in = 44.38	Tcw_in = 45.00
Tchw_in = 10	-3.95	-5.44	-6.93	-8.43	-9.94	-11.45	-12.97	-14.49	-16.02
Tchw_in = 12	-1.11	-2.61	-4.12	-5.63	-7.15	-8.67	-10.20	-11.74	-13.27
Tchw_in = 14	1.77	0.25	-1.27	-2.79	-4.32	-5.85	-7.39	-8.94	-10.49
Tchw_in = 16	4.68	3.16	1.62	0.09	-1.45	-3.00	-4.55	-6.10	-7.67
Tchw_in = 18	7.62	6.09	4.55	3.00	1.45	-0.11	-1.67	-3.24	-4.81

Table 18. Results for the Q_h in [kW] for Thw_in = 70.00 °C, all temperatures are in [°C]

Thw_in = 75.00	Tcw_in = 40.00	Tcw_in = 40.63	Tcw_in = 41.25	Tcw_in = 41.88	Tcw_in = 42.50	Tcw_in = 43.13	Tcw_in = 43.75	Tcw_in = 44.38	Tcw_in = 45.00
Tchw_in = 10	1.14	-0.30	-1.75	-3.20	-4.65	-6.11	-7.58	-9.05	-10.53
Tchw_in = 12	4.00	2.55	1.09	-0.38	-1.84	-3.32	-4.80	-6.28	-7.77
Tchw_in = 14	6.90	5.44	3.97	2.49	1.01	-0.48	-1.97	-3.47	-4.97
Tchw_in = 16	9.85	8.37	6.89	5.40	3.91	2.41	0.90	-0.61	-2.13
Tchw_in = 18	12.83	11.34	9.85	8.34	6.84	5.33	3.81	2.29	0.76

Table 19. Results for the Q_h in [kW] for Thw_in = 75.00 °C, all temperatures are in [°C]

Thw_in = 80.00	Tcw_in = 25.00	Tcw_in = 27.50	Tcw_in = 30.00	Tcw_in = 32.50	Tcw_in = 35.00	Tcw_in = 37.50	Tcw_in = 40.00	Tcw_in = 42.50	Tcw_in = 45.00
Tchw_in = 10	5.91	4.53	3.14	1.75	0.35	-1.06	-2.47	-3.89	-5.31
Tchw_in = 12	8.80	7.40	6.00	4.59	3.17	1.75	0.32	-1.11	-2.55
Tchw_in = 14	11.73	10.32	8.90	7.48	6.05	4.61	3.17	1.72	0.27
Tchw_in = 16	14.70	13.28	11.85	10.41	8.97	7.52	6.06	4.60	3.13
Tchw_in = 18	17.72	16.28	14.83	13.38	11.92	10.46	8.99	7.52	6.04

Table 20. Results for the Q_h in [kW] for Thw_in = 80.00 °C, all temperatures are in [°C]

Thw_in = 85.00	Tcw_in = 40.00	Tcw_in = 40.63	Tcw_in = 41.25	Tcw_in = 41.88	Tcw_in = 42.50	Tcw_in = 43.13	Tcw_in = 43.75	Tcw_in = 44.38	Tcw_in = 45.00
Tchw_in = 10	10.39	9.07	7.74	6.40	5.06	3.71	2.35	0.99	-0.38
Tchw_in = 12	13.29	11.95	10.60	9.25	7.89	6.53	5.16	3.78	2.40
Tchw_in = 14	16.24	14.88	13.52	12.15	10.78	9.40	8.01	6.62	5.22
Tchw_in = 16	19.24	17.87	16.49	15.11	13.72	12.32	10.92	9.51	8.10
Tchw_in = 18	22.28	20.90	19.51	18.11	16.70	15.29	13.87	12.45	11.02

Table 21. Results for the Q_h in [kW] for Thw_in = 85.00 °C, all temperatures are in [°C]

Thw_in = 90.00	Tcw_in = 40.00	Tcw_in = 40.63	Tcw_in = 41.25	Tcw_in = 41.88	Tcw_in = 42.50	Tcw_in = 43.13	Tcw_in = 43.75	Tcw_in = 44.38	Tcw_in = 45.00
Tchw_in = 10	14.55	13.29	12.03	10.75	9.47	8.18	6.89	5.59	4.28
Tchw_in = 12	17.46	16.19	14.90	13.61	12.31	11.00	9.69	8.38	7.05
Tchw_in = 14	20.43	19.14	17.83	16.53	15.21	13.89	12.56	11.22	9.88
Tchw_in = 16	23.45	22.14	20.82	19.49	18.16	16.82	15.48	14.13	12.77
Tchw_in = 18	26.52	25.19	23.86	22.51	21.16	19.81	18.45	17.08	15.71

Table 22. Results for the Q_h in [kW] for Thw_in = 90.00 °C, all temperatures are in [°C]

Thw_in = 95.00	Tcw_in = 40.00	Tcw_in = 40.63	Tcw_in = 41.25	Tcw_in = 41.88	Tcw_in = 42.50	Tcw_in = 43.13	Tcw_in = 43.75	Tcw_in = 44.38	Tcw_in = 45.00
Tchw_in = 10	18.42	17.22	16.01	14.80	13.58	12.36	11.13	9.89	8.64
Tchw_in = 12	21.33	20.12	18.89	17.67	16.43	15.19	13.94	12.68	11.42
Tchw_in = 14	24.31	23.08	21.84	20.59	19.33	18.07	16.81	15.53	14.25
Tchw_in = 16	27.35	26.10	24.84	23.57	22.30	21.02	19.73	18.44	17.14
Tchw_in = 18	30.43	29.17	27.89	26.61	25.31	24.02	22.71	21.41	20.09

Table 23. Results for the Q_h in [kW] for Thw_in = 95.00 °C, all temperatures are in [°C]

Thw_in = 70.00	Tcw_in = 25.00	Tcw_in = 27.50	Tcw_in = 30.00	Tcw_in = 32.50	Tcw_in = 35.00	Tcw_in = 37.50	Tcw_in = 40.00	Tcw_in = 42.50	Tcw_in = 45.00
Tchw_in = 10	13.25	10.90	8.47	5.99	3.44	0.85	-1.79	-4.47	-7.19
Tchw_in = 10.5	13.61	11.25	8.82	6.32	3.77	1.17	-1.48	-4.16	-6.89
Tchw_in = 11	13.97	11.60	9.16	6.66	4.10	1.49	-1.16	-3.85	-6.58
Tchw_in = 11.5	14.33	11.95	9.51	7.00	4.43	1.82	-0.84	-3.54	-6.28
Tchw_in = 12	14.70	12.31	9.86	7.34	4.77	2.14	-0.52	-3.23	-5.97

Table 24. Results for the Q_e in [kW] for Thw_in = 70.00 °C, all temperatures are in [°C]

Thw_in = 75.00	Tcw_in = 25.00	Tcw_in = 27.50	Tcw_in = 30.00	Tcw_in = 32.50	Tcw_in = 35.00	Tcw_in = 37.50	Tcw_in = 40.00	Tcw_in = 42.50	Tcw_in = 45.00
Tchw_in = 10	14.88	12.64	10.33	7.95	5.51	3.02	0.48	-2.10	-4.72
Tchw_in = 10.5	15.25	13.00	10.68	8.29	5.85	3.35	0.80	-1.79	-4.41
Tchw_in = 11	15.61	13.36	11.03	8.63	6.18	3.67	1.12	-1.48	-4.11
Tchw_in = 11.5	15.98	13.72	11.38	8.98	6.52	4.00	1.44	-1.16	-3.80
Tchw_in = 12	16.35	14.08	11.73	9.32	6.85	4.33	1.76	-0.85	-3.50

Table 25. Results for the Q_e in [kW] for Thw_in = 75.00 °C, all temperatures are in [°C]

Thw_in = 80.00	Tcw_in = 25.00	Tcw_in = 27.50	Tcw_in = 30.00	Tcw_in = 32.50	Tcw_in = 35.00	Tcw_in = 37.50	Tcw_in = 40.00	Tcw_in = 42.50	Tcw_in = 45.00
Tchw_in = 10	16.34	14.21	12.02	9.75	7.43	5.04	2.61	0.13	-2.38
Tchw_in = 10.5	16.71	14.58	12.37	10.10	7.76	5.37	2.93	0.45	-2.08
Tchw_in = 11	17.08	14.94	12.72	10.44	8.10	5.70	3.25	0.76	-1.77
Tchw_in = 11.5	17.45	15.30	13.08	10.79	8.44	6.03	3.57	1.07	-1.47
Tchw_in = 12	17.83	15.67	13.44	11.14	8.78	6.36	3.90	1.39	-1.16

Table 26. Results for the Q_e in [kW] for Thw_in = 80.00 °C, all temperatures are in [°C]

Thw_in = 85.00	Tcw_in = 25.00	Tcw_in = 27.50	Tcw_in = 30.00	Tcw_in = 32.50	Tcw_in = 35.00	Tcw_in = 37.50	Tcw_in = 40.00	Tcw_in = 42.50	Tcw_in = 45.00
Tchw_in = 10	17.62	15.62	13.54	11.39	9.18	6.91	4.59	2.22	-0.18
Tchw_in = 10.5	18.00	15.99	13.90	11.74	9.52	7.24	4.91	2.54	0.12
Tchw_in = 11	18.38	16.35	14.25	12.09	9.86	7.57	5.23	2.85	0.43
Tchw_in = 11.5	18.75	16.72	14.61	12.44	10.20	7.90	5.56	3.17	0.73
Tchw_in = 12	19.13	17.09	14.98	12.79	10.54	8.24	5.89	3.49	1.04

Table 27. Results for the Q_e in [kW] for Thw_in = 85.00 °C, all temperatures are in [°C]

Thw_in = 90.00	Tcw_in = 25.00	Tcw_in = 27.50	Tcw_in = 30.00	Tcw_in = 32.50	Tcw_in = 35.00	Tcw_in = 37.50	Tcw_in = 40.00	Tcw_in = 42.50	Tcw_in = 45.00
Tchw_in = 10	18.75	16.87	14.91	12.87	10.78	8.63	6.42	4.17	1.87
Tchw_in = 10.5	19.13	17.24	15.26	13.22	11.12	8.96	6.74	4.48	2.18
Tchw_in = 11	19.51	17.61	15.62	13.57	11.46	9.29	7.07	4.80	2.48
Tchw_in = 11.5	19.89	17.98	15.99	13.93	11.80	9.63	7.39	5.11	2.79
Tchw_in = 12	20.28	18.35	16.35	14.28	12.15	9.96	7.72	5.43	3.10

Table 28. Results for the Q_e in [kW] for Thw_in = 90.00 °C, all temperatures are in [°C]

Thw_in = 95.00	Tcw_in = 25.00	Tcw_in = 27.50	Tcw_in = 30.00	Tcw_in = 32.50	Tcw_in = 35.00	Tcw_in = 37.50	Tcw_in = 40.00	Tcw_in = 42.50	Tcw_in = 45.00
Tchw_in = 10	19.88	18.12	16.28	14.35	12.38	10.34	8.25	6.11	3.93
Tchw_in = 10.5	20.12	18.34	16.48	14.56	12.57	10.53	8.43	6.28	4.10
Tchw_in = 11	20.50	18.71	16.84	14.91	12.91	10.86	8.75	6.60	4.40
Tchw_in = 11.5	20.89	19.08	17.21	15.26	13.26	11.20	9.08	6.92	4.71
Tchw_in = 12	21.28	19.46	17.57	15.62	13.61	11.53	9.41	7.24	5.02

Table 29. Results for the Q_e in [kW] for Thw_in = 90.00 °C, all temperatures are in [°C]

12 Appendix III: components of the SHWS

12.1 Solar flat plate collectors

The flat plate solar collectors modeled in TRNSYS are based on the Hewalex KS 2000 TP comersialized by HEWALEX Sp. z o.o. Sp. k. [6]. Every collector has a gross area of 2.095 m^2, flow rate equal to 240 l/h and tilted at 20 °. The collectors are hooked up in series with three collectors on each line. To model the collectors in TRNSYS the type 1 was used which needs the following values:

Parameter	Value	Unit
Number in series	3	-
Collectors area	control	m^2
Fluid specific heat	4.186	kJ/(kg K)
Efficiency mode	2	-
Tested flow rate	95.46	kg/(hr m^2)
Intercept efficiency	0.696	-
Efficiency slope	3.3	W/(m^2 K)
Efficiency curvature	0.0058	W/(m^2 K^2)
Optical mode 2	2	-
1st-order IAM	0.94	-
2nd-order IAM	0	-
Inlet temperature	component	°C
Inlet flow rate	component	kg/hr
Ambient temperature	weather data	°C
Incident radiation	weather data	kJ/(hr m^2)
Total horizontal radiation	weather data	kJ/(hr m^2)
Horizontal diffuse radiation	weather data	kJ/(hr m^2)
Ground reflectance	weather data	-
Incidence angle	weather data	°
Collector slope	20	°

Table 30. Input parameters for the solar collectors

The inlet temperature and flow rate of the water are taken from the mixing valve of the solar collectors while the radiation values from the weather data. The working flow rate is calculated by multiplying the number of the collectors with the flow rate of each collector and dividing this value by 3 (number of collectors connected in series). The type 1 is based on the publications: of ASHRAE [47], of CEN [15] and of Duffie et al. [21].

12.2 Cool coil

The cool coil was modeled with the type 508b which cools and dehumidifies the air stream as much as possible given the inlet conditions of both the air and the fluid streams. The cooling coil is modeled using a bypass approach where the user specifies a fraction of the air stream that bypasses the coil. The remain air stream is assumed to exit the coil at the average temperature of the fluid in the coil and at saturated conditions.
Two cool coils where used, one to cool the air that goes into the building during the cooling period and one to heat the chilled water by using the environmental air during the heating period. Both cool coils work by controlling the output temperature of the fluid. For the cooling period this temperature is set to 10.5 °C while for the heating period is equal to 10 °C. The input values for the cool coils for both heating and cooling periods are:

Parameter	Value	Unit
Fluid inlet temperature	control	°C
Fluid flow rate	control	kg/h
Air inlet temperature	control	°C
Not used	0.005	-
Air relative humidity (%)	control	% (base 100)
Air flow rate	control	kg/h
Air pressure	1.0	atm
Air-side pressure drop	0.0	atm
Coil bypass fraction	0.15	fraction
Setpoint: outlet fluid temperature	control	°C

Table 31. Input parameters for the cool coil

During cooling, the inlet temperature and relative humidity of the air are taken from the type 56 which is the model of the buildings. The fluid inlet temperature and the flow rate are taken from the control panel. The flow rate of the cooling water during the cooling period is divided by the number of buildings to simulate a system with two buildings because only one type 56 can be added in TRNSYS. The output fluid flow rate from the cool coil is multiplied by the number of buildings before returning to the adsorption chiller. The cool coil gives as output the temperature and the relative humidity of the air which return to the buildings thought the air ventilation.
During heating, the inlet temperature and relative humidity of the air are taken from the control panel. The inlet air is taken from the external air (weather data) The type 508b is taken from the TESS Libraries [8].

12.3 Heat coil

The heat coil was modeled with the type 753e which models a simple heating coil where the air is heated as it passes across a coil containing a hotter fluid. The device contains controls that bypass a fraction of the fluid stream past the coil to maintain a desired outlet air condition. The input values for the heat coil are:

Parameter	Value	Unit
Fluid inlet temperature	component	°C
Fluid flow rate	component	kg/h
Air inlet temperature	control	°C
Not used	0.005	-
Air relative humidity (%)	control	% (base 100)
Air flow rate	control	kg/h
Air pressure	1.0	atm
Air-side pressure drop	0.0	atm
Coil bypass fraction	0.15	fraction
Setpoint: outlet fluid temperature	control	°C

Table 32. Input parameters for the heat coil

The inlet temperature and flow rate of the fluid are taken from the heat exchanger while the temperature and the flow rate of the air from the building. The type 753e is taken from the TESS Libraries [8].

12.4 Mixing and divergent valves

For mixing water the type 649 is used and for diverting water the type 647. These types are taken from the TESS Libraries [8].

12.5 Heat exchanger

The heat exchanger was modeled with the type 761 which models a heat exchanger that is able to control the cold side fluid flow rate into the heat exchanger in order to maintain the user-defined temperature difference of the cold side. The design parameters are:

Parameter	Value	Unit
Heat exchanger flow mode	2	-
Specific heat of hot-side fluid	4.190	kJ/(kg K)
Specific heat of cold-side fluid	4.190	kJ/(kg K)
Rated flow rate of hot-side	5202	kg/h
Rated flow rate of cold-side	1200	kg/h
Maximum rated flow rate of cold side	1200	kg/h
Rated effectiveness of heat exchanger	0.8	-
Minimum control signal value	0	-

Table 33. Design parameters for the heat exchanger

While the input parameters are:

Parameter	Value	Unit
Hot-side inlet temperature	control	°C
Hot-side flow rate	control	kg/h
Cold-side inlet temperature	component	C
Cold-side flow rate	component	kg/h
Cold-side temperature difference	5	ΔC

Table 34. Input parameters for the heat exchanger

The inlet temperature and the flow rate of the hot side fluid are taken from the control panel while the inlet temperature and the flow rate of the cold side fluid from the heat coil. The input flow rate of the hot water is divided by the number of buildings during the heating period to simulate a system with two buildings because only one type 56 can be added in TRNSYS. The outlet flow rate of the hot water is multiplied by the number of buildings before returning to the adsorption chiller. The type 652 is taken from the TESS Libraries [8].

12.6 Tank

The tank was modeled with the type 60d which models a vertically cylindrical tank with one inlet and one outlet flows and one internal heat exchanger. The dimensions of the tank are based on the tanks comercialized by DINOX-H [7]. The parameters for this component that do not change for the four storage volumes are:

Parameter	Value	Unit
User-specified inlet positions	2	-
Tank perimeter	-1	m
Not used (inlet 2)	-1	-
Not used (outlet 2)	-1	-
Tank loss coefficient	0.95	W/K
Fluid specific heat	4.19	kJ/(h K)
Fluid density	1000	kg/m^3
Fluid thermal conductivity	0.667	W/(m K)
Destratification conductivity	0	kJ/(h m K)
Boiling temperature	100	°C
Auxiliary heater mode	2	-
Height of 1st aux. heater	1	m
Height of 1st thermostat	1.25	m
Set point temperature for element 1	55	°C
Deadband for heating element 1	5	ΔT
Height of heating element 2	1	m
Height of thermostat 2	1	m
Set point temperature for element 2	55	°C
Deadband for heating element 2	5	ΔT
Overall loss coefficient for gas flue	0	kJ/(h K)
Flue temperature	20	°C
Fraction of critical timestep	6	-
Gas heater?	0	-
Number of internal heat exchangers	1	-
Equal sized nodes	0	-
Uniform tank losses	0	-
HX Fluid Indicator	1	-
Fraction of glycol	0.75	-
Heat exchanger inside diameter	31.75	mm
Heat exchanger outside diameter	38.1	mm
Heat exchanger fin diameter	38.1	mm
Fins per meter for heat exchanger	100	-
Heat exchanger wall conductivity	401	W/(m K)
Heat exchanger material conductivity	401	W/(m K)

Table 35. Fixed parameters for the tank

While the parameters that change with the storage volume are:

Parameter	Value				Unit
Tank height	1.99	2.36	2.505	2.83	m
Tank volume	0.5	1	2	3	m^3
Height of flow inlet 1	0.065	0.090	0.090	0.11	m
Height of flow outlet 1	1.907	2.020	2.425	2.74	m
Total surface area of heat exchanger	1.8	2.8	3.2	3.3	m^2
Heat exchanger length	18.046	28.071	32.082	33.084	m
Height of heat exchanger inlet	0.890	1.005	1.118	1.25	m
Height of heat exchanger outlet	0.330	0.405	0.510	0.6	m

Table 36. Input parameters for the tank that change with the volume of the tank

The tank is divided in twenty temperature levels which simulates the stratification of the water inside the tank. The environment temperature needed as input is taken from the temperature of the basement because it's assumed that the tank is kept in the basement. The type 60d is based on the publications of: Klein et al. [32] and of Newton B.J [40].

12.7 Boiler

The boiler was modeled with the type 700 which models a fluid boiler. The design and input parameters are:

Parameter	Value	Unit
Rated Capacity	20	kW
Fluid specific heat	4.190	kJ/(kg K)
Minimum turn-down ratio	0.2	-
Inlet fluid temperature	control	°C
Inlet fluid flow rate	control	kg/h
Input Control Signal	0	-
Set-point temperature	control	°C
Boiler Efficiency	0.85	Fraction
Combustion Efficiency	0.9	Fraction

Table 37. Design and input parameters for the boiler

The inlet temperature and the flow rate of the fluid are taken from the control panel. The type 700 is taken from the TESS Libraries [8].

12.8 Cooling Tower

The cooling tower was modeled with the type 510 which models a closed circuit cooling tower. The cooling tower is needed in order to maintain the cooling temperature between 25 °C and 45 °C during the cooling period. The design and input parameters are:

Parameter	Value	Unit
Humidity mode	2	-
Design inlet fluid temperature	38	°C
Design outlet fluid temperature	35	°C
Design fluid flow rate	4608	kg/h
Fluid specific heat	4.186	kJ/(kg K)
Design ambient air temperature	36	°C
Design wet bulb temperature	27.8	°C
Design air flow rate	35500	kg/h
Air pressure at design conditions	1.0	atm
Rated fan power	1.8	kW
Number of power coefficients	3	-
Power coefficient-1	0.0	-
Power coefficient-2	0.0	-
Power coefficient-3	0.0	-
Fluid inlet temperature	control	°C
Fluid flow rate	control	kg/h
Ambient temperature	weather data	°C
Ambient humidity ratio	weather data	-
Ambient % RH	weather data	% (base 100)
Ambient air pressure	weather data	atm
Fan control signal	control	-
Desired Outlet Temperature	control	°C

Table 38. Design parameters for the cooling tower

The inlet temperature and the flow rate of the fluid are taken from the control panel. The type 510 is taken from the TESS Libraries [8].

12.9 Differential controller

Six differential controllers were added by using the type 2 which maintain functioning the SHWS.

- Two controllers are needed to generate the heating and cooling signals. The coils work based on the internal temperature of the buildings. If the internal temperature goes beyond the comfort limits the cooling or the heating is turned on. The input of the controllers is the internal temperature of the buildings. The controllers generate a control function which is equal to 1 if the cooling or heating has to be turned on or equal to 0 if the cooling or heating has to be turned off. The input parameters are different for the cooling and heating control. For the cooling control the inputs parameters are:

Parameter	Value	Unit
Upper input temperature Th	component	°C
Lower input temperature Tl	24	°C
Monitoring temperature Tin	0	°C
Input control function	0	-
Upper dead band dT	3	ΔT
Lower dead band dT	0	ΔT

Table 39. Input parameters for cooling signal

The upper input temperature is the internal temperature of the buildings. The cooling turns on when the temperature goes above 27 °C and turns off when the temperature reaches 24 °C.
For the heating control the inputs parameters are:

Parameter	Value	Unit
Upper input temperature Th	22	°C
Lower input temperature Tl	component	°C
Monitoring temperature Tin	0	°C
Input control function	0	-
Upper dead band dT	3	ΔT
Lower dead band dT	0	ΔT

Table 40. Input parameters for heating signal

The lower input temperature is the internal temperature of the buildings. The heating turns on when the temperature goes below 19 °C and turns off when the temperature reaches 22 °C.
- Two controller were added for the boiler. During cooling period, if the chiller can't cool the buildings then the boiler turns on and heat the hot water. The boiler turns on when the internal temperature reach 28 °C and turns off when the temperature goes below 27.5 °C. For the boiler control during the cooling period the input parameters are:

Parameter	Value	Unit
Upper input temperature Th	component	°C
Lower input temperature Tl	27.5	°C
Monitoring temperature Tin	0	°C
Input control function	0	-
Upper dead band dT	0.5	ΔT
Lower dead band dT	0	ΔT

Table 41. Input parameters for the first boiler signal

The upper input temperature is the internal temperature of the buildings.
During the heating period, The boiler turns on when the hot water goes bellow 75 °C and turns off when the hot water reaches 90 °C. For the boiler control during the heating period the input parameters are:

Parameter	Value	Unit
Upper input temperature Th	90	°C
Lower input temperature Tl	component	°C
Monitoring temperature Tin	0	°C
Input control function	0	-
Upper dead band dT	15	ΔT
Lower dead band dT	0	ΔT

Table 42. Input parameters for the second boiler signal

The lower input temperature is the temperature of the hot water exiting from the tank.
- Two controllers were added for the collectors. One controls the water flow rate coming from the collectors. If the temperature of the water is lower than the temperature of the water in the tank then the collectors water doesn't pass through the internal heat exchanger of the tank. The input parameters for the control of the flowrare of the collectors are:

Parameter	Value	Unit
Upper input temperature Th	0	°C
Lower input temperature Tl	component	°C
Monitoring temperature Tin	0	°C
Input control function	0	-
Upper dead band dT	0	ΔT
Lower dead band dT	0	ΔT

Table 43. Input parameters for the first collectors control signal

The lower input temperature is the temperature of the hot water exiting from the tank.
The second controller for the solar collectors is to avoid temperatures higher than 95 °C inside the tank. If the temperature of the water inside the tank reach 95 °C then the water from the collectors doesn't pass through the internal heat exchanger of the tank. The flow rate is blocked until the temperature of the tank goes below 93 °C.

Parameter	Value	Unit
Upper input temperature Th	component	°C
Lower input temperature Tl	93	°C
Monitoring temperature Tin	0	°C
Input control function	0	-
Upper dead band dT	2	ΔT
Lower dead band dT	0	ΔT

Table 44. Input parameters for the second collectors control signal

The upper input temperature is the temperature of the hot water exiting from the tank.

12.10 Adsorption chiller

The adsorption chiller was model with the type 155 which implements a link with Matlab. This type provides a Matlab script. In this script, first the inputs have to be defined, then the main script has to be added and finally the outputs have to be specified. The parameters values are:

Parameter	Value	Unit
Mode	0	-
Number of inputs	6	-
Number of outputs	7	-
Calling Mode	0	-
Keep Matlab open after simulation	1	-

Table 45. Design parameters for the adsorption chiller

The input parameters are:

Parameter	Unit	
Thw_in	component	°C
Tcw_in	component	°C
Tchw_in	component	°C
sigC	control	-
sigH	control	-
T_air_in	control	°C

Table 46. Input parameters for the adsorption chiller

T_air_in is the internal temperature of the buildings. The Thw_in is taken from the output of the mixing valve of the boiler (mixing valve boiler), the Tcw_in is taken from the output of the mixing valve of the cool water (mixing valve cw) and the the Tchw_in is taken from the output of the mixing valve of the chilled water (mixing valve chw). The output parameters are:

Parameter	Unit
Tchw_out	°C
Tcw_out	°C
Thw_out	°C
Q_h	kW
Q_e	kW
Q_d	kW
Q_a	kW

Table 47. Output parameters of the adsorption chiller

The values SigC, SigH, are send to the control panel which divides the water flow rates to maintain the SHWS in function.

References

[1] Airtechnic. http://www.airtechnic.gr/appdata/documents/airtechnic%20pricelist/pricelist_klimatismos_part_2.pdf. Accessed: 14-07-2018.

[2] Community research and development information service, project id: Nne5/25/2001. https://cordis.europa.eu/project/rcn/61352_en.html. Accessed: 27-07-2018.

[3] Daikin. https://www.daikin.gr. Accessed: 14-07-2018.

[4] nzeb, net zero energy buildings. http://www.nzeb.in/knowledge-centre/hvac-2/desiccant-cooling-system/. Accessed: 27-07-2018.

[5] Ren21, renewables, global status report, 2015. http://www.ren21.net/. Accessed: 27-07-2018.

[6] Solar collector factsheet hewalex ks 2000 tp. http://www.hewalex.eu/pliki/pobierz/spf-c825-certificate-for-solar-collector-ks2000-tp.pdf. Accessed: 18-06-2018.

[7] Standard internal heat exchanger tanks. http://dinox-h.hu/en/standard-internal-heat-exchanger.php. Accessed: 14-07-2018.

[8] Tess component library package. http://www.trnsys.com/tess-libraries/. Accessed: 18-06-2018.

[9] Jérôme Adnot, Dominique Giraud, F Colomines, P Rivière, S Becirspahic, G Benke, et al. Central (commercial) airconditioning systems in europe. In *Proceedings*, volume 5, pages 143–149, 2002.

[10] Amine Allouhi, Tarik Kousksou, Abdelmajid Jamil, Pascal Bruel, Youssef Mourad, and Youssef Zeraouli. Solar driven cooling systems: an updated review. *Renewable and Sustainable Energy Reviews*, 44:159–181, 2015.

[11] Constantinos A Balaras, Gershon Grossman, Hans-Martin Henning, Carlos A Infante Ferreira, Erich Podesser, Lei Wang, and Edo Wiemken. Solar air conditioning in europe—an overview. *Renewable and sustainable energy reviews*, 11(2):299–314, 2007.

[12] P Bourdoukan, E Wurtz, and Patrice Joubert. Experimental investigation of a solar desiccant cooling installation. *Solar Energy*, 83(11):2059–2073, 2009.

[13] F Calise, A Palombo, and L Vanoli. Maximization of primary energy savings of solar heating and cooling systems by transient simulations and computer design of experiments. *Applied Energy*, 87(2):524–540, 2010.

[14] Antonio Capozza, Michele De Carli, Antonio Galgaro, and Angelo Zarrella. Linee guida per la progettazione dei campi geotermici per pompe di calore. *Milan: Ricerca Sistema Energetico*, 2012.

[15] CEN. En 12975-2:2001. *Thermal solar systems and components – Solar collectors – Part 2: Test methods*, 2001.

[16] Soon-Haeng Cho and Jong-Nam Kim. Modeling of a silica gel/water adsorption-cooling system. *Energy*, 17(9):829–839, 1992.

[17] HT Chua, KC Ng, A Malek, T Kashiwagi, A Akisawa, and BB Saha. Modeling the performance of two-bed, sillica gel-water adsorption chillers. *International Journal of Refrigeration*, 22(3):194–204, 1999.

[18] YJ Dai, RZ Wang, HF Zhang, and JD Yu. Use of liquid desiccant cooling to improve the performance of vapor compression air conditioning. *Applied Thermal Engineering*, 21(12):1185–1202, 2001.

[19] Kadoma Daou, RZ Wang, and ZZ Xia. Desiccant cooling air conditioning: a review. *Renewable and Sustainable Energy Reviews*, 10(2):55–77, 2006.

[20] Umberto Desideri, Stefania Proietti, and Paolo Sdringola. Solar-powered cooling systems: Technical and economic analysis on industrial refrigeration and air-conditioning applications. *Applied Energy*, 86(9):1376–1386, 2009.

[21] JA Duffie, William A Beckman, and WM Worek. Solar engineering of thermal processes, 1994.

[22] Τεχνικό Επιμελητήριο Ελλάδας. Τ.ο.τ.ε.ε. 20701-1/2017 *αναλυτικές εθνικές προδιαγραφές παραμέτρων για τον υπολογισμό της ενεργειακής απόδοσης κτηρίων και την έκδοση του πιστοποιητικού ενεργειακής απόδοσης*.

[23] Τεχνικό Επιμελητήριο Ελλάδας. Τ.ο.τ.ε.ε. 20701-3/2010 *κλιματικά δεδομένα ελληνικών περιοχών*.

[24] Eurostat and Union européenne. Commission européenne. *Energy, transport and environment indicators*, volume 2. Office for Official Publications of the European Communities, 2011.

[25] Georgios A Florides, Soteris A Kalogirou, Savvas A Tassou, and LC Wrobel. Modelling and simulation of an absorption solar cooling system for cyprus. *Solar energy*, 72(1):43–51, 2002.

[26] TS Ge, RZ Wang, ZY Xu, QW Pan, S Du, XM Chen, T Ma, XN Wu, XL Sun, and JF Chen. Solar heating and cooling: Present and future development. *Renewable Energy*, 2017.

[27] SP Halliday, CB Beggs, and PA Sleigh. The use of solar desiccant cooling in the uk: a feasibility study. *Applied Thermal Engineering*, 22(12):1327–1338, 2002.

[28] HZ Hassan, AA Mohamad, and R Bennacer. Simulation of an adsorption solar cooling system. *Energy*, 36(1):530–537, 2011.

[29] HM Henning, T Erpenbeck, C Hindenburg, and IS Santamaria. The potential of solar energy use in desiccant cooling cycles. *International journal of refrigeration*, 24(3):220–229, 2001.

[30] Michaelis Karagiorgas, Theocharis Tsoutsos, Vassiliki Drosou, Stéphane Pouffary, Tulio Pagano, Germán Lopez Lara, and José Manuel Melim Mendes. Hotres: renewable energies in the hotels. an extensive technical tool for the hotel industry. *Renewable and Sustainable Energy Reviews*, 10(3):198–224, 2006.

[31] Sibnath Kayal, Sun Baichuan, and Bidyut Baran Saha. Adsorption characteristics of aqsoa zeolites and water for adsorption chillers. *International Journal of Heat and Mass Transfer*, 92:1120–1127, 2016.

[32] Sanford Alan Klein, WA Beckman, and John A Duffie. A design procedure for solar heating systems. *Solar Energy*, 18(2):113–127, 1976.

[33] Daeho Ko, Ranjani Siriwardane, and Lorenz T Biegler. Optimization of a pressure-swing adsorption process using zeolite 13x for co2 sequestration. *Industrial & engineering chemistry research*, 42(2):339–348, 2003.

[34] P Lamp and F Ziegler. European research on solar-assisted air conditioning. *International Journal of refrigeration*, 21(2):89–99, 1998.

[35] Renato M Lazzarin. Solar cooling: Pv or thermal? a thermodynamic and economical analysis. *International Journal of Refrigeration*, 39:38–47, 2014.

[36] Y Liu and KC Leong. Numerical modeling of a zeolite/water adsorption cooling system with non-constant condensing pressure. *International communications in heat and mass transfer*, 35(5):618–622, 2008.

[37] Tiago Mateus and Armando C Oliveira. Energy and economic analysis of an integrated solar absorption cooling and heating system in different building types and climates. *Applied Energy*, 86(6):949–957, 2009.

[38] Barbara Mette, Henner Kerskes, Harald Drück, and Hans Müller-Steinhagen. Experimental and numerical investigations on the water vapor adsorption isotherms and kinetics of binderless zeolite 13x. *International Journal of Heat and Mass Transfer*, 71:555–561, 2014.

[39] Fabio Maria Montagnino. Solar cooling technologies. design, application and performance of existing projects. *Solar Energy*, 154:144–157, 2017.

[40] Brian J Newton. *Modeling of solar storage tanks*. University of Wisconsin–Madison, 1995.

[41] Todd Otanicar, Robert A Taylor, and Patrick E Phelan. Prospects for solar cooling–an economic and environmental assessment. *Solar Energy*, 86(5):1287–1299, 2012.

[42] Valeria Palomba, Salvatore Vasta, Angelo Freni, Quanwen Pan, Ruzhu Wang, and Xiaoqiang Zhai. Increasing the share of renewables through adsorption solar cooling: A validated case study. *Renewable energy*, 110:126–140, 2017.

[43] AM Papadopoulos, S Oxizidis, and Nikolaos Kyriakis. Perspectives of solar cooling in view of the developments in the air-conditioning sector. *Renewable and Sustainable Energy Reviews*, 7(5):419–438, 2003.

[44] E Papoutsis and E Koronaki. *θερμοδυναμική ανάλυση ψυκτικών συστημάτων προσρόφησης*. *Adsorption chiller*, 1:1–256, 2018.

[45] Jean Philippe Praene, Olivier Marc, Franck Lucas, and Frédéric Miranville. Simulation and experimental investigation of solar absorption cooling system in reunion island. *Applied Energy*, 88(3):831–839, 2011.

[46] Bidyut B Saha, Elisa C Boelman, and Takao Kashiwagi. Computational analysis of an advanced adsorption-refrigeration cycle. *Energy*, 20(10):983–994, 1995.

[47] ASHRAE Standard. Standard 93-2003. *Method of testing to determine the thermal performance of solar collector*, 2003.

[48] Th Tsoutsos, E Aloumpi, Z Gkouskos, and M Karagiorgas. Design of a solar absorption cooling system in a greek hospital. *Energy and Buildings*, 42(2):265–272, 2010.

[49] Theocharis Tsoutsos, Joanna Anagnostou, Colin Pritchard, Michalis Karagiorgas, and Dimosthenis Agoris. Solar cooling technologies in greece. an economic viability analysis. *Applied Thermal Engineering*, 23(11):1427–1439, 2003.

[50] Salvatore Vasta, Valeria Palomba, Andrea Frazzica, Fabio Costa, and Angelo Freni. Dynamic simulation and performance analysis of solar cooling systems in italy. *Energy Procedia*, 81:1171–1183, 2015.

[51] Rick Wagner. Multi-linear interpolation. *Beach Cities Robotics*, 2008.

[52] RZ Wang, TS Ge, CJ Chen, Q Ma, and ZQ Xiong. Solar sorption cooling systems for residential applications: options and guidelines. *International Journal of refrigeration*, 32(4):638–660, 2009.

[53] RZ Wang and RG Oliveira. Adsorption refrigeration—an efficient way to make good use of waste heat and solar energy. *Progress in Energy and Combustion Science*, 32(4):424–458, 2006.

[54] Xiaolin Wang and HT Chua. Two bed silica gel–water adsorption chillers: an effectual lumped parameter model. *International Journal of Refrigeration*, 30(8):1417–1426, 2007.

[55] DG Waugaman, A Kini, and CF Kettleborough. A review of desiccant cooling systems. *Journal of Energy Resources Technology*, 115(1):1–8, 1993.

[56] Wei-Dong Wu, Hua Zhang, and Da-Wen Sun. Mathematical simulation and experimental study of a modified zeolite 13x–water adsorption refrigeration module. *Applied Thermal Engineering*, 29(4):645–651, 2009.

[57] ZY Xu and RZ Wang. Simulation of solar cooling system based on variable effect libr-water absorption chiller. *Renewable Energy*, 113:907–914, 2017.